



Quality Management of Flexible Pavement Layers with Seismic Methods

Conducted for:

Texas Department of Transportation and

Research Report 0-1735-3

December 2005

Center for Transportation Infrastructure Systems
The University of Texas at El Paso
El Paso, TX 79968

Quality Management of Flexible Pavement Layers with Seismic Methods

By

Soheil Nazarian, Ph.D., P.E.

Deren Yuan, Ph.D.

Vivek Tandon, Ph.D., P.E.

and

Miguel Arellano, P.E.

Research Report 0-1735-3

**Performed in Cooperation with the
Texas Department of Transportation and
The Federal Highway Administration**

**Research Project 0-1735
Development of Structural Field Testing of
Flexible Pavement Layers**

**Quality Management of ACP and Base Using
Project 1735 Findings**

December 2005

The Center for Transportation Infrastructure Systems
The University of Texas at El Paso
El Paso, TX 79968-0516
(915) 747-6925

The contents of this report reflect the view of the authors, who are responsible for the facts and the accuracy of the data presented herein. The contents do not necessarily reflect the official views or policies of the Texas Department of Transportation or the Federal Highway Administration. This report does not constitute a standard, specification, or regulation.

**NOT INTENDED FOR CONSTRUCTION, BIDDING,
OR PERMIT PURPOSES**

Soheil Nazarian, PhD, PE (69263)
Deren Yuan, PhD
Vivek Tandon, PhD, PE (88219)
Miguel Arellano, PE (90069)

Pages ii and iii are misnumbered in the original.

-- CTR Library Digitization Team

TECHNICAL REPORT STANDARD TITLE PAGE

1. Report No. FHWA/TX-03/0-1735-3	2. Government Accession No.	3. Recipient's Catalog No.	
4. Title and Subtitle Quality Management of Flexible Pavement Layers with Seismic Methods		5. Report Date December 2002	
		6. Performing Organization Code	
7. Author(s) S. Nazarian, D. Yuan, V. Tandon and M. Arellano		8. Performing Organization Report No. Research Report 0-1735-3	
9. Performing Organization Name and Address Center for Transportation Infrastructure Systems The University of Texas at El Paso El Paso, Texas 79968-0516		10. Work Unit No.	
		11. Contract or Grant No. Study No. 0-1735	
12. Sponsoring Agency Name and Address Texas Department of Transportation Research and Technology Implementation Office P.O. Box 5080 Austin, Texas 78763		13. Type of Report and Period Covered Technical Report September 2000 – August, 2002	
		14. Sponsoring Agency Code	
15. Supplementary Notes Research Performed in Cooperation with TxDOT and FHWA			
16. Abstract <p>Under this project several field protocols and test equipment have been developed, which in a rational manner, combine the results from laboratory and field tests with those used for quality control during construction. The significance of the project is that more rational methods for quality control during construction can be developed, at the same time, feedback to the pavement design engineer can be provided in terms of the assumption made to design the pavement. The protocols proposed have potential to provide the first step towards developing performance-based specifications.</p> <p>This report contains the results of an effort to address the issues related to the implementation of the devices recommended in the day-to-day operation of TxDOT. The major issues that are addressed are the repeatability, reproducibility of the methods, means of relating the measured parameters to the design moduli, and relating the parameters to performance of the pavement.</p>			
17. Key Words Pavement Design, Modulus, Laboratory Testing, Flexible Pavements, Resilient Modulus, Quality Control, Seismic Methods		18. Distribution Statement No restrictions. This document is available to the public through the National Technical Information Service, 5285 Port Royal Road, Springfield, Virginia 22161	
19. Security Classif. (of this report) Unclassified	20. Security Classif. (of this page) Unclassified	21. No. of Pages 120	22. Price

Acknowledgements

The authors would like to give their sincere appreciation to Steve Smith of the TXDOT Odessa District and David Head of El Paso District for their ever-present support. We would also like to thank the constructive advice from the Project Advisory Team, especially Mark McDaniel, Caroline Herrera, Dar Hao Chen, John Bilyeu and Joe Leidy.

We would also like to thank the hard working people from districts that generously offered their time. Especially, we would like to thank Tomas Saenz of El Paso District, K.C. Evans of Odessa District, Richard Williammee of Fort Worth District, Miles Garrison of Atlanta District and Raul Palma of Pharr District for arranging the logistics for the field tests.

We are also appreciative to Tom Scullion of TTI for providing assistance in field and lab tests. Arif Chowdhury of TTI provided specimens from the Atlanta project.

Abstract

Under this project several protocols and test equipment have been developed, which, in a rational manner, combine the results from laboratory and field tests with those used for quality control during construction. The significance of the project is that more rational methods for quality control during construction can be developed, at the same time, feedback to the pavement design engineer can be provided in terms of the assumption made to design the pavement. The protocols proposed have potential to provide the first step towards developing performance-based specifications.

This report contains the results of an effort to address the issues related to the implementation of the devices recommended in the day-to-day operation of TxDOT. The major issues that are addressed are the repeatability, reproducibility of the methods, means of relating the measured parameters to the design moduli, and relating the parameters to performance of the pavement.

Executive Summary

Depending upon the thickness of different layers and the mode of failure, different structural parameters play dominant roles. In general, the most important parameters are the thickness and moduli of different layers. Therefore, these parameters should be measured fairly accurately. Tests to measure moduli of different layers are presented in this report.

The focus of the study has been on measuring moduli with four inter-related seismic devices that measure moduli of materials nondestructively. Two of these are laboratory devices: the free-free resonant column device for testing base and subgrade and the ultrasonic device for testing AC cores and briquettes. The other two are field devices: the Portable Seismic Pavement Analyzer (PSPA) for testing AC layers and a version of it that works on the base and prepared subgrade layers (affectionately called DSPA for Dirt Seismic Pavement Analyzer).

Procedures have been developed to measure the moduli of each pavement layer shortly after placement and after the completion of the project. These procedures allow rapid data collection and interpretation. Thus, any problem during construction process can be identified and adjusted. The outcomes from this project exhibit that the proposed equipment and methodologies may strike a balance between the existing level of sophistication in the design methodology, laboratory testing and field testing. Performing the simplified laboratory and field tests along with more traditional tests may result in a database that can be used to smoothly unify the design procedures and construction quality control.

The major advantage of seismic methods is that similar results are anticipated from the field and laboratory tests as long as the material is tested under comparable conditions. This unique feature of seismic methods in material characterization is of particular significance, if one is interested in implementing performance-based specifications. The use of seismic moduli in pavement design, which is the other issue of significance, is currently being addressed under Project 0-1780 entitled Design Moduli from Seismic Measurements.

This report contains the results of an effort to address the issues related to the implementation of the methods and devices recommended in the day-to-day operation of TxDOT. The major issues addressed are the repeatability, reproducibility of the methods, means of relating the measured parameters to the design moduli and relating the parameters to performance of the pavement.

Implementation Statement

An implementation project has already been approved for this project. The tasks to be undertaken as per the implementation plan are:

- Develop and deliver a comprehensive training course for engineers and technicians who conduct tests
- Assist TxDOT personnel to evaluate and modify procedures and test equipment to ensure their usefulness, user friendliness and versatility
- Recommend initial specifications for implementation of the methods by TxDOT personnel
- Compare existing QC/QA results with the outcome of these methods
- Recommend final specifications

ASPHALT CONCRETE LAYER	42
BASE LAYER	53
CHAPTER 7 - CLOSURE	67
REFERENCES	69

Figure 5.9 – Seismic Modulus of Specimens Prepared with Precautionary Measures.....	38
Figure 5.10 – Overall Modulus-Moisture Plot for Sandy Materials.....	38
Figure 6.1 – Variation in Modulus Measured with PSPA with Air Voids from I-20 Sites.....	44
Figure 6.2 – Comparison of Moduli Measured In Situ, on Cores Retrieved from Field and from Specimens Prepared from Loose Material Retrieved during Paving.....	46
Figure 6.3 – Typical Results from Complex Modulus and Seismic Tests on a AC Specimen.....	48
Figure 6.4 – Comparison of Master Curves with and without Seismic Data	49
Figure 6.5 – Variation in Lab and Field Moduli from Sites Tested in Texas.....	49
Figure 6.6 – Variation in Lab and Field Moduli from Sites Tested outside Texas.....	52
Figure 6.7 – Resilient Modulus Test Setup.....	54
Figure 6.8 – Typical Resilient Modulus Test Results.....	55
Figure 6.9 – Typical Variation in Resilient Modulus with Strain.....	56
Figure 6.10 – Relationship between Seismic and Low-Strain Resilient Moduli.....	56
Figure 6.11 – Correlation between Strength Parameter and Compression Wave Velocity of Bases Tested	57
Figure 6.12 – Performance as Related to Angle of Internal Friction from New Triaxial Method (Tex-143-E).....	63
Figure 6.13 – Performance as Related to Seismic Modulus from Free-Free Resonant Column	63
Figure 6.14 – Performance as Related to Dielectric Values from Tube Suction Tests.....	64
Figure 6.15 – Performance as Related to Seismic Modulus with DSPA.....	65
Figure 6.16 – Variation in Modulus and Moisture Content with Time for a Typical Base.....	65
Figure 6.17 – Performance as Related to Seismic Modulus Ratio	66

List of Tables

Table 5.1 – Physical Properties of Synthetic Material Used in This Study	26
Table 5.2 – Repeatability of Ultrasonic Device in Modulus Measurement as a Function of Diameter and Height of Synthetic Specimens	27
Table 5.3 – Repeatability of Free-free Resonant Column Device in Modulus Measurement as a Function of Diameter and Height of Synthetic Specimens	29
Table 5.4 – Evaluation of Repeatability of Free-Free Resonant Column and PSPA (from Alexander, 1996)	39
Table 6.1 – Gradations of Mixtures Used in I-20 Site	43
Table 6.2 – Volumetric Information for Mixture Used in I-20 Site	44
Table 6.3 – Variation in Modulus Measured with PSPA and Volumetric Information from I-20 Sites	44
Table 6.4 – Comparison of Moduli Measured with PSPA In Situ and Ultrasonic Device on Cores from I-20 Site.....	45
Table 6.5 – Variation in Modulus Measured with Ultrasonic Device and Volumetric Information from Briquettes Made from I-20 Sites Materials.....	46
Table 6.6 – Description of Sites Tested inside Texas	50
Table 6.7 – Description of Sites Tested outside Texas	52
Table 6.8 – Loading Sequence for Resilient Modulus Test.....	53
Table 6.9 – Description of Sites Tested	59
Table 6.10 – Index Properties of Sites Tested	61
Table 6.11 – Strength and Stiffness Parameters of Sites Tested.....	62

Chapter 1

Introduction

Aside from traffic and environmental loading, the primary parameters that affect the performance of a flexible pavement section are the modulus, thickness and Poisson's ratio of each layer. Current TxDOT procedure for structural design of flexible pavements considers these parameters. The state-of-the-art equipment to perform laboratory resilient modulus tests on AC, base and subgrade materials have also been acquired. TxDOT can perform nondestructive field tests to estimate the in-place moduli of different layers. Unfortunately, the construction specifications and acceptance criterion are not based on the same engineering properties. The acceptance criteria are typically based on adequate thickness, and adequate density of the placed and compacted materials. To successfully implement any mechanistic pavement design procedure and to move toward performance-based specifications, it is essential to develop tools that can measure the modulus and thickness of each layer in the field. The main objective of this project is to develop inexpensive, accurate and precise devices for project level studies to measure modulus.

The primary goal of this project has been to develop realistic field test protocols and equipment, which in a rational manner, combine the results from laboratory and field tests with those used for quality control during construction. A series of simplified laboratory tests that are compatible with the field tests have been recommended. All these tests have several features in common. They can be performed rapidly (less than three minutes), they are inexpensive and their data reduction processes are simple and almost instantaneous. These technologies can be transferred to TxDOT.

The significance of this project is evident. These types of tests are one of the major components needed to develop a mechanistic pavement design and performance-based construction specifications. A gradual transition from the existing specifications to performance-based specifications may be necessary. Performing the simplified laboratory and field tests on pavement materials will allow us to develop a database that can be used to smoothly unify the design procedures and construction quality control.

In two previous reports, the feasibility of the protocols and procedures for quality management of the AC layer are comprehensively addressed. In this report, the results of an effort to address the issues related to the implementation of the devices recommended in the day-to-day operation of TxDOT are included. The major issues addressed are the repeatability and reproducibility of the methods, means of relating the measured parameters to the design moduli, and relating the parameters to performance of the pavement. To be effective in practical use, a device should have four major features. First, it should measure fundamental properties of materials (i.e., it should not be an index test). Second, the device should be sensitive enough to the parameter of interest so that good and bad quality materials can be readily delineated. Third, the measurements should be accurate enough so that they can provide feedback to the designer and the laboratory personnel. Fourth, the device should be precise enough so that it can be readily used in the QA/QC process.

The report consists of seven chapters. A brief description of each device and method is included in Chapter 2. The methodology to convert the measured seismic moduli to those used in design is included in Chapter 3. The overall test protocols are summarized in Chapter 4. The operational aspects of the devices in terms of precision and accuracy are addressed in Chapter 5. Chapter 6 is dedicated to relating the measured values to performance parameters. Summary, conclusions and the future work plan are described in Chapter 7.

Chapter 2

Test Equipment

The focus of the study has been on measuring moduli with four inter-related devices. Two of these devices are used in the laboratory: the free-free resonant column device for testing base and subgrade specimens and the ultrasonic device for testing AC cores and briquettes. The other two devices are the Portable Seismic Pavement Analyzer (PSPA) for testing AC layers nondestructively in the field and a version of it that works on the base and prepared subgrade materials (affectionately called DSPA for Dirt Seismic Pavement Analyzer). Each device is described below.

Laboratory Testing

Free-free Resonant Column Test

The free-free resonant column (FFRC) test is a simple laboratory test for determining the modulus of pavement materials. The modulus measured with this method is the low-strain seismic modulus. The method is originally developed for testing Portland cement concrete specimens; however, with appropriate modifications in hardware and software, it is also applicable to specimens of base and subgrade materials as well as certain AC specimens. Since the tests are nondestructive, a membrane can be placed around the specimen so that it can be tested later for stiffness (resilient modulus). Performing both tests simultaneously will allow TxDOT to develop a database that can be used to smoothly unify the design parameters and the parameters used in construction quality control.

When a cylindrical specimen is subjected to an impulse load at one end, seismic energy over a large range of frequencies will propagate within the specimen. Depending on the dimensions and the stiffness of the specimen, energy associated with one or more frequencies are trapped and magnified (resonate) as they propagate within the specimen. The goal with this test is to determine these resonant frequencies. Since the dimensions of the specimen are known, if one can determine the frequency(ies) that are resonating (i.e. the resonant frequencies), one can

readily determine the modulus of the specimen using principles of wave propagation in a solid rod (see Richart et al., 1970 for the theoretical background).

The procedure used in the seismic test is to find the Young's modulus by measuring the velocity that a wave propagates through a cylindrical specimen and combining those results with other measurable properties. The schematic of the test set up is shown in Figure 2.1. To perform the test an accelerometer is placed securely at one end of a specimen, and the other end is tapped with a hammer that has a load cell attached to it. The two sensors are connected to a data acquisition system placed in a computer. Software has been developed to acquire and manipulate the time records from the accelerometer and the load cell. Typical time records are shown in Figure 2.2. The load consists of a short-duration half-sine pulse. The response measured with the accelerometer contains an oscillation that corresponds to the standing wave energy trapped within the specimen.

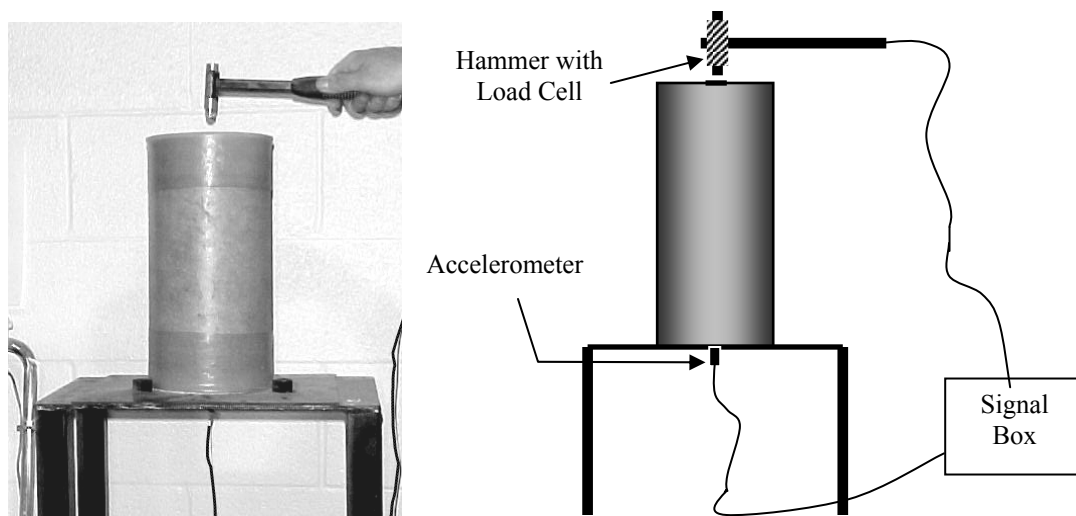


Figure 2.1 – Free-free Resonant Column Test Setup

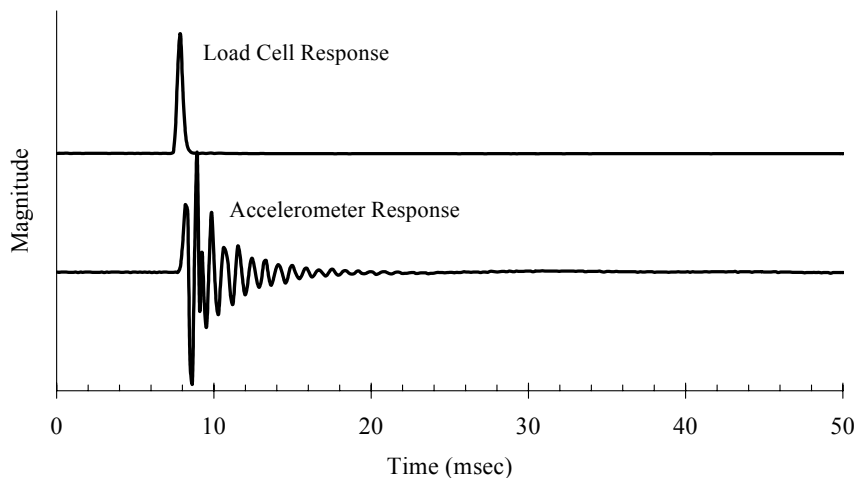


Figure 2.2 – Typical Load Cell and Accelerometer Responses from Free-Free Resonant Column Test

A more convenient way of determining the frequency of oscillation consists of transforming the two signals into the frequency-domain using a fast-Fourier transform and then normalizing the acceleration amplitude with the load amplitude. The variation of normalized amplitude as a function of frequency, which is called a transfer function, contains peaks that correspond to the oscillation of the standing waves. A typical transfer function is shown in Figure 2.3 with the peak frequencies clearly marked. Knowing the longitudinal resonant frequency, f_p , mass density, ρ , and the length of the specimen, L , Young's modulus, E , can be found using

$$E = \rho (2 f_p L)^2 = \rho (V_p)^2 \quad (2.1)$$

where V_p is the compression wave velocity.

The sample preparation described for the resilient modulus test is also applicable here. Similar to the resilient modulus tests, a length-to-diameter ratio of 2 is recommended for specimens. However, if necessary, this can be relaxed to 1.5. In that case, the determination of shear resonance, f_s , is rather difficult. Another important practical issue is securing the accelerometer to the specimen. We have found that a roofing nail embedded in the specimen during compaction provides a convenient pedestal for securing the accelerometer with a magnet. We have also found that a nail placed on the opposite side will provide a nice anvil for the hammer.

Ultrasonic Test Setup

The ultrasonic test methods were first used to evaluate the quality of concrete more than 50 years ago (Naik and Malhorta, 1991). The laboratory setup used in this study is shown in Figure 2.4. The elastic modulus of a specimen is measured using a device (marketed as a V-meter) containing a pulse generator and a timing circuit, coupled with piezoelectric transmitting and receiving transducers. The dominant frequency of the energy imparted to the specimen is 54 kHz. The timing circuit digitally displays the time needed for a wave to travel through a

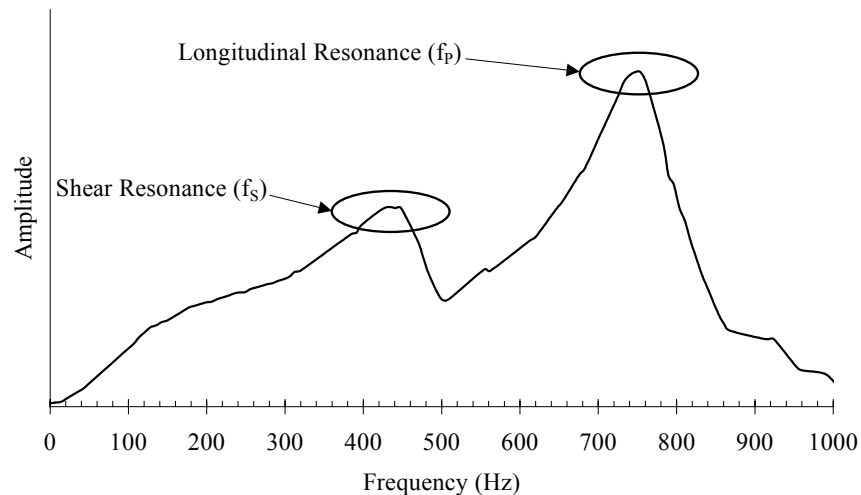


Figure 2.3 – Typical Transfer Function from Free-Free Resonant Column Test

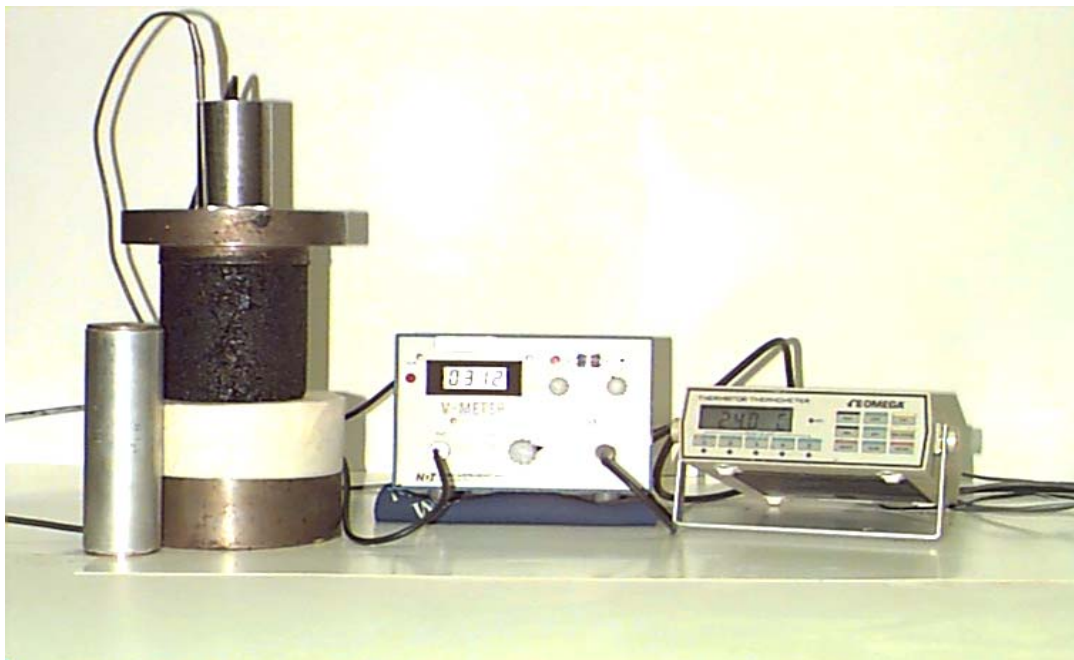
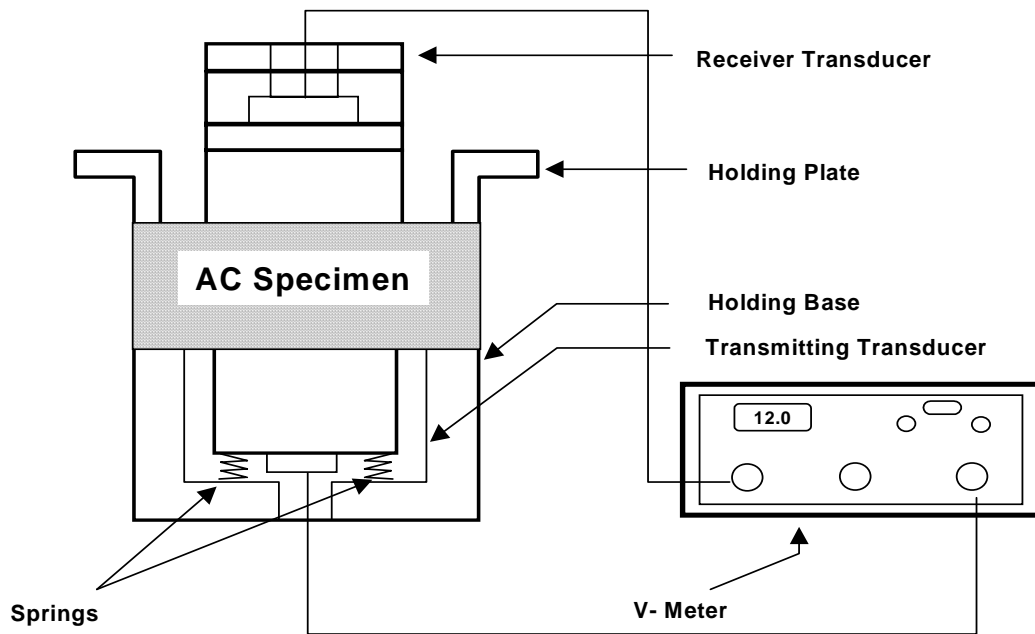


Figure 2.4 – Ultrasonic Test Device for AC Specimens

specimen. To ensure full contact between the transducers and a specimen, special removable epoxy couplant caps are used on both transducers. To secure the specimen between the transducers, a loading plate is placed on top of it, and a spring-supporting system is placed underneath the transmitting transducer. Compression wave (P-wave) velocity, V_p , is calculated

by dividing the length of the specimen by the corresponding travel time. The modulus, M_v , is then calculated using

$$M_v = \rho V_p^2, \quad (2.2)$$

where ρ is the bulk density of the specimen. For practical use, Equation 2.2 can be rewritten as

$$M_v = \frac{WH}{(\pi R^2 t_v^2)}, \quad (2.3)$$

where W , R and H are the mass, radius and height of the specimen, and t_v = travel time. The size of the sensors used with the test device is large relative to the wave travel path. The modulus measured with the V-meter, M_v , is the so-called constraint modulus. The constraint modulus, M_v can then be converted to Young's modulus, E_v through a theoretically-correct relationship in the form of

$$E_v = M_v \frac{(1+\nu)(1-2\nu)}{(1-\nu)} \quad (2.4)$$

where ν is Poisson's ratio.

Portable Seismic Pavement Analyzer

The Portable Seismic Pavement Analyzer (PSPA), as shown in Figure 2.5, is a device designed to determine the average modulus of a concrete or asphalt layer.

The PSPA, shown in Figure 2.5, consists of two receivers (accelerometers) and a source packaged into a hand-portable system, which can perform high frequency seismic tests. The device is operable from a computer. This computer is tethered to the hand-carried transducer unit through a cable that carries power to the transducers and hammer and returns the measured signal to the data acquisition board in the computer.

The operating principle of the PSPA is based on generating and detecting stress waves in a medium. The Ultrasonic Surface Wave (USW) method, which is an offshoot of the SASW method (Nazarian et al., 1997), can be used to determine the modulus of the material. The major distinction between these two methods is that in the USW method the modulus of the top pavement layer can be directly determined without an inversion algorithm.

To collect data with a PSPA, the technician initiates the testing sequence through the computer. The high-frequency source is activated four to six times. The outputs of the two receivers from the last three impacts are saved and averaged (stacked). The other (pre-recording) impacts are used to adjust the gains of the amplifiers. The gains are set in a manner that optimizes the dynamic range.

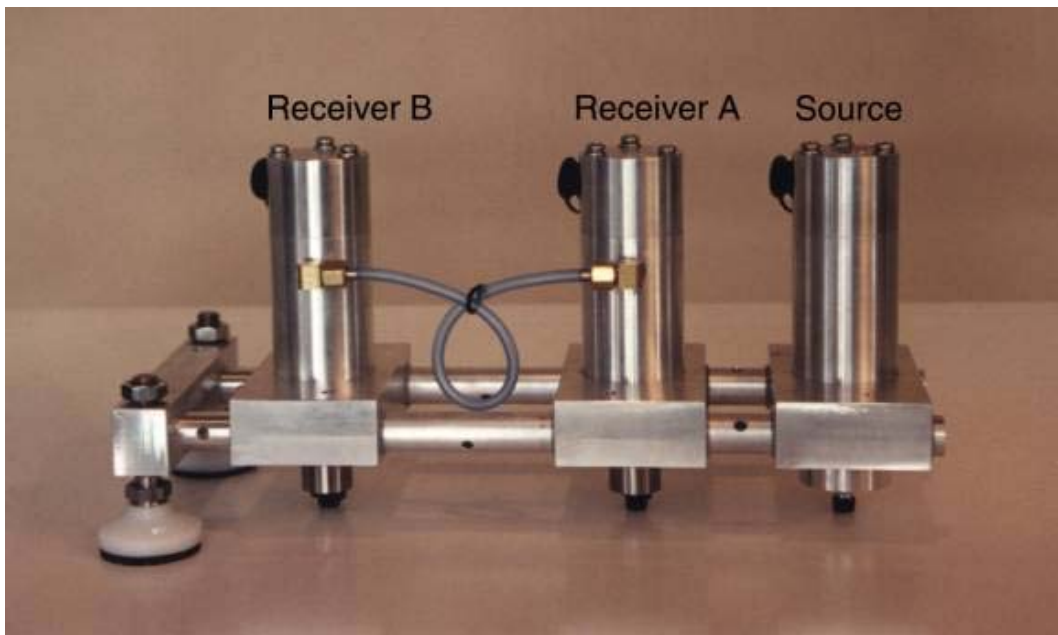


Figure 2.5 – Portable Seismic Pavement Analyzer

Typical voltage outputs of the two accelerometers are shown in Figure 2.6. To ensure that an adequate signal-to-noise ratio is achieved in all channels, signals are normalized to the maximum amplitude of one. In this manner, the main features of the signals can be easily inspected.

The relationship amongst velocity, V , traveltime Δt , and receiver spacing, ΔX , can be written in the following form:

$$V = \frac{\Delta X}{\Delta t} \quad (2.5)$$

In the equation, V can be the propagation velocity of any of the three waves [i.e. compression wave, V_P ; shear wave, V_S ; or surface (Rayleigh) wave, V_R]. Knowing wave velocity, the modulus can be determined in several ways. Young's modulus, E , can be determined from shear modulus, G , through the Poisson's ratio, ν , using:

$$E = 2(1 + \nu)G \quad (2.6)$$

Shear modulus can be determined from shear wave velocity, V_S , using:

$$G = \rho V_s^2 \quad (2.7)$$

To obtain the modulus from surface wave velocity, V_R is first converted to shear wave velocity using

$$V_S = V_R (1.13 - 0.16\nu) \quad (2.8)$$

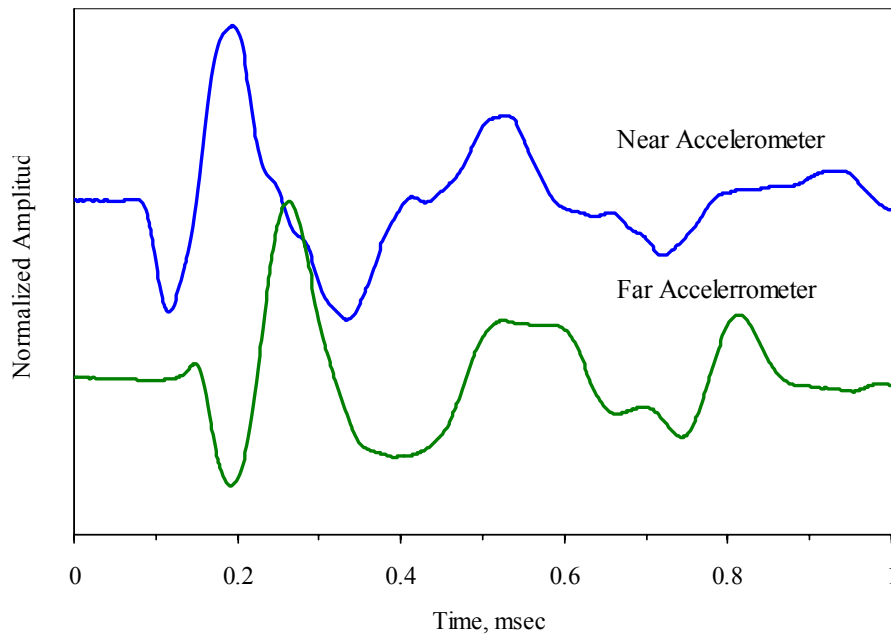


Figure 2.6 – Typical Time Records from PSPA

The shear modulus is then determined by using Equation 2.7. Surface waves (or Rayleigh, R-wave) contain most of the seismic energy in this case. As such, the most dominant arrivals are related to the surface waves making it easy to measure. The Ultrasonic Surface Wave (USW) method is an offshoot of the SASW method (Nazarian et al., 1997).

As sketched in Figure 2.7, at wavelengths less than or equal to the thickness of the uppermost layer, the velocity of propagation is independent of wavelength. Therefore, if one simply generates high-frequency (short-wavelength) waves and if one assumes that the properties of the uppermost layer are uniform, the shear wave velocity of the upper layer, V_s , can be calculated from Equation 2.8.

The modulus of the top layer, E , can be determined from

$$E = 2 \rho V_s^2 (1 + \nu). \quad (2.9)$$

where V_{ph} = velocity of surface waves, ρ = mass density, and ν = Poisson's ratio.

The PSPA has been modified so that it can be functional on base materials as well as prepared subgrade. This version of PSPA, which is affectionately called the Dirt SPA, DSPA, only differs in the source and some electronic components. The source is equipped with a conical shape hammer so that it can provide intimate contact with the soil, and the electronic components are optimized for the response of the granular materials.

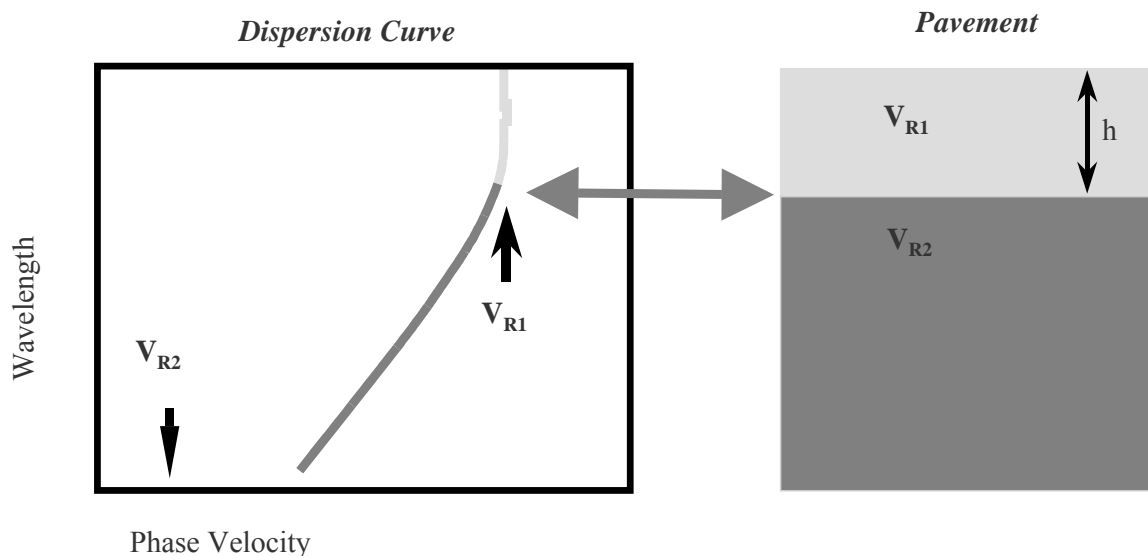


Figure 2.7 – Schematic of USW Method

Chapter 3

Design Modulus from Seismic Modulus

Moduli obtained with seismic measurements are low-strain high-strain-rate values. Vehicular traffic causes high strain deformation at low strain rates. One of the main concerns of the pavement community throughout the years has been how seismic moduli can be used in the design. It is of utmost importance to address this question before further discussion in the methodology is carried out. Project 0-1780 is focused on this subject. Because of the interdependence of this and Project 0-1780, a brief discussion of the design process is included here.

Under the AASHTO 2002 program, a concentrated national effort is on the way to develop and implement mechanistic pavement design in all states. In that study, as well as a number of other ones, the base and subgrade layers are considered to behave nonlinearly under the loads applied to it. For the AC layer, the viscoelastic and temperature-dependent variation in the stiffness parameters of the AC layer should be considered in the design.

In AASHTO 2002 design guide as well as many other mechanistic-empirical approaches, one of many analytical or numerical models with different levels of sophistication can be used in pavement design. With these models, the remaining lives of the pavement are estimated from the critical stresses, strains and deformations within a pavement structure. The focal point of all these models is the moduli of different layers.

The linear elastic model is rather simple since the modulus is considered as a constant value independent of the state of stress applied to the pavement. As such, the modulus of each layer does not change with the variation in load applied to a pavement. Most current algorithms used in pavement analysis and design take advantage of this type of solution. The advantage of these models is that they can rapidly yield results. Their main limitation is that the results are rather approximate if the loads are large enough for the material to exhibit a nonlinear behavior.

The nonlinear constitutive model adopted by most agencies and institutions can be generalized as

$$E = k_1 \sigma_c^{k_2} \sigma_d^{k_3} \quad (3.1)$$

where k_1 , k_2 and k_3 are coefficients preferably determined from laboratory resilient modulus tests. In the absence of the resilient modulus tests, several empirical relationships exist that can be used. In Equation 3.1, the modulus at a given point within the pavement structure is related to the state of stress. The advantage of this type of models is that it is universally applicable to fine-grained and coarse-grained base and subgrade materials.

Barksdale et al. (1997) have summarized a number of variations to this equation. Using principles of mechanics, all those relationships can be converted to the other with ease. The so-called two-parameter models advocated by the AASHTO 1993 design guide can be derived from Equation 3.1 by assigning a value of zero to k_2 (for fine-grained materials) or k_3 (for coarse-grained materials).

For seismic testing, the nonlinear material model for base and subgrade, based on Equation 3.1 is in the form of:

$$E_{\text{design}} = E_{\text{seis}} \left(\frac{\sigma_{c_ult}}{\sigma_{c_init}} \right)^{k_2} \left(\frac{\sigma_{d_ult}}{\sigma_{d_init}} \right)^{k_3} \quad (3.2)$$

where E_{design} and E_{seis} are the design modulus and seismic modulus, respectively. Parameters σ_c and σ_d are the confining pressure and deviatoric stress at the representative depth, respectively. Subscripts “ult” and “init” correspond to the condition when the maximum truckload is applied to the pavement and the free-field condition, respectively. The derivation of this equation can be found in Ke et al. (2001). The significance of Equation 3.2 is that the seismic modulus is an independent measurement that is fundamentally related to the linear-elastic modulus of a material. Currently, this is the only method that can provide such an independent parameter.

Inspecting either Equation 3.1 or 3.2, if one assumes that the base or subgrade layer behave nonlinearly, the design modulus for the layer changes with the thickness and seismic modulus of the layer. As such, the structural model and the input modulus values should be considered together. The practical implication of this matter is best shown through an example. Let us consider a typical pavement in Texas. The asphalt layer is considered as 3 in. (75 mm) thick with a modulus of 500 ksi (3.5 GPa). For simplicity, let us assume that the subgrade is a linear-elastic material with a modulus of 10 ksi (70 MPa). The base is assumed to be nonlinear according to Equation 3.1 with k_1 , k_2 and k_3 values of 7 ksi (49 MPa), 0.4 and -0.1, respectively. The base thickness of 8 in. (200 mm) is assumed. This pavement section is subjected to an 18-kip (40 kN) wheel load. If the thickness of the base is varied between 4 in. (100 mm) and 12 in. (300 mm), the variation in base modulus with depth varies as shown in Figure 3.1 in a normalized fashion. In all three cases, the moduli are not constant and decrease with depth within the base. As the thickness of the base increases, the contrast between the top and bottom modulus becomes more evident. In the existing design programs used by TxDOT, a representative value has to be considered for this layer so that the critical strains in the pavement profile can be determined. In most damage models, the tensile strain at the bottom of the AC layer and compressive strain on top of the subgrade are considered as critical. It is intuitive that if the average modulus, corresponding say to the middle of the base layer is considered the estimated critical strains may be in error.

Program SMART (Seismic Modulus Analysis and Reduction Tool) developed under project 0-1780 will allow the user to combine the seismic modulus with the nonlinear parameters of the layers to

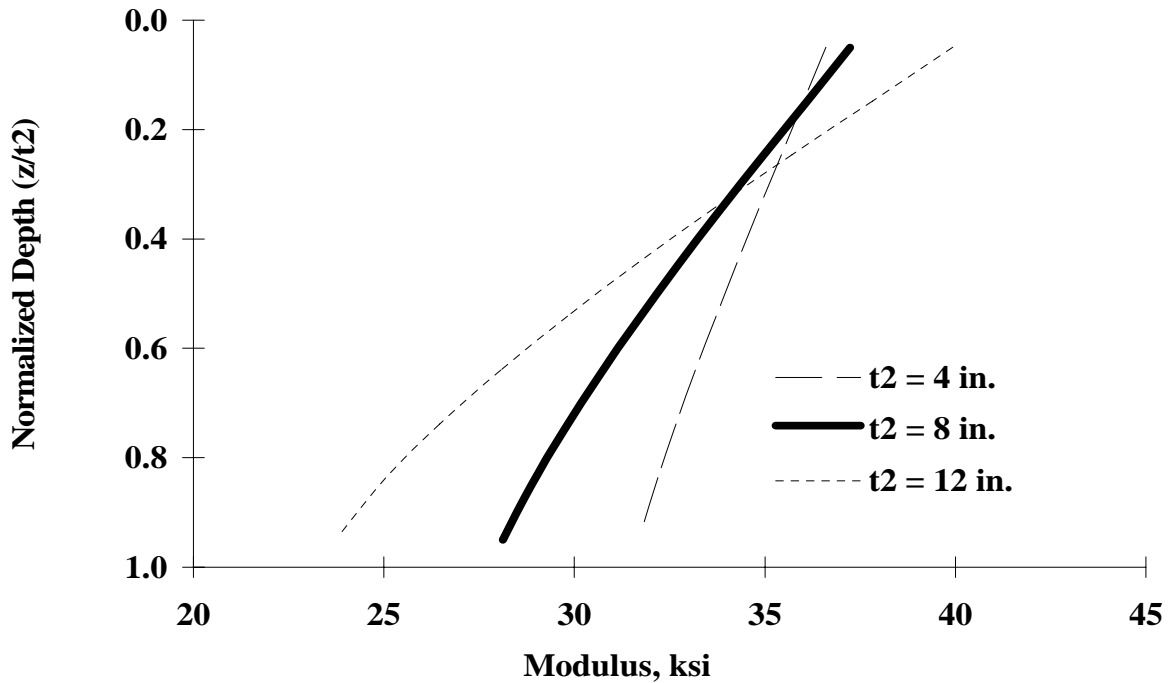


Figure 3.1 – Impact of Layer Thickness on Variation in Modulus within Base layer

obtain the structure-dependent nonlinear modulus. In SMART an iterative process is employed. To implement the algorithm, nonlinear layers are divided into several sublayers. One stress point is chosen for each nonlinear sub-layer. An initial modulus is assigned to each stress point. The stresses and strains are calculated for all stress points using a multi-layer elastic computer program. The confining pressure and deviatoric stress can then be calculated for each stress point. A new modulus can then be obtained from Equation 3.2. The assumed modulus and the newly calculated modulus at each stress point are compared. If the difference is larger than a pre-assigned tolerance, the process will be repeated using the updated moduli. The above procedure is repeated until the modulus difference is within the tolerance and, thus, convergence is reached. Finally, the required stresses and strains are computed using final moduli for all nonlinear sub-layers. The limitations and advantages of this procedure are described in detail in Abdallah et al. (2003).

Program SMART also uses the master curve concept incorporated in AASHTO 2002 Design Guide. For the AC layer, the most desirable way of calculating the design modulus is to develop the master curve based on the recommendations of Witczak et al. (1999). The response of a viscoelastic material, such as AC, is dependent on the loading frequency and temperature. A typical distribution of dynamic modulus with frequency and temperature of an asphalt concrete mixture is shown in Figure 3.2. The general practice has been that the testing is performed at various temperatures at similar loading frequencies and a master curve is generated at a reference temperature by using time-temperature shift factors. The master curve is then developed based on the assumption that asphalt concrete is a thermo-rheologically simple material. The results presented in Figure 3.2 are shifted horizontally to develop a master curve. A sigmoid function proposed by Ferry (1970) can be used to generate a master curve. The sigmoid function is

$$\log(E^*) = \delta + \frac{\alpha}{1 + e^{\beta + \gamma \times \log t_r}} \quad (3.3)$$

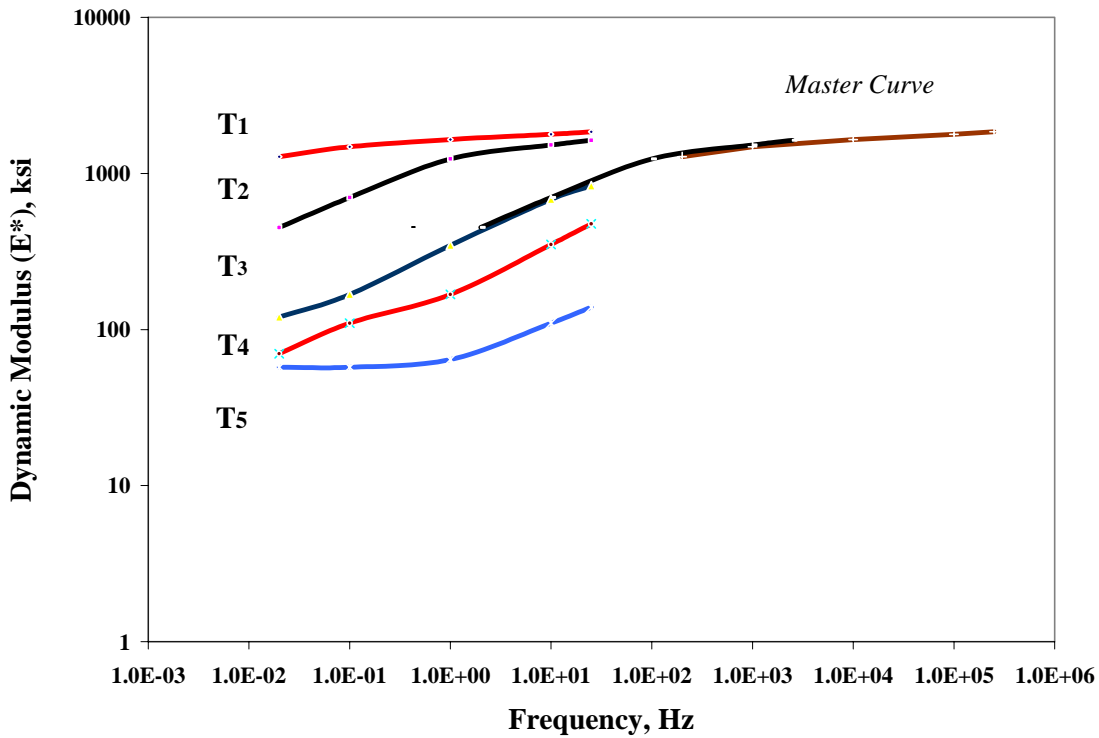


Figure 3.2 – Master Curve Concept

where E^* = dynamic modulus, T_r = loading period, δ = Minimum value of dynamic modulus, $\delta + \alpha$ = Maximum value of dynamic modulus and β, γ = sigmoidal function shape parameter. Once the master curve is established, the design modulus can be readily determined from the design vehicular speed and the design temperature as recommended in the AASHTO 2002 Design Guide.

Saeed and Hall (2001), based on tests on a half a dozen specimens, have shown that the seismic modulus and the master curve from complex modulus correlate well. An example from one site is shown in Figure 3.3. Typical results from one material when the seismic and dynamic moduli are combined are shown in Figure 3.4. The process of defining the design modulus is marked on the figure as well. First, a reference temperature is defined for the regional. A design frequency is then determined based upon the vehicular speed. The desired design modulus based on these two input parameters can be readily defined.

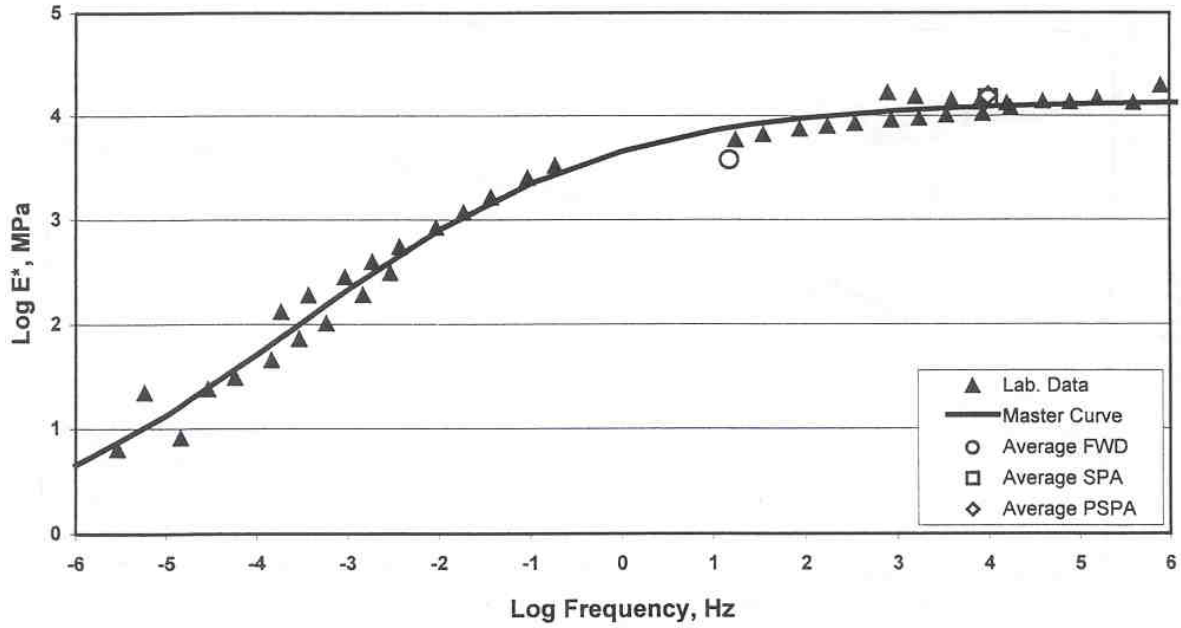


Figure 3.3 – Master Curve from Complex Modulus Compared with Moduli measured from Different NDT Tests

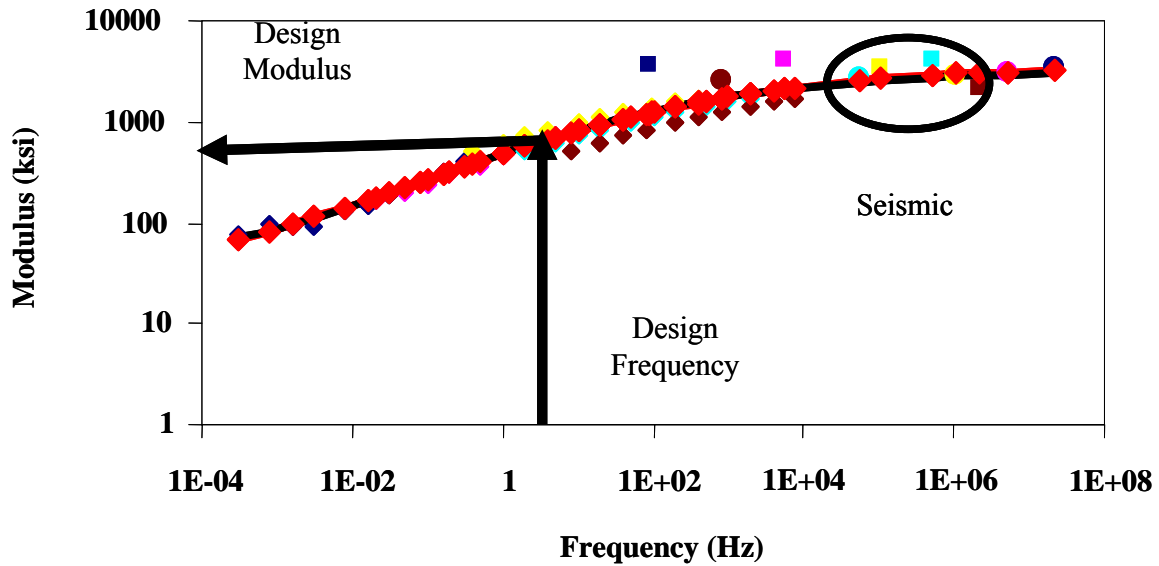


Figure 3.4 – Master Curve Concept for Defining Seismic Modulus

Chapter 4

Overall Protocol

The current state of quality assurance-quality control (QA/QC) practice in construction of transportation and infrastructure projects is mostly concerned with the constructability and durability of the materials rather than parameters specified for design. To make sure that the specified design parameters are met in the field, the QA/QC procedure has to incorporate several inter-related items. First, the major parameters considered in this process should be related to the parameters used in the design. Pre-construction laboratory tests for determining the suitability of a material should also be, to a large extent, based on the selected design parameters. In addition, the acceptable values for the selected parameters should be based on the same laboratory tests. Finally, the quality control during construction has to ensure that the acceptable levels are achieved.

Base materials used in the construction of pavements are good clarifying examples. In most design procedures, the modulus of the base is used to determine the layer thickness. However, most state highway agencies (SHAs) do not measure modulus of the placed based material. Instead, the selection of the base material depends on adequate gradation, plasticity, and nature of coarse aggregates. These parameters have shown to be valuable in ensuring a durable layer. However, they cannot ensure that the design modulus is achieved. The acceptable construction characteristics to be controlled in the field are based on obtaining the densest state possible identified in the laboratory for that material. Although it is desirable to conduct laboratory tests on specimens to determine the design modulus, most highway agencies assign a presumptive value to this parameter since laboratory tests are time-consuming. The densest state of the material may not provide the adequate modulus assumed by the designer. Finally, the adequacy of density is measured in the field without any consideration to the achievement of adequate modulus. As long as such disconnect among the design process, laboratory testing and field quality control exists, the implementation of a performance-based specifications or warranty-based construction will be difficult. To achieve these goals, the current practice has to be supplemented by methods that will provide continuity between the design, laboratory and construction.

The goal in any construction project is to produce a durable material that will perform satisfactorily throughout its expected design life. Aside from environmental factors, the primary parameters that affect the performance of a compacted layer are the modulus and/or strength of that layer. Based on this discussion, the goal of performance-based quality management is to ensure that the moduli or strengths throughout the project are similar to the design values within a specific tolerance. As such, the quality is defined as meeting a structural-related target variable with a minimal variance.

Quality Control Steps

The proposed QA/QC procedure consists of several steps. The first step consists of selecting the most suitable material or mix for a given project. The second step is dedicated to determining the variation in modulus with the primary parameter of interest and determining the desired modulus. For base and subgrade materials, this step consists of developing a moisture-modulus curve (similar to moisture-density curve). For AC materials, this step consists of developing voids in total mix (VTM)-modulus curve. In the third step, the variation in modulus with environmental factors is considered. For example, the variation in modulus with moisture of a base layer can be determined in the laboratory. In the case of AC, the variation in modulus with temperature is important. The fourth step consists of determining the desirable modulus for the material. The final step is to compare the field modulus with the acceptable laboratory modulus. Each step is described below.

Step 1: Selecting Most Suitable Material

For the last century, the focus of the highway agencies has been towards developing the most durable pavement layers. For the most part, the characteristics of a durable material for a given layer depend on the collective experience of a large and diverse group of scientists and practitioners. For example, Item 247 in TxDOT specification clearly defines how to obtain a durable material. Parameters such as angularity of the aggregates, the hardness of aggregates, percent allowable fines, allowable plasticity and degree and method of compaction impact the modulus and strength of a base layer. However, the selection of acceptable levels for these parameters is for the most part experienced based. Very little effort has been focused to routinely define the impact of these parameters on the modulus of the layer.

Similar procedures are also followed for the AC layers. The volumetric design, from the simplest form (Marshall Method) to the most sophisticated one (SHRP Method) ensures a constructible and durable material. Despite the recent recommendations by SHRP and academic circles, the desirable modulus of the material is not defined during or after mix design. Wheel tracking tests can provide an experimental way of ensuring durability but they do not provide any insight into the parameters that the designer requires for estimating the adequate thickness to ensure performance.

Based on this discussion, durability and performance go hand in hand. The material selection and mix design should be based on know-how acquired by the highway community. However, the design should be carried out based on the measured modulus of the material.

Step 2: Selecting Most Suitable Modulus

After the material is selected and its constructability is ascertained, the next step is to determine the most feasible modulus for the given material. To do so, the modulus has to be related to one of the primary construction parameters. For example, for base materials the modulus can be related to moisture content. For AC materials, the modulus can be related to the compaction effort (i.e. VTM).

To develop the moisture density curve, several specimens with different moisture contents are prepared using the same compaction energy. The same specimens can be used for determining the modulus with the free-free resonant column device. Similar to the moisture-density curve, the moisture-modulus curve is developed. In this way, the moisture content at which the maximum seismic modulus is obtained can be determined. Alternatively, the seismic modulus at the traditional optimum moisture content can be estimated.

As an example, the moisture modulus curve for a typical base is shown in Figure 4.1. The optimum moisture content of the material is about 6.5%. The maximum seismic modulus occurs at a moisture content closer to 6%. As such, the maximum modulus may occur at a lower moisture content than at the optimum moisture content determined by the Proctor method.

The variation in modulus with VTM for one AC mixture is shown in Figure 4.2. A linear trend can be observed between the modulus and the VTM. As the VTM increases, the modulus decreases.

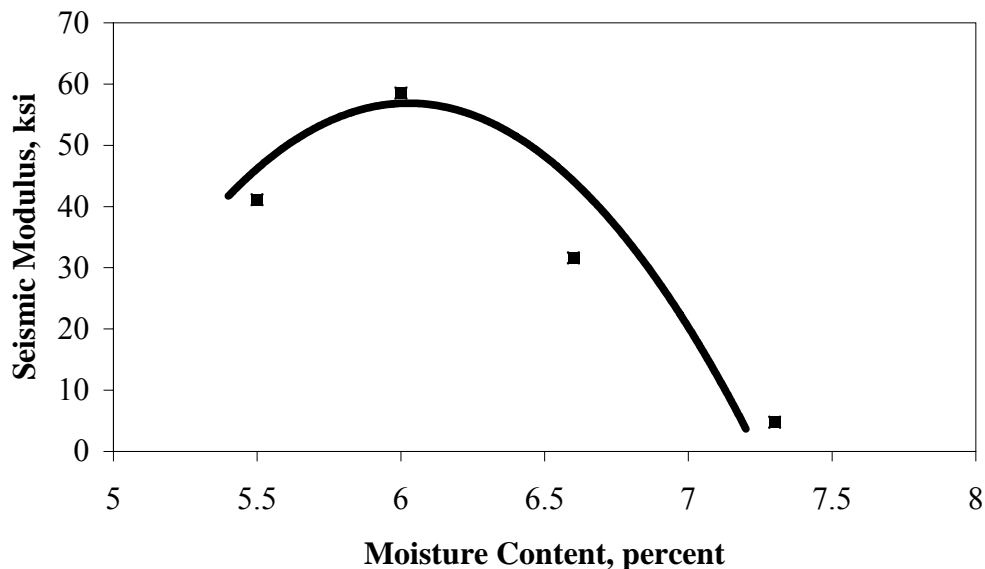


Figure 4.1 – Variation in Modulus with Moisture under Constant Compaction Effort

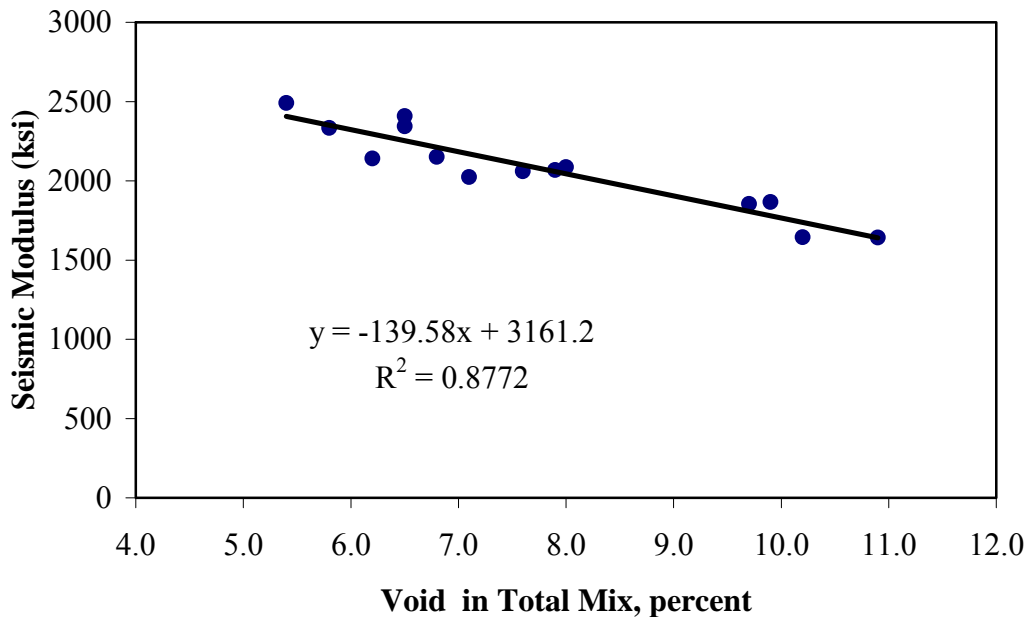


Figure 4.2 – Variation in Modulus with Voids in Total Mix

Step 3: Simulating Seasonal Variation in Modulus

After the compaction of a layer is completed, it may be exposed to environmental factors that could impact its behavior. One of the major input parameters in many pavement design procedures for most base and subgrade materials is the seasonal variation in modulus with exposure to moisture. In terms of performance, the water retention potentials of some materials have shown to have detrimental impact on the strength and stiffness parameters and, as such, their performance (Saarnketo and Scullion, 1997). For the AC pavement, the primary parameter is the variation in modulus with temperature. The new mechanistic design procedures, such as the AASHTO 2002 Design Guide, require this input.

To address this concern for base and subgrade materials, a specimen is prepared at the optimum moisture content and placed in an oven normally used for moisture content specimens and dried until all the moisture is removed. The specimen is weighed, and the FFRC test is performed on it daily. Since the test is nondestructive, the same specimen can be used repeatedly. When the moisture content approaches to zero, the specimen is placed on a saturated porous stone in a pan filled with water. The gain in weight of the specimen and the change in modulus with time are then monitored until the moisture content is about the optimum moisture content. By inspecting the change in modulus with moisture content, the behavior of the material can be judged. For a more comprehensive analysis, these tests can be combined with the tube suction test advocated by Saarnketo and Scullion (1997).

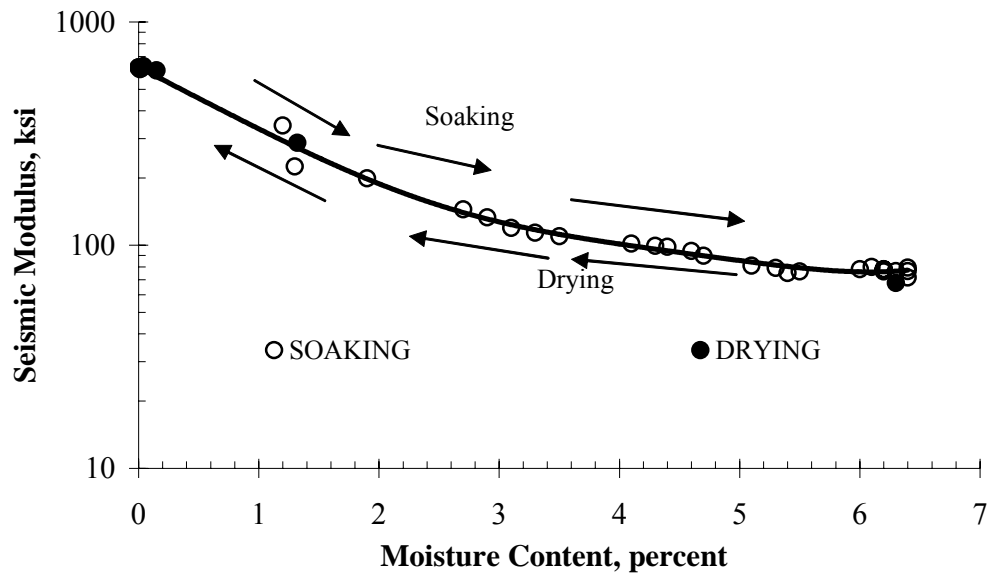


Figure 4.3 – Variation in Modulus with Moisture during Drying and Soak Tests

The variation in modulus with moisture for the same base material shown in Figure 4.1 is shown in Figure 4.3. A significant difference (about an order of magnitude) in modulus can be detected.

The drying cycle can be potentially associated with the change in the properties of the exposed soil during hot summer days after the completion of compaction. The soaking cycle can be related to the occasional rainstorms experienced by the soil. To incorporate the annual seasonal variation in modulus in the pavement design in a more systematic way, this modulus-moisture curve could potentially be used. For structural pavement management during the life of the pavement, the moisture content of the material in the field can be measured and considered in the analysis during the periodic pavement evaluation.

For the AC layer, the simplest way of relating modulus to temperature consists of preparing a specimen at the job mix formula and subjecting it to a sequence of temperatures suitable for the region being considered. At the end of each temperature sequence, the specimen is then tested. An example for the variations in modulus with temperature at a 4% and an 8% VTM for one mixture are shown in Figure 4.4. In both cases, the modulus decreases with an increase in temperature.

A more comprehensive procedure consists of developing a master curve from the complex modulus tests and seismic tests performed on the same specimen. This matter was discussed in Chapter 3.

Step 4: Determining Desirable Modulus of Material

For the base and subgrade layers, knowing the moisture-density curve and moisture-modulus curve, one can then make a decision on the desirable modulus for the material. If the main concern is to achieve the maximum stiffness, the moisture content at which maximum modulus is achieved should be used. The downside of this selection is that the compacted material will be brittle and may be too permeable. On the other hand, if the moisture content is somewhat above the optimum, the modulus may decrease but the permeability of the material and the potential for cracking also decreases. Different base materials exhibit different levels in the reduction in modulus with increase in moisture content. For some materials, the reduction is dramatic (as much as a factor of four reduction in modulus when moisture is about 2% above optimum). For some other materials, the reduction in modulus may be as low as a factor of 1.5. In short, depending on the goals of the project, the engineer has to decide on the most desirable moisture content to use. For the AC layer, the modulus can be based on the modulus VTM curve. After deciding on the degree of compaction at placement, the desired modulus is determined.

When the decision on the desirable modulus for the selected moisture content (for base and subgrade) and VTM (for AC layer) is made, the seismic modulus should be translated to a design modulus. This step is necessary because seismic moduli are low-strain, high-strain-rate values; whereas the design moduli are based on high-strain, low-strain-rate values.

For the base and subgrade materials, the state of stress under representative loads should be determined in order to calculate the design modulus. A summary of the approach was described in Chapter 3. It is important to emphasize that the design modulus is dependent on the thickness

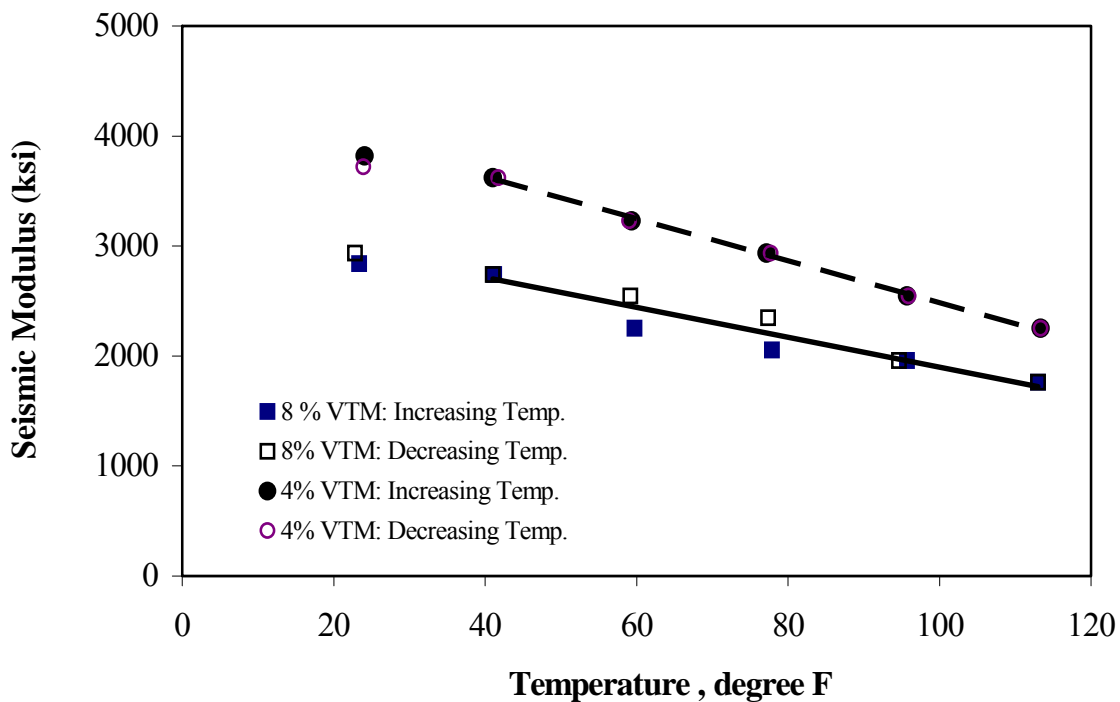


Figure 4.4 – Variation in AC Modulus with Temperature

of the structure and the nonlinear behavior of each layer. For example if 12 in. (300 mm) of the base material shown in Figure 4.1, is overlain with 3 in. (75 mm) of a typical AC, over a typical Texas subgrade with a modulus of 10 ksi (70 MPa), the representative design modulus for the base will be about 28 ksi (170 MPa) if the moisture content of 6% (moisture content at which maximum modulus is obtained as per Figure 4.1) is specified and will be about 23 ksi if the traditional optimum moisture content of 6.5% is used.

If the modulus assumed by the designer and the one obtained from this analysis are significantly different, either an alternative material should be used, or the layer thickness should be adjusted. In that manner, the design and material selection can be harmonized. One of the attractive attributes of this process is that the feasibility of using thicker, lower quality local materials can be explored.

For the AC layer, the most desirable way of calculating the design modulus is to develop the master curve based on the recommendations of Witczak et al. (1999). Then the design modulus can be readily determined from the design vehicular speed and the design temperature as discussed in Chapter 3.

Step 5: Field Quality Control

Field quality control is then carried out using the portable devices described in Chapter 2. Tests are carried out at regular intervals or at any point that the construction inspector suspects segregation, lack or excess moisture, or any other construction related anomalies. Similar to the statistical-based acceptance criteria used for moisture-density measurements, the field moduli should be greater than the representative seismic modulus (not design modulus) determined in the previous step. It is important to make a distinction between the design modulus reported to the designer and the lab seismic modulus used as a guideline for quality control. As mentioned above, these two are inter-related. However, the design modulus is also a function of the pavement structure and nonlinear properties of the base and subgrade and viscoelastic behavior of AC. As indicated before, a close relationship between the laboratory seismic modulus and field seismic modulus should be anticipated, provided the field moisture and compaction efforts are similar to those obtained in the field.

Results from a base section of a road during construction are shown in Figure 4.5. Each data point is approximately 30 ft apart. On the average, the field seismic moduli are greater than the designated lab modulus. However, at several points, the field values are lower than the designated lab values. These points that passed the density and moisture criteria during the inspection process happened to correspond to a finer than anticipated area. This area can be reworked to achieve the design modulus.

The variation in modulus of the AC layer along a road, adjusted to a temperature of 77°F (25°C), is shown in Figure 4.6. The modulus values were fairly constant, and within the acceptable range of moduli of 1700 ksi (12 GPa) and 2400 ksi (17 GPa), except for an area between 80 ft (27 m) and 100 ft (33 m). This area coincides with the entrance to a business entity where a new drainage pipe was installed. On an average, the modulus of the AC layer was about 2000 ksi (14 GPa) when all points were included and 2100 ksi (15 GPa) when the results from the area

between 80 ft (27 m) and 100 ft (33 m) were ignored. Therefore, the area between the 80 ft (27 m) and 100 ft (33 m) is substandard and should be considered for some type of improvement or penalty.

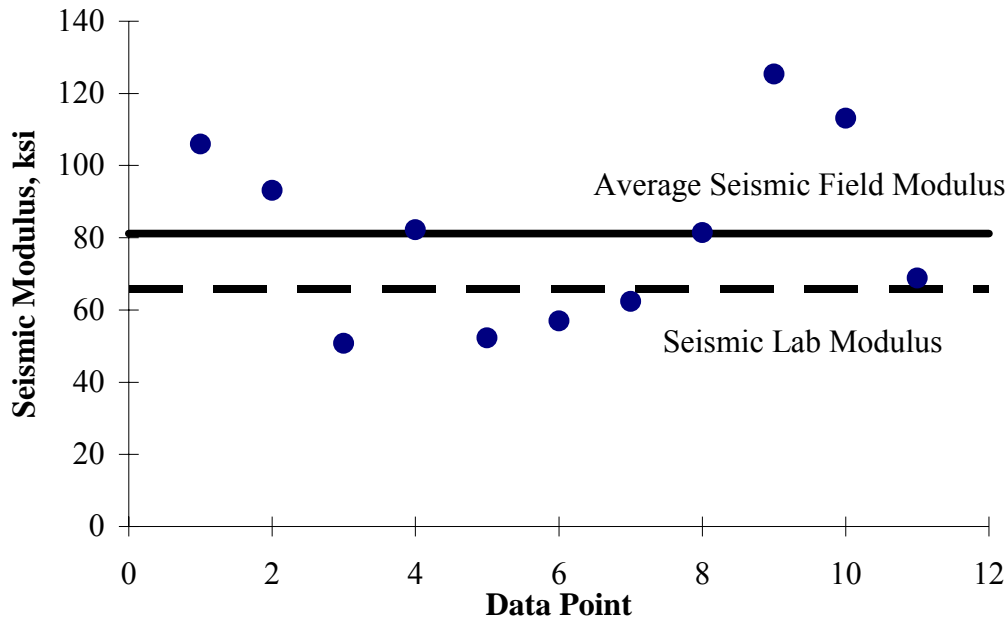


Figure 4.5 – Typical Results from Field Measurement of Base Moduli

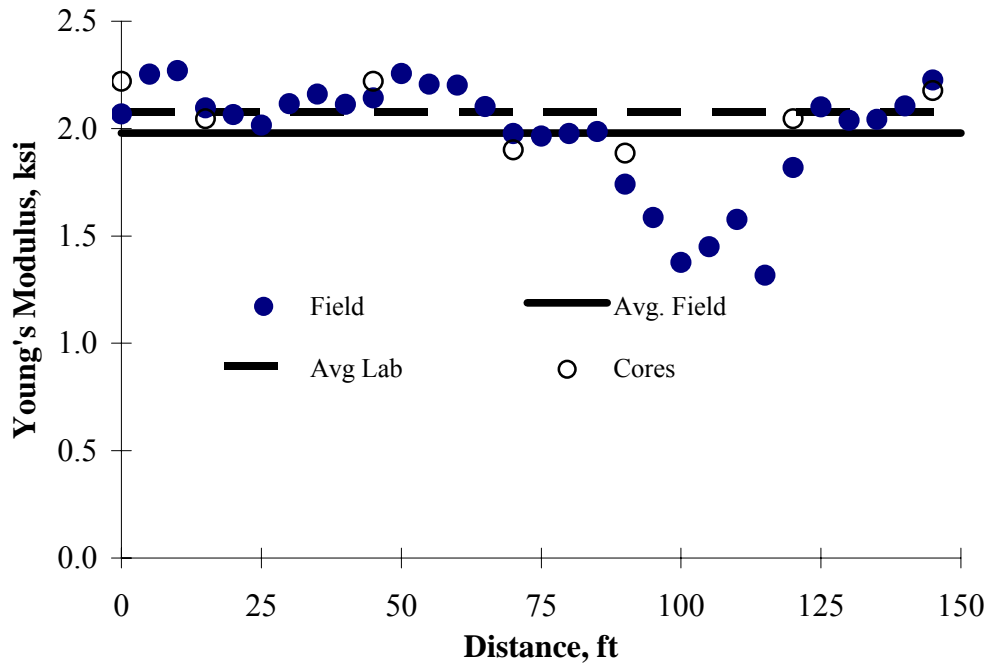


Figure 4.6 – Typical Results from Field Measurement of AC Moduli

Chapter 5

Operational Aspect of Devices

As indicated previously, a device should have certain features to make it practical and easy to implement. First, it should measure fundamental properties of materials (i.e., it should not be an index test). Second, the device should be precise enough so that it can be readily used in the QA/QC process. Third, the measurements should be accurate enough so that they can provide feedback to the designer and the laboratory personnel. In Chapters 2 and 3, the first item was addressed. In this chapter, the matter of precision and accuracy are addressed.

Precision of Devices

The precision of the three devices (PSPA, ultrasonic device and FFRC device), were extensively studied in this project. Since precision of PSPA has been evaluated and reported a number of times before, the focus of this report is to demonstrate precision and accuracy of ultrasonic and free-free resonant column devices.

Ultrasonic Device on Asphalt Concrete Materials

The ultrasonic device has been used for the last thirty years by many organizations. The consensus has been that the device is quite repeatable but not reproducible. In other words, the results are always consistent but the measured values change when a new user tests the same specimens or when the same user repeats the same test at different times. The lack of reproducibility is mostly related to the amount of hold down pressure applied to bond the sensors to the specimen. To minimize this problem, a special stand was designed so that the amount of pressure applied to the specimen is controlled. In addition, synthetic specimens similar in shape and stiffness to the standard briquettes are provided with each device. The operator is strongly encouraged to use these specimens to calibrate her/himself before performing tests on actual specimens. In other words, we calibrate the habits of the operator in addition to calibrating the device.

To demonstrate the level of repeatability in measurements, a series of synthetic specimens of different diameters and lengths were utilized first. Each specimen was tested at several temperatures to observe the impact of temperature on the reproducibility.

The synthetic material used is manufactured by Dupont under the commercial name Delrin[®]. The mechanical properties of the material used in this study as specified by the manufacturer, and the ASTM method used to measure them are summarized in Table 5.1. The stiffness of the material is close to that of typical asphalt concrete, but it exhibits much less viscoelastic behavior. The modulus of the material is temperature dependent, but the dependence on frequency (loading time) is minimal.

Since Superpave gyratory compactors (SGC) can prepare specimens with nominal diameters of either 4 in. (100 mm) or 6 in. (150 mm), all synthetic specimens used here were prepared at these two diameters. To estimate reliable strength or stiffness properties from a cylindrical specimen using compressive shear test, the consensus is that the height of the specimen should be at least twice its diameter. Witczak et al. (1999) have suggested that specimens with height-to-diameter-ratios as low as unity can be successfully used. To validate this hypothesis, the 4-in. (100-mm) diameter specimens were fabricated to the heights of 4 in. (100 mm, H/D = 1), 6 in. (150 mm, H/D = 1.5) and 8 in. (200 mm, H/D = 2). Similarly the 6-in. (150-mm) diameter specimens were fabricated to the heights of 6 in. (150 mm, H/D = 1), 8 in. (200 mm, H/D = 1.3) and 12 in. (300 mm, H/D = 2).

The repeatability of the method was evaluated at nominal temperatures of 14 °F, 40 °F, 60 °F, 73 °F, and 104 °F (-10 °C, 4 °C, 15 °C, 23 °C, and 40 °C). The tests were repeated three times. The average moduli and other relevant statistical information are summarized in Table 5.2. The data sheet provided by the supplier of Delrin[®] did not provide its Poisson's ratio. The seismic data collected on the specimens were analyzed using two different Poisson's ratios. A Poisson's ratio of 0.35 was selected because it is similar to that of a typical AC and a Poisson's ratio of 0.45 because it is similar to that of other synthetic materials similar to Delrin. The test results summarized in Table 5.2 suggest that estimated modulus from the seismic modulus depends on the Poisson's ratio. This matter is even more critical when the Poisson's

Table 5.1 – Physical Properties of Synthetic Material Used in This Study

Mechanical Property	Value	ASTM Standard
Specific gravity	1.42	D 792
Density	89 pcf (14 KN/m ³)	D 792
Tensile Strength	11 ksi (76 MPa)	D 638
Tensile Modulus	450 ksi (3.1 GPa)	D 638
Compressive Strength	16 ksi (110 MPa)	D 785
Compressive Modulus	450 ksi (3.1 GPa)	D 695
Flexural Strength	13 ksi (90 MPa)	D 790

Table 5.2 – Repeatability of Ultrasonic Device in Modulus Measurement as a Function of Diameter and Height of Synthetic Specimens

Specimen Size, in. (mm)		Statistical Parameters	Poisson's Ratio									
D	H		0.35					0.45				
			Test Temperature °F (°C)					Test Temperature °F (°C)				
		14 (-10)	40 (4)	60 (15)	73 (23)	104 (40)	4 (-10)	40 (4)	60 (15)	73 (23)	104 (40)	
4 (100)	4 (100)	Mean, ksi (GPa)	1263 (8.7)	1165 (8.0)	1095 (7.5)	1082 (7.5)	982 (6.8)	544 (3.7)	501 (3.5)	472 (3.2)	466 (3.2)	423 (2.9)
		COV, %	1.21	1.81	1.51	1.23	0.87	1.21	1.81	1.51	1.23	0.87
	6 (150)	Mean, ksi (GPa)	1274 (8.8)	1200 (8.3)	1132 (7.8)	1105 (7.6)	1071 (7.4)	549 (3.8)	517 (3.6)	487 (3.4)	476 (3.3)	461 (3.2)
		COV, %	1.55	1.82	1.50	0.82	0.66	1.55	1.82	1.50	0.82	0.66
	8 (200)	Mean, ksi (GPa)	1256 (8.7)	1188 (8.2)	1122 (7.7)	1099 (7.6)	994 (6.8)	541 (3.7)	512 (3.5)	483 (3.3)	473 (3.3)	428 (2.9)
		COV, %	0.50	0.80	0.83	0.60	0.32	0.50	0.80	0.83	0.60	0.32
6 (150)	6 (150)	Mean, ksi (GPa)	1254 (8.6)	1223 (8.4)	1128 (7.8)	1107 (7.6)	1021 (7.0)	540 (3.7)	526 (3.6)	486 (3.3)	477 (3.3)	439 (3.0)
		COV, %	1.37	0.91	1.29	0.6	0.85	1.37	0.91	1.29	0.6	0.85
	8 (200)	Mean, ksi (GPa)	1243 (8.6)	1215 (8.4)	1137 (7.8)	1113 (7.7)	1013 (7.0)	535 (3.7)	523 (3.6)	490 (3.4)	479 (3.3)	436 (3.0)
		COV, %	2.04	1.80	1.66	0.80	1.28	2.04	1.80	1.66	0.80	1.28
	12 (300)	Mean, ksi (GPa)	1211 (8.3)	1189 (8.2)	1122 (7.7)	1096 (7.5)	1009 (7.0)	521 (3.6)	512 (3.5)	483 (3.3)	472 (3.3)	434 (3.0)
		COV, %	1.57	1.27	1.47	0.81	0.64	1.57	1.27	1.47	0.81	0.64

ratio is close to 0.5. A change of the Poisson's ratio from 0.35 to 0.45, results in a change in the estimated Young's modulus by about a factor of 2. Therefore, it is imperative to measure the Poisson's ratio of the material, or more practically, to calibrate the results from ultrasonic testing with the PSPA.

The test results also suggest that seismic modulus from the ultrasonic device is practically independent of the diameter or the height-to-diameter ratio of the specimen. As reflected in Table 5.2, for a Poisson's ratio of 0.45 at room temperature (73 °F or 23 °C), the modulus of Derlin varied from 466 ksi (3.2 GPa) to 479 ksi (3.3 GPa) for six different specimens with different lengths and diameters.

In the next step, the repeatability was established by testing a number of AC specimens. About 53 cores with different stiffness and thickness from ten different sites were tested. Four operators were selected. Two of them were experienced operators. The third operator was

trained as per the training program put together for TxDOT as part of this project. The last operator was familiar with the test procedure but was only occasionally involved in testing. Each operator tested each specimen four times. The largest coefficient of variation from all specimens and all operators was 6.5% with overwhelming majority of the COVs being less than 2%. To determine the reproducibility, the average travel times recorded on each specimen by the four operators are compared in Figure 5.1. The two experienced operators and the newly-trained operator obtained very similar results, while the occasional user reported numbers that on the average were 3% higher than the experienced user. This demonstrates the value of daily calibration and the importance of periodical training of the users.

Free-free Resonant Column (FFRC) Device (Asphalt Concrete Materials)

The variations in seismic moduli from the FFRC tests as a function of height-to-diameter ratio for the 4-in. (100-mm) and 6-in. (150-mm) diameter specimens are included in Table 5.3. The trends are quite similar for all five temperatures studied. The moduli from the FFRC are practically independent of the diameter of the specimen. However, as expected, measured moduli vary with the height-to-diameter ratio. The FFRC method is based on the propagation and reflection of waves in long solid rods. Typically an H/D ratio of two or greater is recommended for this test. For the two specimens with the H/D ratio of two, the moduli are quite similar since they are usually within 5% of one another (see Figure 5.2). For the H/D ratio of unity, the moduli from FFRC are always smaller than those specimens with H/D ratio of two. For the H/D ratio of 1.3 and 1.5, the moduli are only slightly less than the moduli measured on specimens with H/D ratio of 2. In summary, the FFRC tests are repeatable independent of the diameter of the specimen. Also it seems that the seismic moduli can be reliably measured for specimens with H/D ratio of 1.5 (and perhaps 1.3).

As an emphasis, the moduli measured with the ultrasonic device on the same specimens used for the FFRC tests are also shown in Figure 5.2. In this case, the modulus is independent of both the diameter and the length-to-diameter ratio.

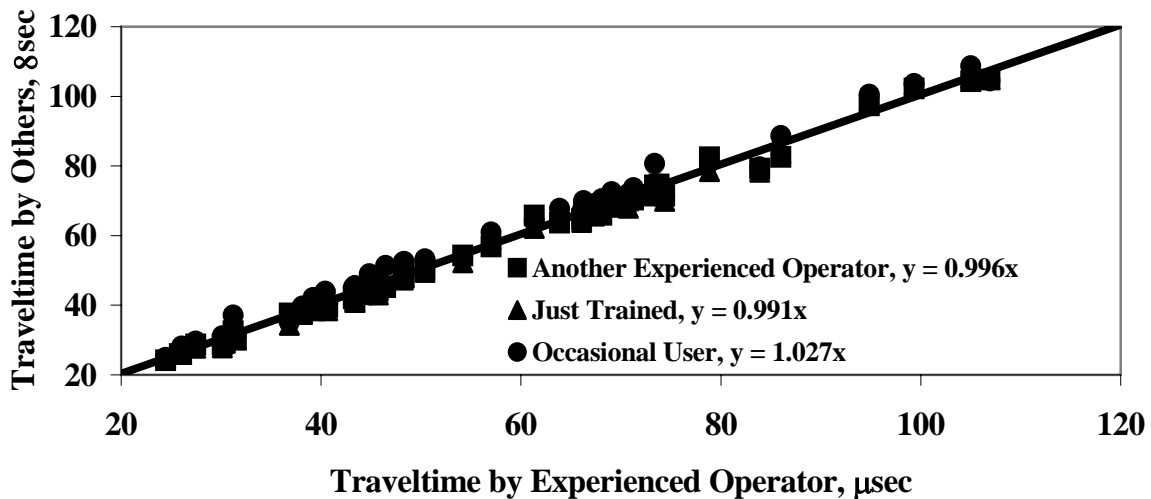


Figure 5.1 – Reproducibility of Ultrasonic Device as Adopted in This Study

Table 5.3 – Repeatability of Free-free Resonant Column Device in Modulus Measurement as a Function of Diameter and Height of Synthetic Specimens

Nominal Specimen Size		Statistical Parameters	Test Temperature °F (°C)				
Diameter	Height		14 (-10)	40 (4)	60 (15)	73 (23)	104 (40)
4 in. (100 mm)	4 in. (100 mm)	Mean, ksi (GPa)	508 (3.50)	462 (3.18)	431 (2.97)	414 (2.85)	334 (2.30)
		COV, %	2.36	1.52	1.39	0.72	1.80
	6 in. (150 mm)	Mean, ksi (GPa)	557 (3.84)	516 (3.56)	489 (3.37)	449 (3.09)	364 (2.51)
		COV, %	1.44	0.97	1.23	0.67	1.10
	8 in. (200 mm)	Mean, ksi (GPa)	571 (3.93)	523 (3.60)	504 (3.47)	478 (3.29)	401 (2.76)
		COV, %	1.53	1.11	0.29	1.22	1.09
6 in. (150 mm)	6 in. (150 mm)	Mean, ksi (GPa)	507 (3.49)	475 (3.27)	452 (3.11)	419 (2.89)	364 (2.51)
		COV, %	0.39	0.63	0.66	0.72	1.10
	8 in. (200 mm)	Mean, ksi (GPa)	557 (3.84)	523 (3.60)	494 (3.40)	464 (3.20)	410 (2.82)
		COV, %	0.54	0.76	1.01	0.65	1.22
	12 in. (300 mm)	Mean, ksi (GPa)	584 (4.02)	544 (3.75)	524 (3.61)	503 (3.47)	415 (2.86)
		COV, %	1.20	1.10	0.76	0.99	1.20

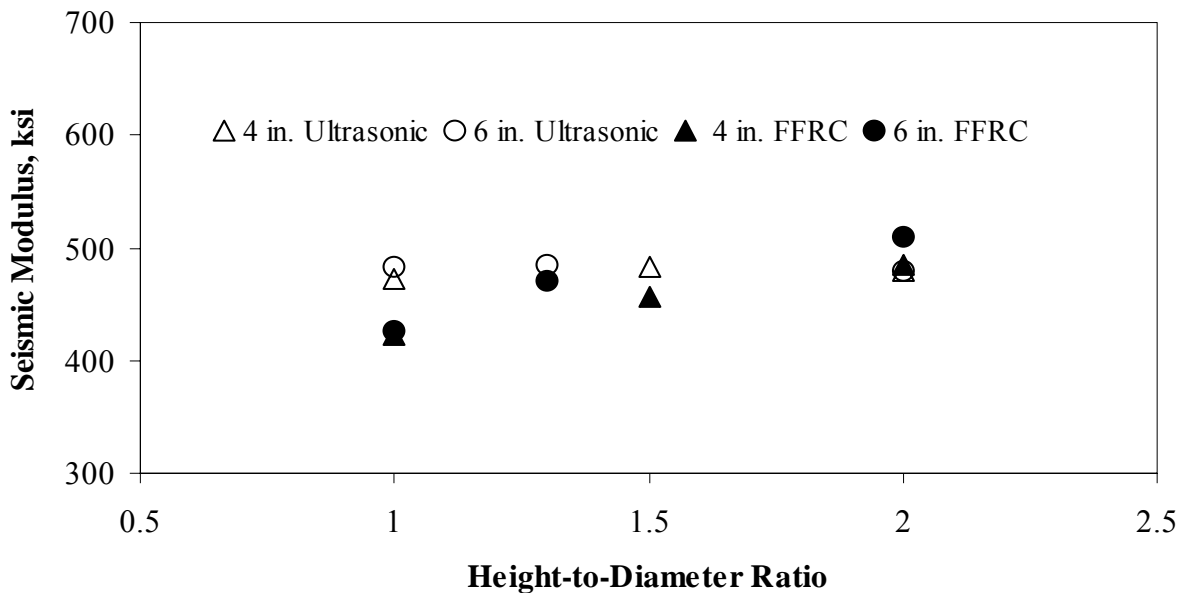


Figure 5.2 – Comparison of Moduli Measured with Ultrasonic and FFRC Devices at a Temperature of 73 °F (23 °C)

Complex Modulus Tests on Asphalt Concrete Materials

It would be appropriate to demonstrate the variation in dynamic modulus from the complex modulus tests of the synthetic specimens with temperature and frequency as well as its interrelationship to seismic modulus. The average dynamic modulus data for each frequency and test temperature measured for a 4 in. (100 mm) by 6 in. (150 mm) specimen is shown in Figure 5.3a. In the figure, the dynamic modulus decreases with an increase in temperature. However, the change in the dynamic modulus with frequency is rather minimal at any given test temperature. This confirms that the materials behavior is affected by temperature and is independent of frequency.

The data were shifted to a reference temperature of 73 ° F (23 °C) based on the assumption that the synthetic specimen is made of a thermo-rheologically simple material. The variation in the shift factor with temperature is shown in Figure 5.3b. A reasonably good linear relationship exists between the two parameters as the coefficient of determination of the best fit line through the data is close to unity.

The variation in dynamic modulus with the so-called reduced frequency (i.e. the master curve) for this material is shown in Figure 5.3c. The moduli vary little with the change in reduced frequency indicating that the material does not exhibit significant viscoelastic behavior.

To determine the feasibility and the impact of incorporating the seismic moduli in the master curve, the same exercise was repeated but this time the seismic moduli from the ultrasonic and FFRC tests were also included in the process. The variations in measured moduli from the complex modulus tests and the two seismic tests with frequency are shown in Figure 5.4a and 5.5a for Poisson's ratio of 0.35 and 0.45, respectively. The results from the complex modulus tests are identical to that shown in Figure 5.3a. The seismic moduli from the ultrasonic device are shown at a frequency of 54 kHz, the central frequency of the transducer. Since the raw data from the FFRC test is a resonant frequency, the moduli measured with that setup are shown at their actual resonant frequency (between 5 kHz and 6 kHz).

The variation in the shift factor with temperature for the combined data is shown in Figure 5.4b and 5.5b. The least-squares best fit regression line through the data, once again yielded a coefficient of determination close to unity. The equations of the shift factor-temperature lines for the case when the seismic moduli were not considered and were considered (Figure 5.3b, Figure 5.4b and 5.5b) suggest that they compare quite closely for Poisson's ratio of 0.45 but differ for Poisson's ratio of 0.35. Therefore, it is essential that the accurate Poisson's ratio of the material be used for field applications. For Poisson's ratio of 0.45, the seismic moduli complement the complex modulus data as shown in Figure 5.5b.

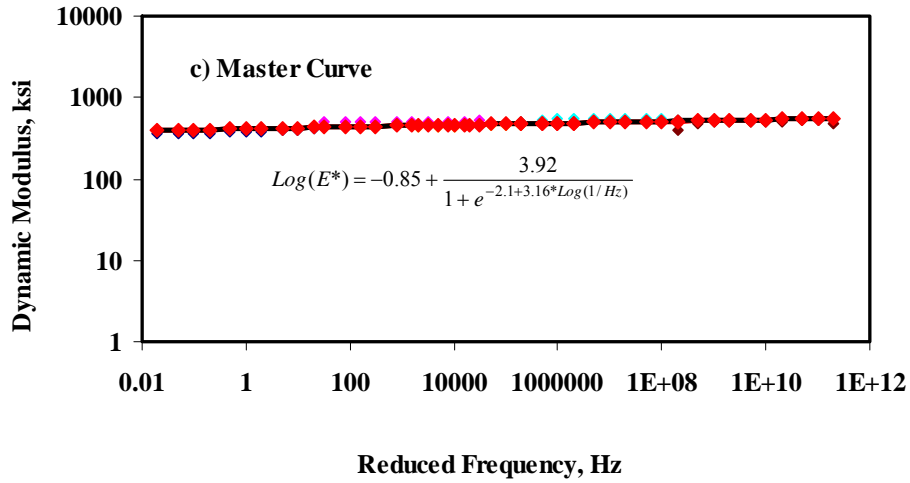
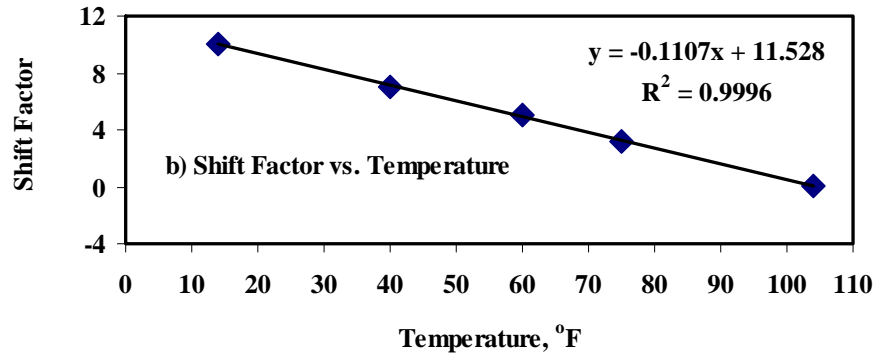
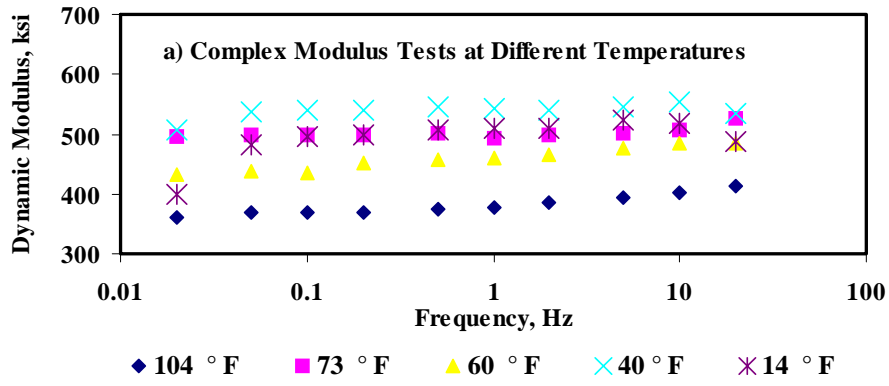


Figure 5.3 – Development of Master Curve from Complex Modulus Test Results

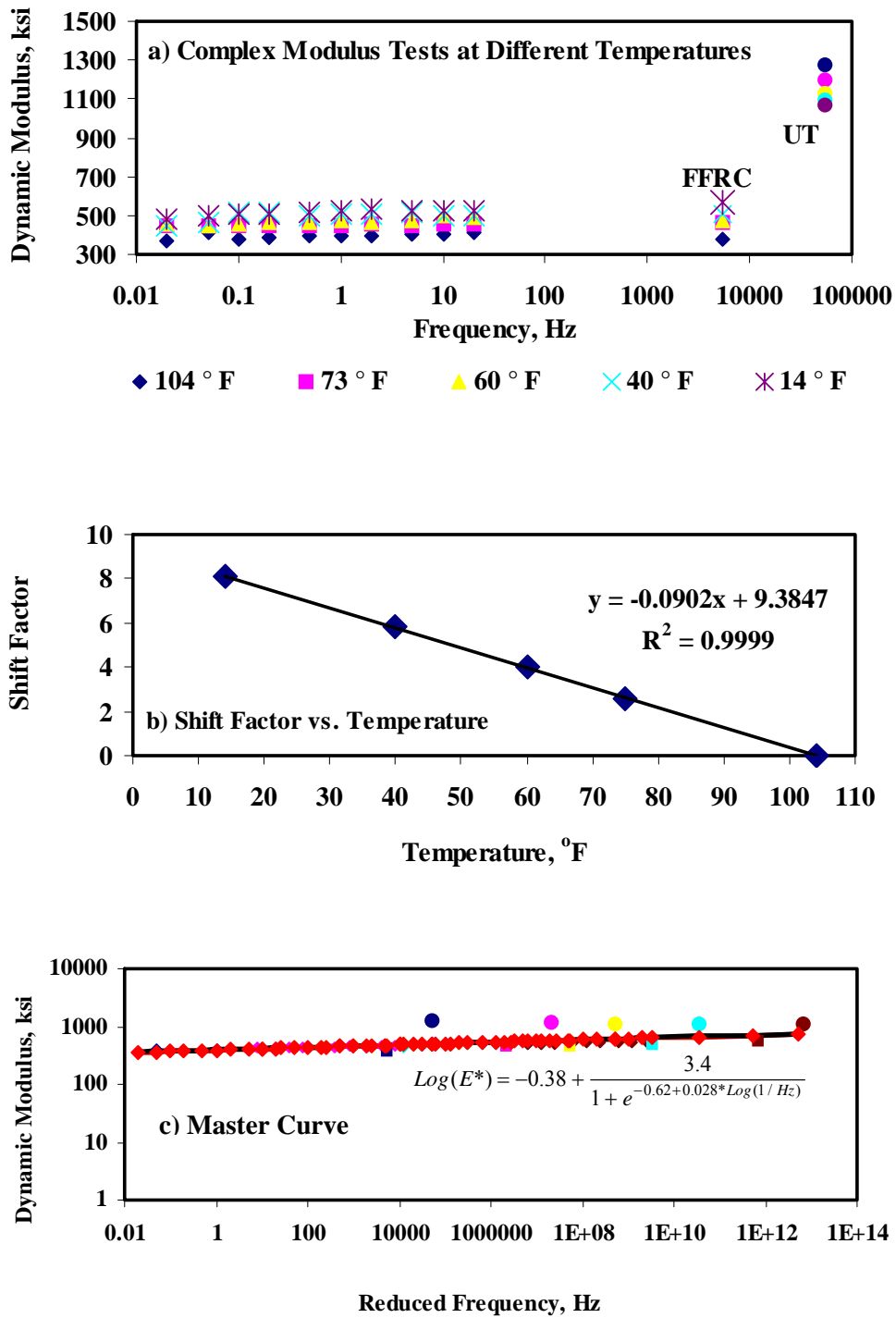


Figure 5.4 – Development of Master Curve from Combined Complex and Seismic Modulus Test Results (with a Poisson's Ratio of 0.35)

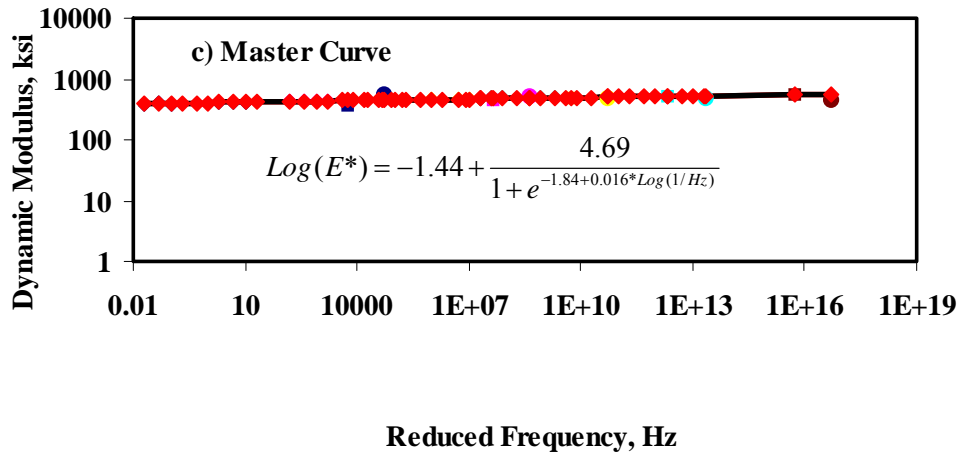
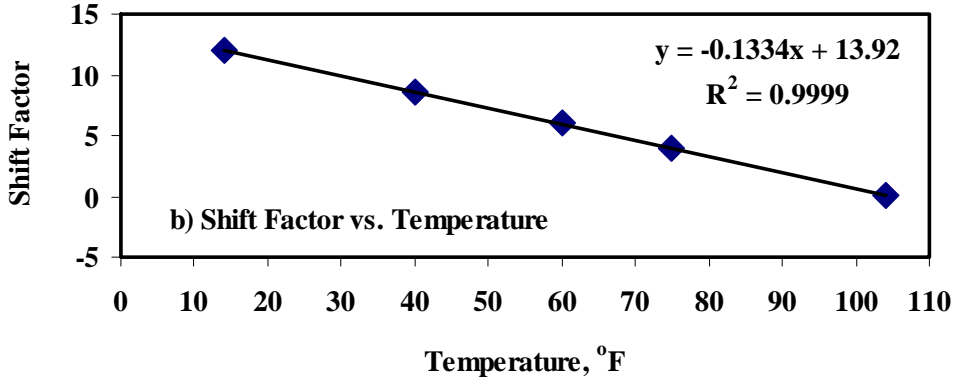
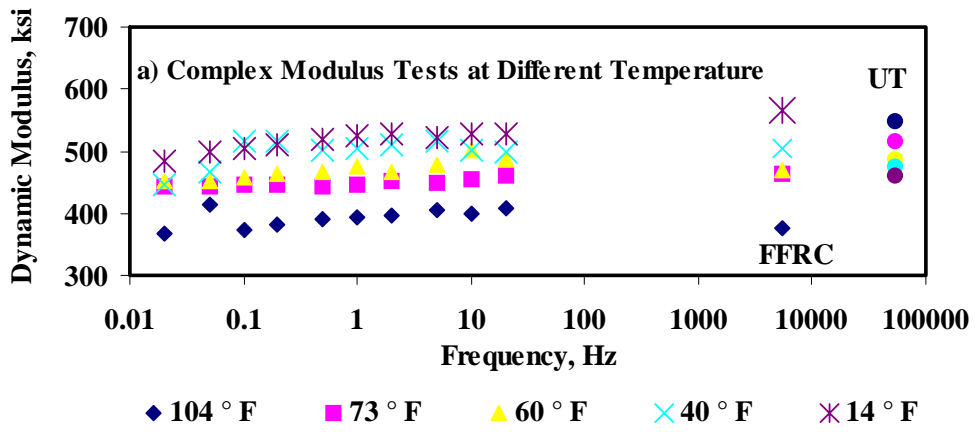


Figure 5.5 – Development of Master Curve from Combined Complex and Seismic Modulus Test Results (with a Poisson's Ratio of 0.45)

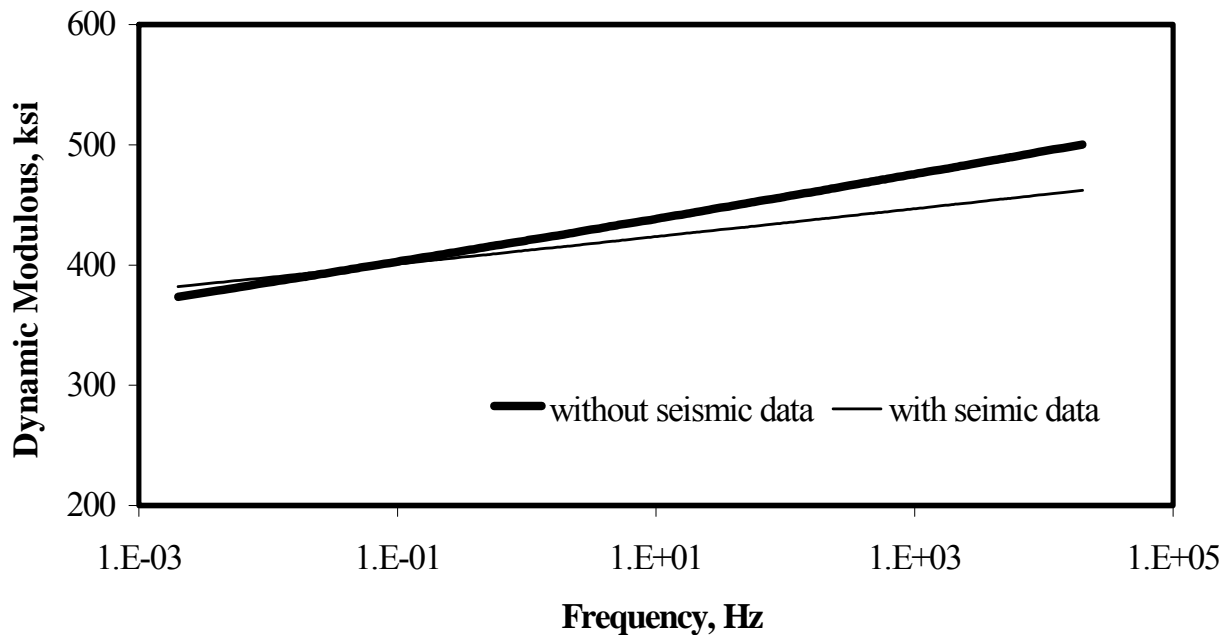


Figure 5.6 – Comparison of Master Curve with and without Seismic Data

The master curves for a reference temperature of 73°F (23°C) from the combined seismic and complex moduli are incorporated in Figure 5.4c and 5.5c. The master curves of Figure 5.3c and 5.5c fit the data quite well and are comparable to each other. However, the master curve of Figure 5.4c shows that the seismic modulus estimated using a Poisson’s ratio of 0.35 does not belong to the master curve.

The sigmoidal fit function proposed in Chapter 3 was used to develop mathematical equations for the master curves. The three equations are included in Figures 5.3c, 5.4c and 5.5c. Although the parameters of the equations are significantly different, the equations generate similar master curves as shown in Figure 5.6. As such, the differences in parameters from the master curve have to do with the nature of the curve fitting and not the fundamental differences in the physical behavior of the material.

Free-free Resonant Column (FFRC) Device (Base and Subgrade Materials)

Alexander (1996) estimated that the repeatability of the method on concrete specimens is better than 2%. But because of the attenuation of signals in softer granular materials, and because of the sensitivity of the modulus to change in moisture and uniformity of compaction, such a level of repeatability cannot be achieved in base and subgrade materials. Even though the resonant frequencies in the seismic tests are not sensitive to the locations of the accelerometer and impact on the specimen ends, the amplitude associated with each resonance varies with these two parameters. Fortunately, the amplitudes are not important at all and only the frequencies at which the peak amplitudes (resonant frequencies) occur are significant. However, it is desirable to propose locations where the results are more robust.

A series of tests were conducted on about eight-dozen specimens to study this phenomenon. As reflected in Figure 5.7, thirty-five possible combinations of impact and receiver (accelerometer) that would produce a primary wave were tried on each specimen. For convenience, the specimens were impacted on top. Thumbtacks were placed in a sideways “T” shape to distinguish the different locations and to provide a platform to hit the specimen. The bottom of the specimen, where the receiver is placed, consists of an “L” shape with location A being across from 1, B from 2, and so on.

Statistically, the majority of the tests configurations yielded repeatable results. The best test setups seem to be when the source is placed near the center of the specimen (within one-third of the radius). The location of the receiver works best when it is placed on the same half of the specimen as the source but not beyond two-thirds radius out from the center. Locations A1, C1, and E1 provide results that are highly repeatable. If only the A1 (center-to-center) test combination is used, there is less of a chance to generate detectable shear energy. Thus, it is recommended to test with the C1 or E1 configuration in addition to A1.

Three materials (a typical base, a sand, and a clay) were used for determining the repeatability of the tests for granular materials. The base specimens were nominally 6 inches in diameter by 12 inches long while the sand and clay specimens were nominally 4 inches by 8 inches. The clay material is a highly-plastic clay from Dallas area, and mainly consisted of materials passing No. 200 sieve. The liquid and plastic limits of that material were 65% and 24%, respectively. The sand is primarily fine and medium sand with some small amount of silt also from the Dallas area. The optimum moisture contents of the two materials were about 18% and 8% for the fine-grained and coarse-grained materials, respectively.

The variation in modulus with moisture for the clay, sand and base materials are shown in Figure 5.8. From Figure 5.8a, the clay exhibits a peak seismic modulus at moisture content of about 13%. For moisture contents wet from the moisture content at which the peak modulus occurs, the modulus decreases with an increase in moisture. Also a sharp drop in modulus for moisture contents less than that of the peak modulus is observed. A relatively large number of specimens were prepared to demonstrate the repeatability and reproducibility of the test method. The goal

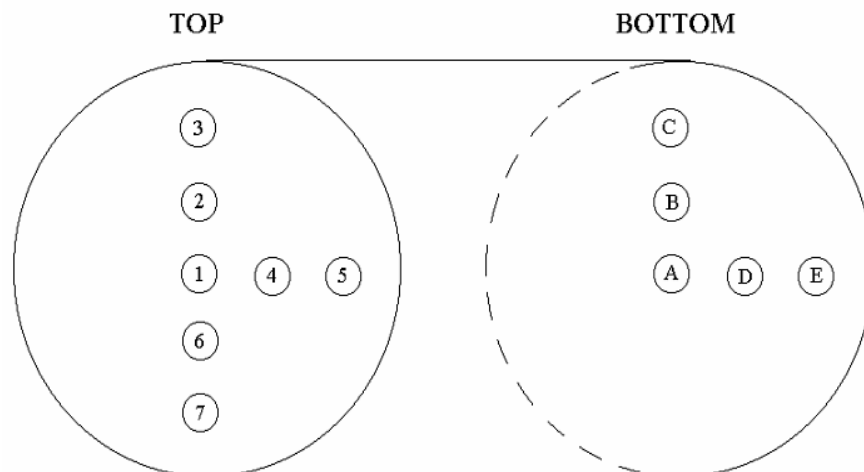


Figure 5.7 – Source and Receiver Locations Studied

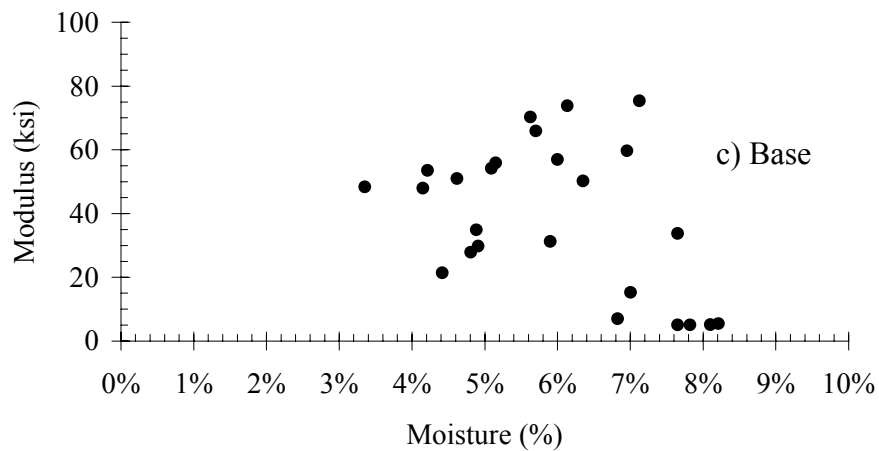
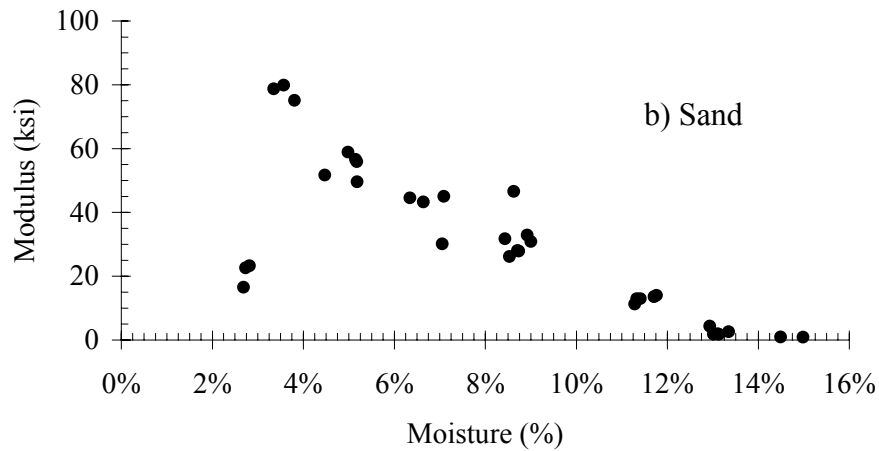
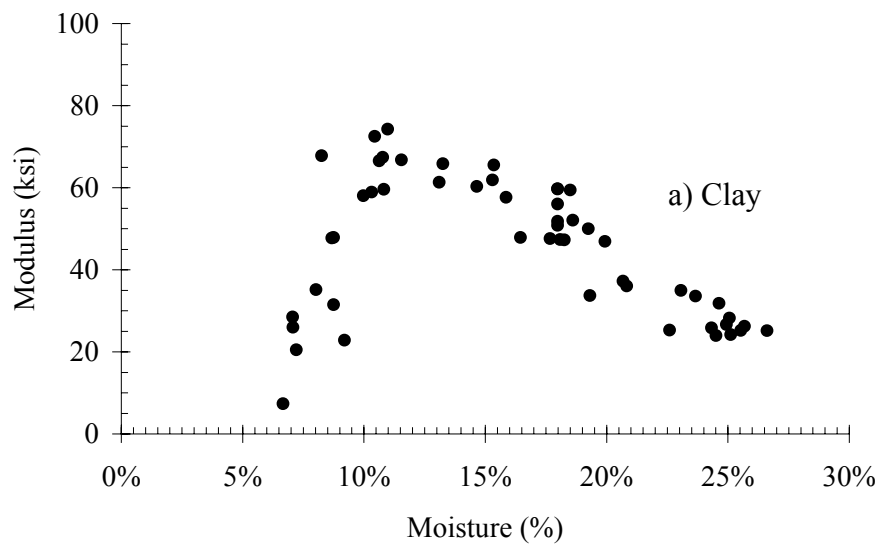


Figure 5.8 – Moisture-Modulus Plots for Three Types of Granular Materials

was to prepare the specimens at six discrete moisture contents. Some variability between the target and actual moisture contents are observed. Nevertheless, the results follow a reasonably tight trend, demonstrating the reproducibility of the results.

The sandy material demonstrates a different trend as reflected in Figure 5.8b. The modulus increases with a decrease in moisture content until a point (say 3%). Below that moisture content, the specimens are so fragile that they could not stand alone without cracking. As such, their measured moduli are quite low. Ignoring the moduli from specimens with moisture contents below 3%, the results are again reasonably repeatable and follow a tight trend.

The base material, as shown in Figure 5.8c, initially exhibited large variability in our experiment. Since the test method is repeatable on other materials, the variability was attributed to the specimen preparation method. A visual observation of the specimen demonstrated segregation of materials during specimen preparation. Several steps were taken to address this issue. The sample preparation method was modified to incorporate a thorough mixing of the materials before and during the specimen preparation. The materials used for each lift were ensured to visually contain a balance distribution of all aggregates. Aggregates larger than 1 in. (25 mm) were also removed from the sample. Each lift was deeply scarified to ensure intimate and seamless contact between each layer.

The other parameter studied was the method of compaction – manual (hand) or mechanical (machine). We determined that the two methods provide consistent results as long as the compaction device is routinely and carefully maintained and its cables were stretched properly. After these modifications, another repeatability study was carried out. The specimens prepared using the machine yield similar results with a much smaller coefficient of variation. As is evident in Figure 5.9, similar specimens prepared with precaution yield repeatable results with only one outlier. The coefficient of variation drops from 18% to 9% when the outlier is removed. In summary, these corrective measures not only have significantly improved the repeatability of the seismic tests on base materials, they have also improved the repeatability of the resilient modulus and triaxial tests conducted. Machine compaction is recommended because there is less variation from specimen-to-specimen and operator-to-operator than arises with hand compaction.

The other parameter that should be controlled in this and other tests is the time between the preparation of the specimen and testing. On one hand, the specimen “cures” with time; that is its strength and modulus increases. On the other hand, the specimen “dries out” with time. To minimize the loss of moisture with time, it is essential to cover the specimen as soon as it is prepared. Figure 5.10 demonstrates the impact of time from specimen preparation on the measured modulus for a sandy material when proper precautions are not taken to minimize moisture loss. The modulus changed from day-to-day in magnitude. Specimens dry of and near the peak on the modulus-moisture curve tended to have moduli that increased slightly as the days progressed. Specimens wet of the peak generally had moduli that decreased slightly or stayed the same with time. With increase in time between specimen preparation and test, the curves became also increasingly scattered. For the first 24 hours, similar specimens yield similar moduli. A careful observation of Figure 5.10 demonstrates that different specimens prepared at similar moisture content lose moisture at different rates, hence more scatter in the test results.

Based on this study, we recommend that either sand specimens be tested about 24 hours after preparation or the specimens be maintained in a manner that the moisture loss is minimal.

Similar experiment was carried out for the clay. Even though not shown here, the clay material can be tested on any day with virtually no difficulties and with relatively small changes in the modulus from day to day as long as it is protected from moisture loss. Over the four days of testing, the modulus changed very little and the data did not scatter for individual specimens.

Under the new specimen preparation protocol, the base became easier to test as the days progressed since the specimen was maturing. The optimum time to test the base material was the first 48 hours after the preparation of the specimen with appropriate attention to minimizing the loss of moisture.

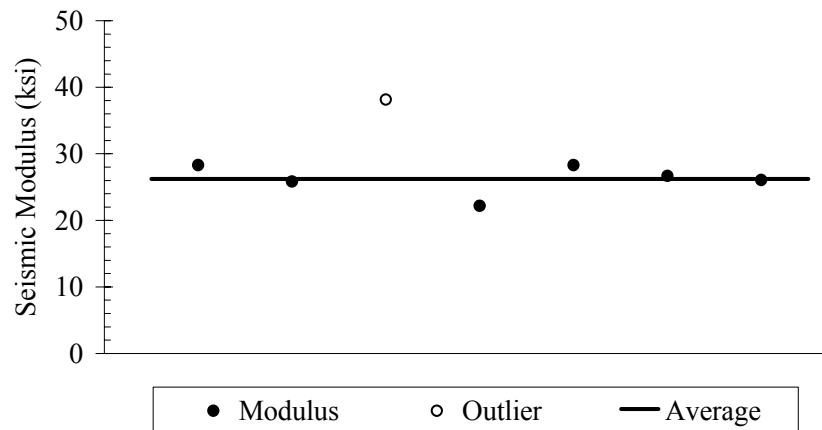


Figure 5.9 – Seismic Modulus of Specimens Prepared with Precautionary Measures

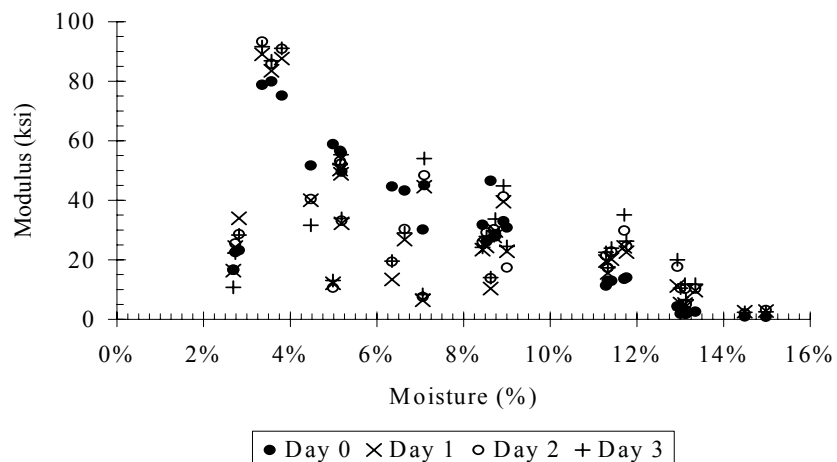


Figure 5.10 – Overall Modulus-Moisture Plot for Sandy Materials

PSPA Devices

The repeatability of the PSPA and DSPA has been evaluated in a number of TxDOT project in the last few years. The consensus is that the results are quite repeatable. As such, this matter was not emphasized in this phase of the project. As an example, the results of a repeatability study by Alexander (1996) are shown in Table 5.4. Alexander also demonstrated that the velocities measured with the PSPA and free-free resonant column tests are highly correlated.

The results of the evaluation of the seismic laboratory and field tests performed by Alexander (1996) are included in Table 5.1. He concluded that the repeatability of the tests was better than those carried out by traditional strength tests.

Table 5.4 – Evaluation of Repeatability of Free-Free Resonant Column and PSPA (from Alexander, 1996)

Test Type	No. of Data Sets [Replicates]	Range of Means, fps	Range of Std. Dev., fps	Average and [Range] for CV(%)
Free-Free P-Wave Velocity for Sawn Beams - between replicates on a single beam	63 [3]	11545 to 14230	0 to 845	1.2 [0 to 6.9]
Free-Free P-Wave Velocity for Sawn Beams - between beams for a single mixture	16 [4]	11670 to 14090	39 to 465	1.6 [0.3 to 3.6]
Free-Free P-Wave Velocity for Field Cores ^a - between replicates on a single core	24 [10]	12725 to 17265	0 to 110	0.2 [0.0 to 0.8]
Free-Free P-Wave Velocity for Field Cores ^a - between cores for a single mixture	6 [4]	12875 to 15880	45 to 1020	2.0 [0.4 to 6.4]
Free-Free P-Wave Velocity for Lab-Molded Beams - between replicates on a single beam	33 [3]	9870 to 14535	7 to 270	0.6 [0.1 to 1.9]
Free-Free P-Wave Velocity for Lab-Molded Beams - beams for a single mixture	12 [3]	9980 to 14390	13 to 430	1.0 [0.1 to 4.1]
Free-Free P-Wave Velocity for Lab-Molded Cylinders ^b - between replicates on a single cylinder	72 [3]	9650 to 14110	0 to 480	0.8 [0.0 to 3.7]
Free-Free P-Wave Velocity for Lab-Molded Cylinders ^b - between beams for a single mixture	24 [3]	12400 to 14020	8 to 340	1.0 [0.1 to 2.6]
PSPA R-Wave Velocity for Slabs ^c - between readings at the same location	2 [30]	7360 to 8090	31 to 40	0.5 [0.4 to 0.5]
PSPA R-Wave Velocity for Slabs ^c - between locations in close proximity	48 [3 to 5]	6020 to 8640	10 to 250	0.8 [0.1 to 3.5]
^a includes 6-, 4-, and 3-inch diameter specimens				
^b 6x12-inch cylinders only				
^c 6-inch thick slabs				

Chapter 6

Relating Seismic Moduli to Performance

One of the tasks of this project was to relate the performance of the AC and base materials to their seismic properties. The performance of a given pavement section is due to a complex interaction between the material properties and the pavement structure. In other words, a high quality material placed too thin would deteriorate as badly as a low-quality material placed with adequate thickness. The performance of a material can be related to a given strength or stiffness parameter in the following ways: 1) through observations and 2) through relating the parameters of interest to other known performance indicators.

To carry out this task through observations, a large number of sites constructed from similar materials with different levels of distress should be visited. The materials should be tested in situ and then retrieved for laboratory tests. The exact reason for the distress at each site, preferably through cradle to grave monitoring, should be identified and isolated. In that manner, the performance can be empirically related to a specific parameter. The advantage of this method is that a direct observation can be made. The disadvantages of this method are few. First delineating whether the structural inadequacy or the quality of the material is the source of a given distress in some cases is difficult. In many cases, by the time that the distress is visible, it can be attributed not only to the inadequacy of one specific layer but to the interaction of among two or more layers. In addition, it is expensive to gather all the information. A good example of this type of activity is the long-term-pavement performance (LTPP) database.

The alternative approach consists of relating the parameter of interest to one of the acceptable performance indicators of the materials. These performance indicators can be one that is preferably used in the mechanistic design. For example, it would be very desirable to relate the seismic modulus of the base materials to their traditional resilient modulus, since the resilient modulus is one of the primary parameters used in the design of flexible pavements. This approach has the advantage that in a shorter period of time relationships between the parameter of interest and the performance indicator can be established. In addition, these types of relationships are necessary for the development of performance-based specifications. In this study, we initiated a small scale study for the first approach but extensively developed the second

approach. Specifically, we visited about seventeen test locations in five districts. However, we pooled a large number of test points where we had conducted seismic and other tests.

Asphalt Concrete Layer

Our focus of the AC layer testing has been an experimental test section in east Texas. The site is located near Marshall in Atlanta district on IH-20 consisting of a 4 in. (100 mm) overlay placed on top of a Portland cement concrete pavement (PCCP). The 4 in. (100 mm) overlay was placed in two lifts. The bottom 2 in. (50 mm) was a typical TxDOT type mixture, the top layer was a combination of nine different mixtures. In summary, the nine mixtures consisted of a combination of three aggregates using traditional TxDOT and Superpave gyratory compactors to obtain the job mix formula. The gradations of the mixtures are summarized in Table 6.1. All mixes met the Superpave gradation requirements. All mixes except for Section 5 pass below the restricted zone. The other relevant information is included in Table 6.2. The design voids in total mix (VTM) are 4% for all mixtures. The asphalt contents varied between 4.5% and 5%. For all nine mixtures the same PG 76-22 asphalt binder was used.

Tests were carried out in three phases: 1) field control using the PSPA shortly after the completion of the project, 2) testing cores extracted from field with the ultrasonic device, and 3) conducting the ultrasonic and complex modulus tests on lab prepared specimens.

The modulus values obtained from measurements made in the field using the PSPA for the nine sites are shown in Table 6.3. The moduli vary from a minimum of 515 ksi (3.5 GPa) for the CHMB mixture with sandstone aggregate to 683 ksi (4.7 GPa) for the CMHB mixture with the siliceous gravel. The number of samples and the coefficient of variation for each section are also included in Table 6.3. Typically 30 points were tested per section. The coefficient of variation in the measurements for each section is about 10%.

Table 6.3 also contains the average VTM and asphalt content for each section. It would have been desirable to report results from individual test points where the coring and PSPA were carried out concurrently. However, due to time constraint, the in situ volumetric information has to be determined from cores obtain from other locations than PSPA tests. A comparison of Tables 6.2 and 6.3 indicates that the field AC content is fairly close to the design AC content of 4.5% to 5% for all sections except Sections 5 and 7. The field VTM is between a low of 5.7% at Section 4 and a high of 10.4% at Section 2. For most sections the VTM is about 8% to 9%.

The variation in modulus with VTM is presented in Figure 6.1. The mixtures follow more or less the same trend. As the VTM increases, the modulus decreases. The best fit line through the data provides an R^2 of about 0.78. When the variation in the AC content was considered, the best fit line provided the following relationship:

$$E = 624 + 46.20 AC - 28.76 VTM \quad (R^2 = 0.85) \quad (6.1)$$

Table 6.1 – Gradations of Mixtures Used in I-20 Site

a) Superpave Mix

Sieve Size (mm)	Cumulative Percent Passing		
	Siliceous Gravel (Section 1)	Sandstone (Section 2)	Quartzite (Section 3)
19.0	100.0	100.0	100.0
12.5	92.0	92.1	93.7
9.5	84.8	79.4	81.7
4.75	52.4	49.0	45.5
2.36	30.9	29.2	31.4
1.18	20.4	22.4	21.0
0.6	13.9	18.9	17.7
0.3	8.8	14.9	11.8
0.15	4.5	10.2	8.2
0.075	3.2	6.5	5.6
Pan	0.0	0.0	0.0

b) CMHB Mix

Sieve Size	Cumulative Percent Passing		
	Siliceous Gravel (Section 4)	Sandstone (Section 5)	Quartzite (Section 6)
7/8 in	100.0	100.0	100.0
5/8 in	99.7	100.0	99.6
3/8 in	64.5	65.4	65.6
# 4	34.3	38.0	34.2
# 10	21.8	24.0	24.0
# 40	16.2	16.4	14.5
# 80	9.8	10.9	9.1
# 200	6.4	6.4	5.9
Pan	0.0	0.0	0.0

c) Type C mix

Sieve Size	Cumulative Percent Passing		
	Siliceous Gravel (Section 7)	Sandstone (Section 8)	Quartzite (Section 9)
7/8 in	100.0	100.0	100.0
5/8 in	100.0	99.8	99.8
3/8 in	75.8	80.7	79.1
# 4	49.2	46.2	51.4
# 10	31.5	30.9	34.0
# 40	18.2	15.6	17.9
# 80	11.7	9.6	10.0
# 200	5.8	5.8	5.3
Pan	0.0	0.0	0.0

Table 6.2 – Volumetric Information for Mixture Used in I-20 Site

Section No.	Mix Method	Major Aggregate	Properties from Job Mix Formula			
			G _{mb}	G _{mm}	VTM ^{*, %}	AC, %
1	Superpave	Siliceous	2.328	2.425	4.0	5.0
2		Sandstone	--	--	--	--
3		Quartz	3.352	2.456	4.0	5.1
4	CMHB-C	Siliceous	2.280	2.381	4.0	4.7
5		Sandstone	2.245	2.339	4.0	4.7
6		Quartz	2.315	2.412	4.0	4.8
7	Type C	Siliceous	2.315	2.411	4.0	4.4
8		Sandstone	2.275	2.370	4.0	4.5
9		Quartz	2.342	2.440	4.0	4.6

Table 6.3 – Variation in Modulus Measured with PSPA and Volumetric Information from I-20 Sites

Section No.	Mix Method	Major Aggregate	Field Modulus			Field Volumetric Information	
			No. of Samples	Average, ksi	COV, %	VTM, %	AC Content, %
1	Superpave	Siliceous	27	577	10.8	8.8	4.4
2		Sandstone	42	560	5.9	10.4	4.5
3		Quartz	51	621	7.7	7.0	4.5
4	CMHB-C	Siliceous	35	683	12.0	5.7	4.6
5		Sandstone	44	515	8.6	10.1	3.9
6		Quartz	50	609	13.4	8.9	4.8
7	Type C	Siliceous	40	573	11.5	8.2	4.0
8		Sandstone	42	531	8.0	9.3	4.6
9		Quartz	29	566	7.2	8.9	4.7

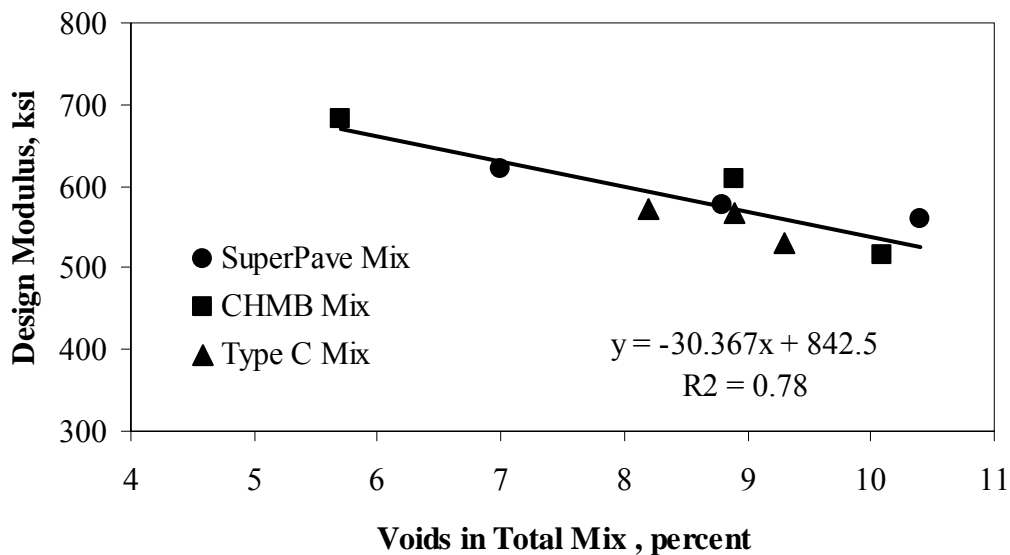


Figure 6.1 – Variation in Modulus Measured with PSPA with Air Voids from I-20 Sites

This relationship can be improved by considering one mixture at a time. This study clearly shows a trend between the modulus and VTM. As such, with proper calibration for a given mixture, the VTM may be potentially estimated from the modulus.

From each section, the cores used for verifying the thickness were shipped to UTEP for laboratory ultrasonic testing. The statistical information from this activity is included in Table 6.4. From Equation 2.4, the Poisson's ratio of the material is needed to obtain the seismic modulus from ultrasonic tests. To do so the results from one core is used to calibrate the results.

The average moduli from the cores and the PSPA are compared in Figure 6.2. For the most part, the two moduli are quite close. In one occasion, Section 6, the results differ by about 20%. The reason for such a difference is unknown at this time.

Several 6-in. (150-mm) high, 4-in. (100-mm) diameter briquettes were prepared from AC mixtures collected during construction by the staff of the Texas Transportation Institute and shipped to UTEP. The dynamic modulus and seismic measurements were carried out on the specimens. The seismic moduli are summarized in Table 6.5. The results from Section 2 are not included because sufficient material was not available to prepare specimens. In general, the moduli from the specimens prepared in the lab (pills) were higher than those obtained from the cores or the PSPA (see Figure 6.2). The AC contents of the specimens were typically slightly greater than the job mix formula reported in Table 6.2. The VTM values, on the other hand, were generally lower than those obtained from the cores. In some instances, the VTM values were even lower than the design value of about 4%. This study shows that the laboratory prepared specimens may not be representative of the field condition. Any quality control based on lab prepared specimens should be done with caution. Part of the explanation for higher moduli observed in the field can be attributed to the differences in the method of compaction and the thickness of the layers.

Table 6.4 – Comparison of Moduli Measured with PSPA In Situ and Ultrasonic Device on Cores from I-20 Site

Section No.	Mix Method	Major Aggregate	Average Field Modulus, ksi	Core Modulus		
				No. of Samples	Average, ksi	COV, %
1	Superpave	Siliceous	577	4	575	9.2
2		Sandstone	560	4	593	5.2
3		Quartz	621	4	626	10.7
4	CMHB-C	Siliceous	683	4	663	4.8
5		Sandstone	515	4	514	3.2
6		Quartz	609	4	507	11.2
7	Type C	Siliceous	573	4	637	0.9
8		Sandstone	531	4	542	4.8
9		Quartz	566	4	590	2.7

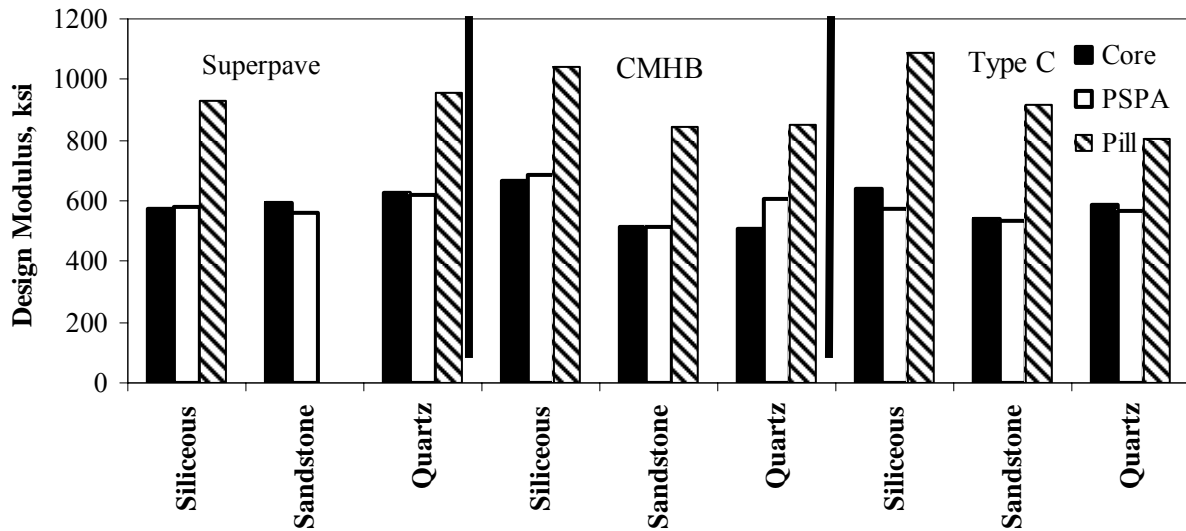


Figure 6.2 – Comparison of Moduli Measured In Situ, on Cores Retrieved from Field and from Specimens Prepared from Loose Material Retrieved during Paving

Table 6.5 – Variation in Modulus Measured with Ultrasonic Device and Volumetric Information from Briquettes Made from I-20 Sites Materials

Section No.	Mix Method	Major Aggregate	Seismic Modulus			Volumetric Information	
			No. of Samples	Average, ksi	COV, %	AC Content, %	VTM, %
1	Superpave	Siliceous	4	927	7.9	4.6	4.9
2		Sandstone	--	--	--	--	--
3		Quartz	4	957	3.2	6.4	2.7
4	CMHB-C	Siliceous	4	1043	1.9	5.1	2.5
5		Sandstone	4	847	2.3	5.2	2.4
6		Quartz	4	851	2.0	5.6	3.1
7	Type C	Siliceous	4	1088	3.7	5.0	1.3
8		Sandstone	4	914	9.4	5.3	4.2
9		Quartz	4	807	6.4	5.3	1.9

In the next step, the same specimens were subjected to the dynamic modulus tests. Measurements were carried out on four specimens from Sections 3, 4, and 8. Two specimens for Sections 1, 5, 6, 7, and 9 were tested because of the level of repeatability observed in the results from the previous sections.

The raw data from one specimen is shown in Figure 6.3a. Tests were carried out at about ten discrete frequencies in the range of about 0.02 Hz to 25 Hz, and at five temperatures ranging from 14°F to 104°F (-10°C to 40°C). Also shown in the figure are the measurements carried out with the ultrasonic device at the five temperatures. These data are plotted at a frequency of about 50 kHz. In addition, the free-free resonant column tests were carried out on the specimens. These data are also plotted at a frequency of about 5 kHz in Figure 6.3a.

After shifting the curves to a reference temperature of 73°F (23°C), the shift factor-temperature relationship shown in Figure 6.3b is obtained. The shift factors more or less form a straight line indicating that the material exhibits a rheologically-simple viscoelastic behavior.

The so-called master curve for a reference temperature of 73°F (23°C) is compared with the shifted data points in Figure 6.3c. The curves follow the data points quite nicely. The raw data, shift factor-temperature relationships, and master curves from all specimens tested for this study from I-20 site are included in Appendix A. This type of behavior was observed for all specimens.

To demonstrate the impact of incorporating the seismic moduli in the construction of the master curve, the master curve shown in Figure 6.3c is compared with that when the seismic data are not included in the development of the master curve (Figure 6.4). The fit parameters associated with the two models are quite different but the shapes of the curves are quite similar. This discrepancy is simple to describe. A number of combinations of fit parameters yield essentially the same curve when the sigmoidal function selected is used. Essentially all nine sites provided similar results as reflected in Appendix A.

This case study demonstrates that the quality control of the AC layer can be carried out with the seismic data. The moduli measured in situ with PSPA and on cores are reasonably close. The seismic and dynamic moduli of a given material can be readily related through a master curve. The use of lab-prepared specimens to characterize the field performance of a given material should be carried out with caution.

Besides the comprehensive case study described above, we have tested more than a dozen sites in the state of Texas. In most cases, the cores were not available to us because of concerns with the damage to the site. Cores were provided at four sites in Texas and five other states. The results from these case studies have tremendously assisted us to improve the protocol provided in Chapter 3. The best way of summarizing these results seems to be by comparing the moduli from the PSPA and the ultrasonic device conducted on the cores. The results and the lessons learned are described here.

The location and the nature of the sites are included in Table 6.6. The variations in moduli measured with the PSPA and the ultrasonic device for the districts tested in Texas are included in Figure 6.5. Also shown on the figure is the line of equality and the 20% error bound. In general point-by-point results are within 20% of one another, with the best fit line through all data having a slope of 1.04. That indicates that overall the difference is about 4%. Even though both lab and field seismic tests are proven to be repeatable, there are several parameters that should be

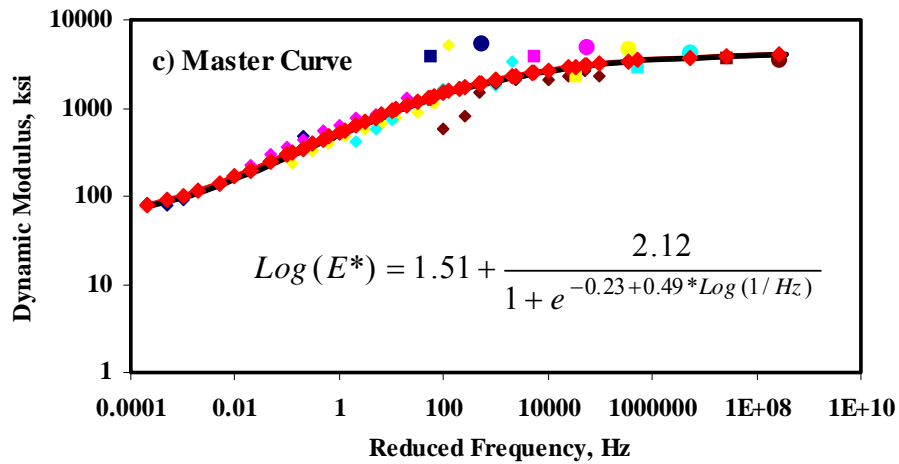
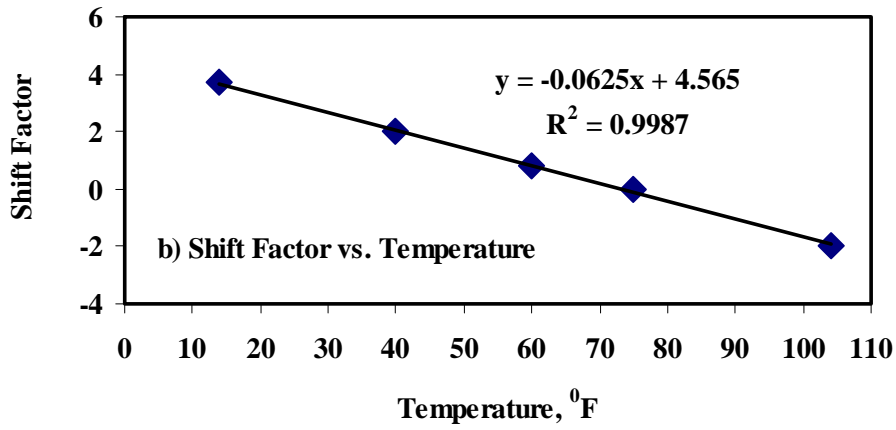
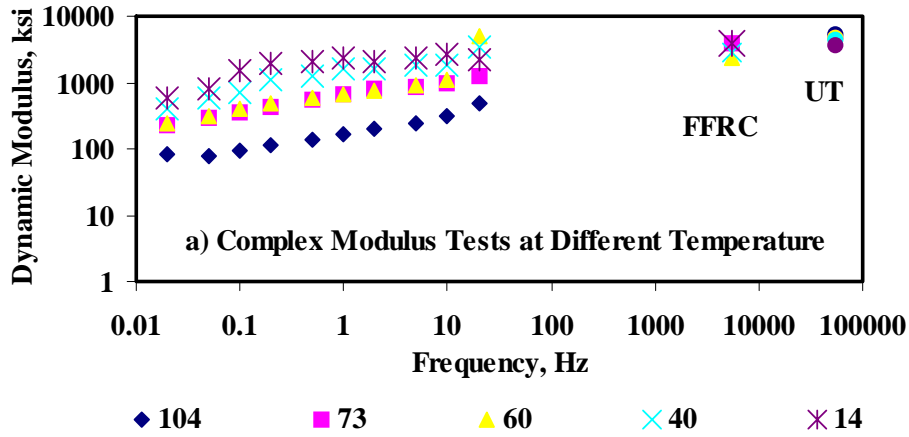


Figure 6.3 – Typical Results from Complex Modulus and Seismic Tests on a AC Specimen

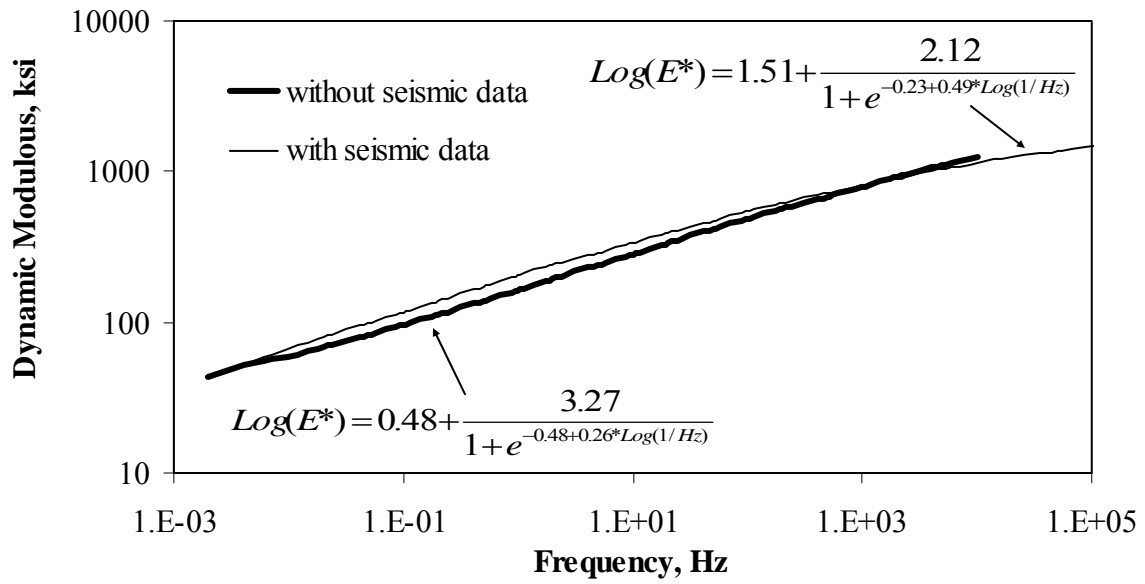


Figure 6.4 – Comparison of Master Curves with and without Seismic Data

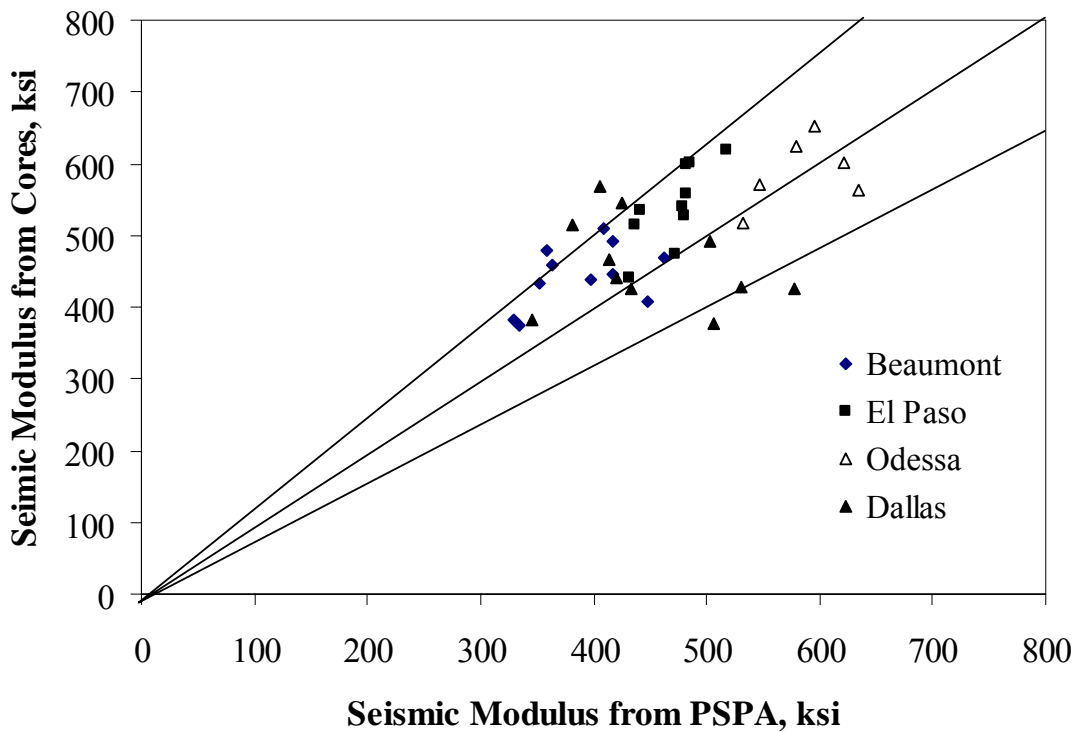


Figure 6.5 – Variation in Lab and Field Moduli from Sites Tested in Texas

Table 6.6 – Description of Sites Tested inside Texas

District	Location	Type of Construction	Nominal AC Surface Thickness (in.)	Base Type
Beaumont	SH 73	Flexible	3.0	Aggregate
Dallas	US 67	Flexible	6.0	Aggregate
El Paso	Loop 375	Flexible	3.0	Aggregate
Odessa	I-20	Flexible	7.0	Aggregate

carefully considered. The temperature of the AC layer has an impact on the modulus measured in the field. While the PSPA tests are carried out at the field temperature, the lab ultrasonic tests are carried out at the room temperature. Therefore it is of utmost importance to accurately measure the temperature of the AC layer during field tests. Even though a temperature gun seems to be doing a reasonable job, it may be more desirable to measure the AC temperature directly. One way of addressing this is perhaps to incorporate a temperature probe in the PSPA device that is in direct contact with the AC layer. The other practical way is by installing a temperature probe in the middle of the AC layer and to calibrate the temperature measured with the gun to the pavement temperature.

Aside from the accuracy of temperature measurement, the relationship used to convert the modulus from one temperature to another may introduce some approximations. Throughout this study (except for the I-20 Marshall project) we used the simplified equation proposed by Aouad et al. (1993). The complex modulus approach, described in Chapter 3, may be a more accurate way of considering the impact of the temperature on modulus.

The third approximation in the analysis has to do with the frequency-dependency of the modulus measured. The ultrasonic device measures the modulus at a frequency of about 54 kHz; whereas depending on the thickness and stiffness of the AC layer, the central frequency associated with the PSPA is between 5 kHz to 15 kHz. As discussed in Chapter 3, this phenomenon may also bring in some approximation into the comparison between the lab and field moduli. This matter can also be addressed by the complex modulus procedure described in Chapter 3 as well.

The condition of the pavement layer also impacts the moduli measured in the field and lab. In the lab the waves are transmitted and received perpendicular to the AC layer; whereas the direction of propagation of waves in the PSPA is primarily in the horizontal direction. As such, the lab measurements are quite sensitive to cracks and debonding in the horizontal direction and the PSPA is more sensitive to the cracks perpendicular to the surface of the ACP. For example an unusually thick layer of tack coat or the onset of debonding of two layers will reduce the modulus measured in the lab; but it would have minimal impact on the USW method that is used to make measurements of the modulus with the PSPA. This concern should be of small consequence to the quality management of pavements, because they are typically new and the quality management is done layer by layer.

The only truly new pavement tested was the Odessa site. In this case, about 60 points were tested about 2 weeks after the completion of project. Six cores were retrieved from the site. The

mixture was a crumb rubber modified mixture typically used in that district. The comparison between the cores and the PSPA results are quite close with the largest difference being about 10%.

The Dallas site consisted of 6 in. (150 mm) of AC placed in three lifts. The last lift was fresh when the tests were carried out. Even though the coring was carried out on the day of field testing, the lab testing was not carried out until a month later because the specimens were in transit. This site demonstrates the largest variability between the lab and field moduli. Nevertheless, the lab and field moduli are within 20%. This is a site that would have benefited the most from a calibration of the results between the core and the PSPA measurements during the field tests.

The site at El Paso district consisted of two layers of AC with a combined thickness of about 3 in. (75 mm). At some points the two layers were debonded. A favorable comparison between the lab and field moduli is obtained except at the debonded cores where the lab values are somewhat higher.

The Beaumont site consisted of about 3 in. (75 mm) of AC. The modulus of the cores is typically slightly higher because of the existence of vertical micro-cracks in the AC layer that impact the PSPA measurements more than the lab tests.

The results from the sites tested outside the state of Texas are included in Figure 6.6. The Mississippi site was graciously provided by the Army Corps of Engineers staff in conjunction with Project 1780. The results from the other three states are provided from a completed national study (see Saeed and Hall, 2001). In general, the lab and field seismic moduli compare quite well. For the most part, the moduli are well within 10% of one another.

The moduli obtained from three sites in North Carolina are summarized in Table 6.7. The thickness of the layers and the underlying base were substantially different. Except in a few occasions, the lab and field moduli are within 10%.

The Ohio site contains the results from three cells in the Ohio test track. Once again, the results from the lab and field compare well. The results reported for Minnesota were collected at four sites with three from Minn-Road facility. Once again, the lab and field results are in close agreement.

As indicated before, Saeed and Hall (2001) compared the seismic moduli with the master curve obtained from complex modulus tests on the specimens. An example was shown in Chapter 3. For all sites where the lab and field moduli were available, the comparison was reasonably close.

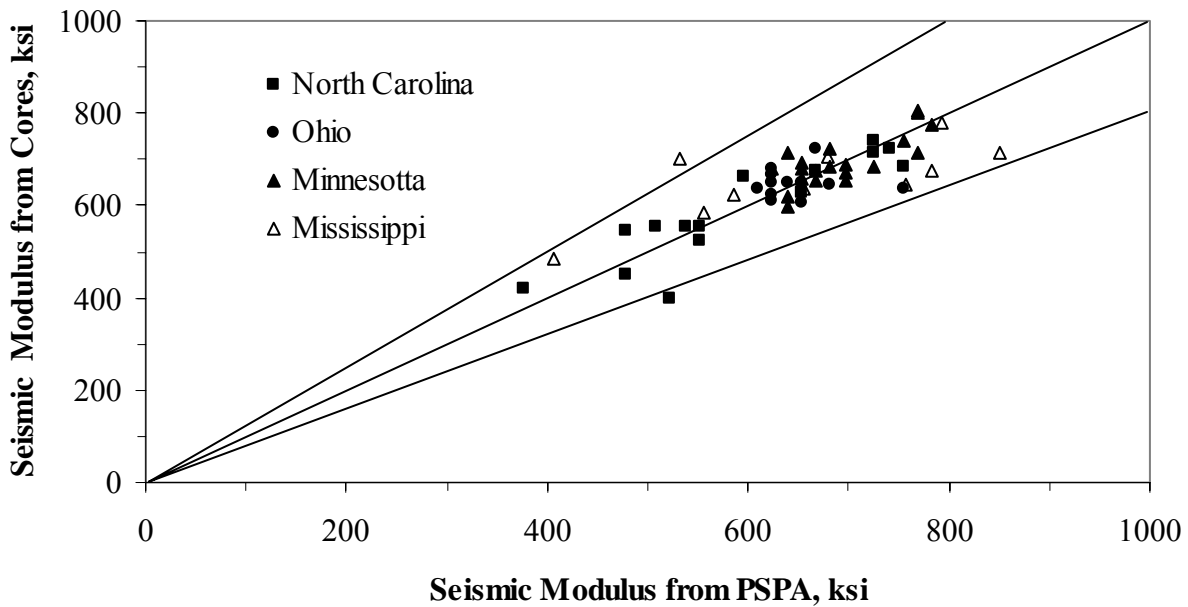


Figure 6.6 – Variation in Lab and Field Moduli from Sites Tested outside Texas

Table 6.7 – Description of Sites Tested outside Texas

State	Location	Type of Construction	Nominal AC Surface Thickness (mm)	PCC Slab Thickness (in.)	Base Type
North Carolina	US 25	Flexible	6.0	--	Aggregate
	IH 26	AC/JCP	2.5	9	Aggregate
	IH 26	AC/Crack&Seat	9.0	9	Aggregate
Ohio	Ohio Test Track	Flexible	4.0	--	ATB
		Flexible	7.5	--	ATB
		Flexible	7.5	--	ATB
Minnesota	Minn Road	Flexible	8.0	--	Aggregate
		Flexible	3.0	--	--
		Flexible	5.0	--	Aggregate
	US 169	AC/JCP	3.0	8	Sand
Mississippi	Item 5	Flexible	2.2	--	Aggregate
	Item 6	Flexible	2.4	--	Aggregate
	Item 7	Flexible	3.9	--	Aggregate
	Item 8	Flexible	3.9	--	Aggregate
	Item 9	Flexible	4.1	--	Aggregate
	Item 10	Flexible	3.9	--	Aggregate
	Item 11	Flexible	5.0	--	Aggregate
	Item 12	Flexible	4.3	--	Aggregate

Base Layer

For the base layer our focus has been on relating the performance to two traditional performance indicators, the resilient modulus of the material and the angle of internal friction. The process followed and the results obtained are summarized here.

This portion of the project was carried out in close collaboration with TxDOT. A number of test results reported and the development and maintenance of the database containing the results were carried out by TxDOT personnel.

The resilient modulus of the base layer is the primary design parameter in many existing mechanistic pavement design procedures as well as the new AASHTO 2002 design guide. A review of the fundamentals of resilient modulus testing and the state-of-practice in performing these tests can be found in Barksdale et al. (1997). The step-by-step procedure used to determine the resilient moduli of different materials can be found in Nazarian et al. (1999). Either 4 in. by 8 in. (100 mm by 200 mm, for subgrade) or 6 in. by 12 in. (150 mm by 300 mm, for base) specimens were compacted in cylindrical molds. The resilient modulus tests consisted of applying various deviatoric stresses at different confining pressures. Table 6.8 contains the sequence for base materials. The loading sequence used was a modified form of the sequence found in AASTHO TP46-94. Three tests at zero confinement were added because seismic tests are carried out at zero confining pressure.

Table 6.8 – Loading Sequence for Resilient Modulus Test

Confining Pressure (psi)	Deviatoric Stress (psi)
15	15 (conditioning cycle)
0	1
0	2
0	3
3	3
3	6
3	9
5	5
5	10
5	15
7	10
7	20
7	30
15	7
15	15
15	30
20	15
20	20
20	40

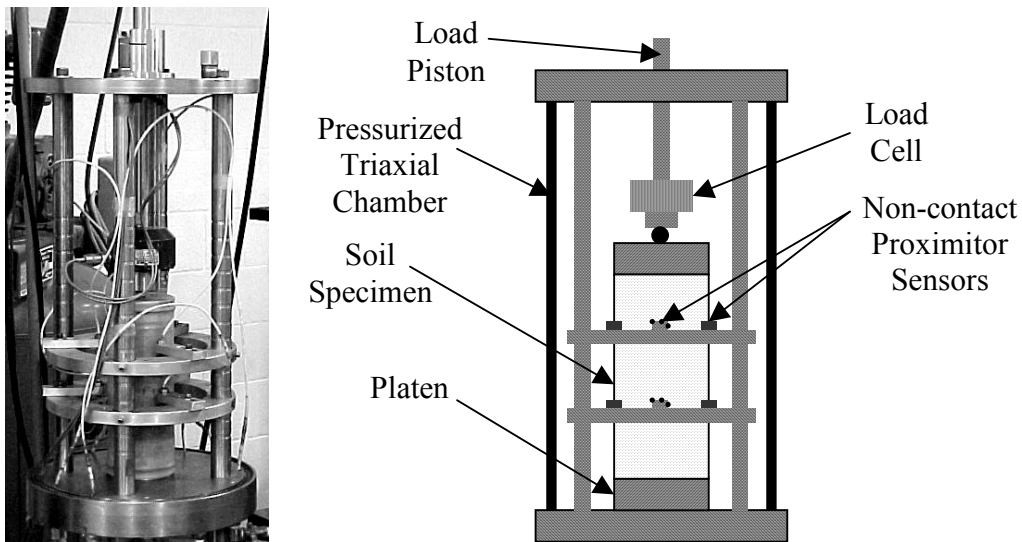


Figure 6.7 – Resilient Modulus Test Setup

The axial deformations are measured along the middle one-third of the specimen with six non-contact proximitor sensors as shown in Figure 6.7. Twenty-five cycles of loading are applied at every stage to optimize testing time, and to minimize the degradation of the specimen. From the measured axial displacements at a particular deviatoric stress and confining pressure, the resilient modulus of the specimen was determined.

As indicated in Chapter 3, the constitutive model used to describe the results of the resilient modulus tests is

$$M_R = k_1 \sigma_d^{k_2} \sigma_c^{k_3} \quad (6.2)$$

where σ_d and σ_c are the deviatoric stress and confining pressure, respectively. Parameters k_1 , k_2 , and k_3 are statistically determined coefficients. Typical results from one test are shown in Figure 6.8. Again, since seismic tests are performed at a confining pressure of zero, a set of three resilient modulus tests was performed at zero confining pressure to facilitate the establishment of relationships.

The resilient modulus test is categorized as a stress-controlled test; that is, at any confining pressure, a certain deviatoric stress is applied to the specimen irrespective of its stiffness. As such for a softer material, the strain experienced by the specimen at a given deviatoric stress is higher than that when a stiff specimen is subjected to the same deviatoric stress. Since base materials normally exhibit strain-softening behavior, the reduction in modulus will be more drastic for softer materials. In addition, a limitation of the resilient modulus tests is that it is difficult to conduct the test reliably at very small-strain moduli. Since seismic methods provide moduli at very small strains this inconsistency has to be addressed. The way we approached this problem is by extrapolating the low-strain modulus of the base at zero confining pressure.

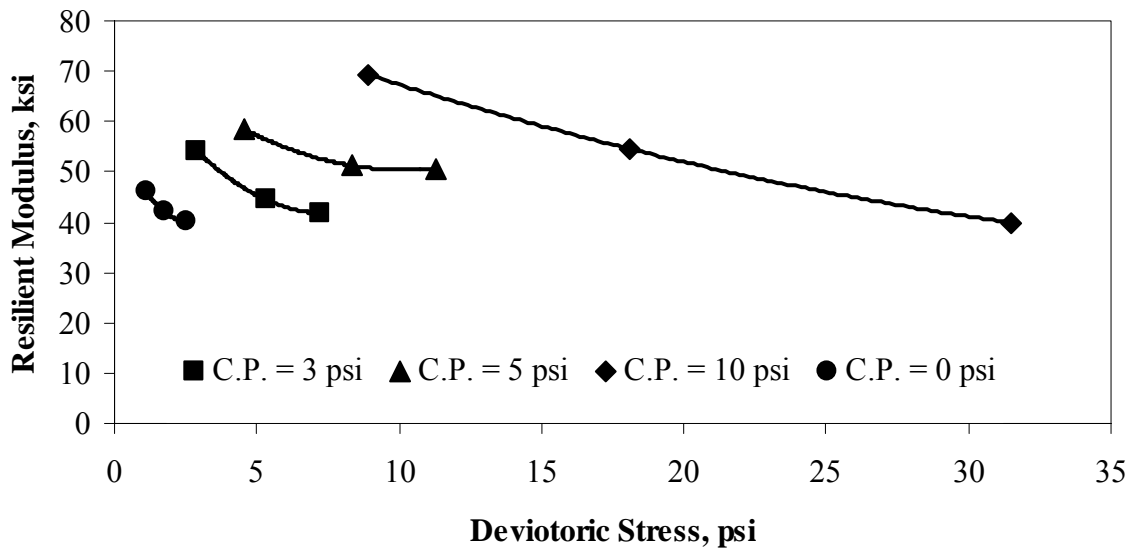


Figure 6.8 – Typical Resilient Modulus Test Results

To estimate the small-strain modulus of a material, the deviatoric stress is converted to axial strain first as shown in Figure 6.9. This task is simply carried out by dividing the deviatoric stress at each point with the resilient modulus corresponding to that point. Note that the strains are plotted in a logarithm scale in the figure. This is the standard way of demonstrating the strain-softening of a material in geotechnical earthquake engineering (see Kramer, 1996). A sigmoid function is then fitted to the three data points tested at zero confining pressure as shown in Figure 6.9. With trial and error, the most appropriate model is in the form of

$$M_R = \frac{\beta}{1 + e^{-\alpha\varepsilon}} \quad (6.3)$$

where M_R is the resilient modulus, ε is the axial strain and α and β are the fit parameters. The parameter β provides a low-strain asymptote that can be considered as the low-strain modulus at the zero confining pressure of the material. This value can be compared with the seismic modulus measured on the same specimen before it is subjected to the resilient modulus tests.

So far we have applied this procedure to about three dozen specimens with a large variation in stiffness and material type (from clayey subgrade to high quality base). The comparison between the low-strain resilient modulus and seismic modulus is shown in Figure 6.10. A reasonably close relationship between the two parameters is obtained.

This approach has several advantages. First, a means of estimating the resilient modulus from the seismic modulus is obtained. In that manner, the seismic modulus can be readily converted to the design modulus. In addition, the need for extensive resilient modulus testing is substantially reduced. The quality control can be carried out much more rapidly as well.

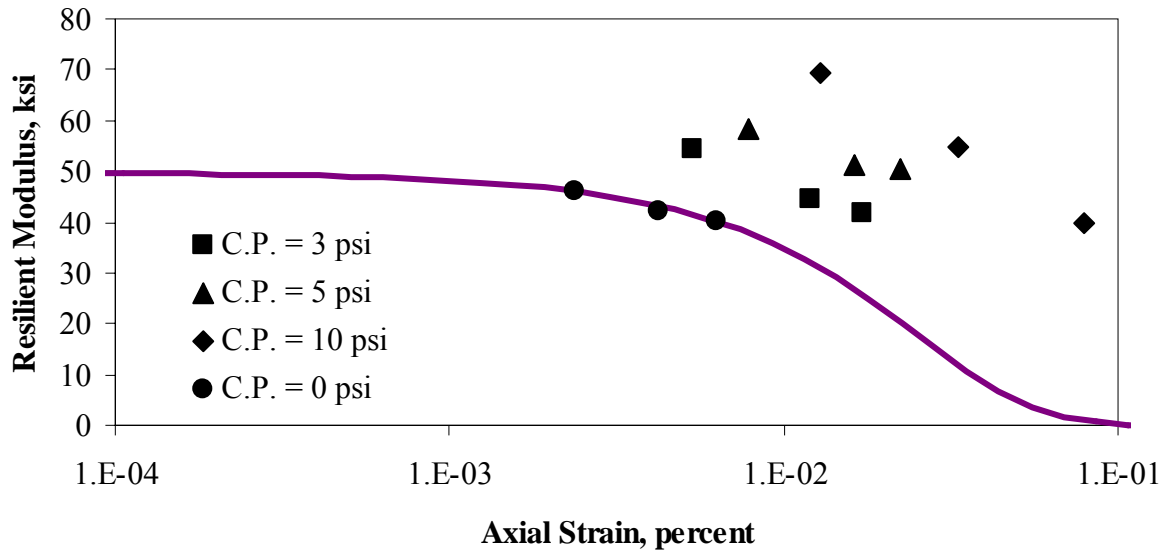


Figure 6.9 – Typical Variation in Resilient Modulus with Strain

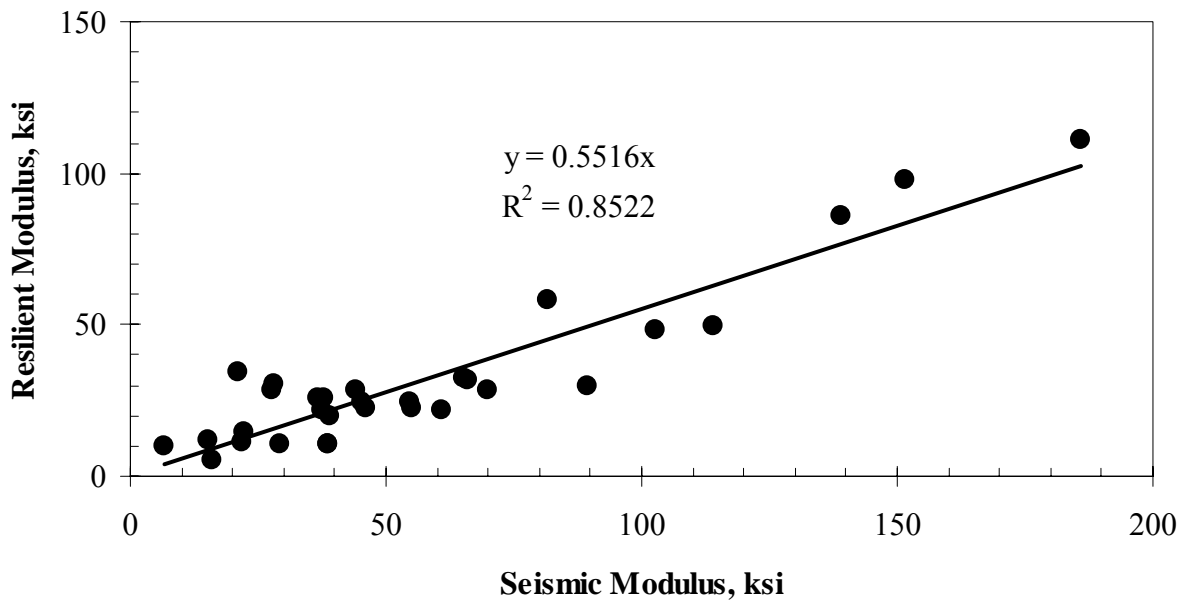


Figure 6.10 – Relationship between Seismic and Low-Strain Resilient Moduli

One important quality indicator of a material in Texas is its triaxial strength of a material. For the last fifty years, the so-called Texas Triaxial Classification (Tex-117-E) has been used. Recognizing the limitations of Tex-117-E, TxDOT is currently advocating Tex-143-E for conducting triaxial tests. The new procedure is quite similar to standard unconsolidated undrained triaxial tests. Specimens, 6 in. (150 mm) in diameter and 8 in. (200 mm) in height, are prepared using a compaction method similar to the Proctor method (Tex-113-E). The specimens are then conditioned and subjected to a confining pressure and then a deviatoric stress. The Mohr circles from this operation are plotted to determine the undrained strength parameters (cohesion and angle of internal friction for a given soil). The new classification is primarily based on the angle of internal friction.

The second attempt to relate the seismic parameters to the established performance indicators was to relate the results from the new triaxial tests to the seismic wave velocity measured on the same specimens. TxDOT staff primarily carried out this task with our assistance.

The variation in compression wave velocity, V_p , with the angle of internal friction, ϕ , is shown in Figure 6.11. As Equation 2.1 indicates, the compression wave velocity and seismic modulus are related through density. Since the compression wave velocity is an independent variable whereas the modulus is related to two independent variables (compression wave velocity and density), it is more desirable to develop correlations based on this parameter. This will eliminate the effects of density when comparing the compression wave velocity to the angle of internal friction. The correlation between these two parameters (V_p and ϕ) is quite reasonable. Correlations such as the one shown could permit an evolutionary transition from the standard quality control based on moisture-density to a more mechanistic-based approach that takes into account other parameters such as modulus and angle of internal friction.

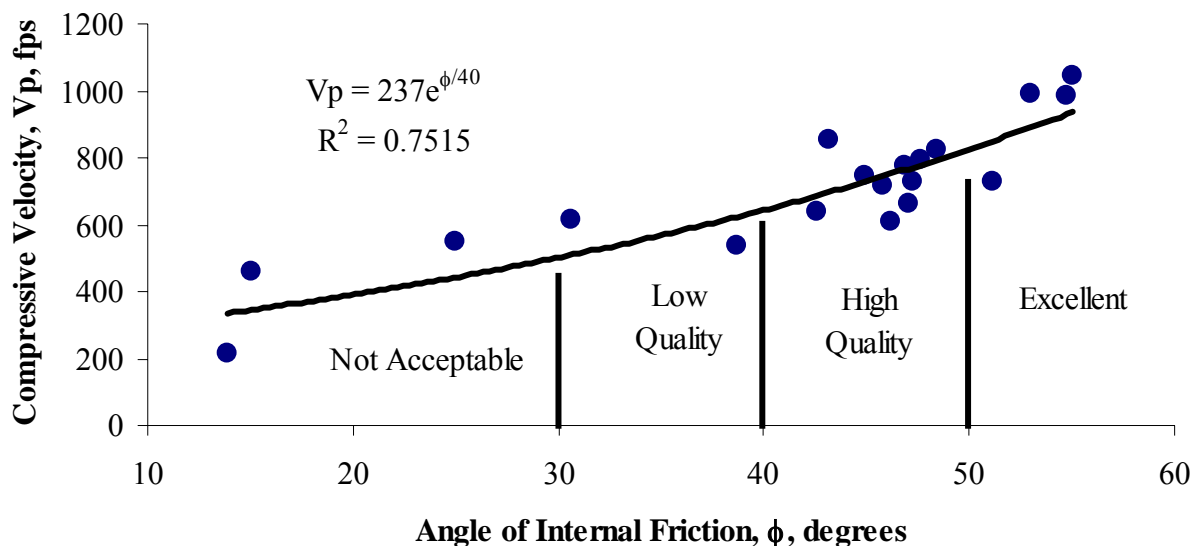


Figure 6.11 – Correlation between Strength Parameter and Compression Wave Velocity of Bases Tested

For the base layer, the material properties were related to the performance as well. To do so about eighteen trenches in four districts were installed. The field test protocol consisted of several telephone calls to a given districts to discuss the requirements of the project. After the district selected a number of sites, the research team visited the district and the sites to determine the suitability of the locations for the project. The next step consisted testing of the sites with the FWD, GPR and the SPA (if possible) to select the section of the road most suitable for the project. The selections of the trench locations were based on the preliminary analysis of the NDT data as well as visual distress. In the selected area, SPA and FWD tests were carried out in the vicinity of the trench to obtain the variation in modulus of the pavement layers with each device. The detailed results from these two devices and the comparison of them are outside the scope of this report. But they are included in Abdallah et al. (2003).

The trenching operation, which was coordinated by the Materials and Pavement (MAP) section of TxDOT, consisted of the following step

- A section of AC was removed. This operation was carried out with no or little water to minimize changes to the moisture of base.
- About half-a-dozen DSPA tests were carried out on top of the base.
- About three moisture and density tests were carried out on top of the exposed base layer using a nuclear-density device.
- About 600 lbs (250 kg) of the base material was carefully removed and bagged for lab testing by UTEP, MAP and TTI.
- Several random specimens were retrieved so that the in-place moisture content of the base can be verified.
- The trench was thoroughly cleaned to the top of the subgrade by removing the excess base material from it.
- About half-a-dozen DSPA tests were carried out on top of the subgrade.
- About 300 lb (120 kg) of the subgrade material was removed and bagged for lab testing by UTEP.
- The pavement section was backfilled and repaired.

The lab tests carried out consisted of

- Index Tests (Gradation, Plasticity Index, Moisture-Density)
- Strength Tests (Triaxial Tests, Tex 117-E and Tex-143-E)
- Modulus Tests (Resilient Modulus Test)
- Seismic Tests (Free-free Resonant Column Test)
- Miscellaneous (Tube Suction Test)

The districts consisted of El Paso, Fort Worth, Odessa and Pharr. The locations of the sites and there performance as judged from their condition during trenching is shown in Table 6.9. As indicated before, the intension of the team was to select locations that the base layer was distressed and not distressed. The selection of the trench locations was dictated primarily by the deflections from FWD, GPR and SPA output. As reflected in the remarks in the table, in several occasions, either the three NDT devices provided contradictory results. In most cases, the SPA, FWD and GPR provided complementary results. In highly distressed area, the FWD deflections

Table 6.9 – Description of Sites Tested

District	Site	Trench	Base Condition	Layer Thickness (in.)		Remarks
				AC	Base	
El Paso	Loop 375	1	Good	4	14	Sites were selected in an area that has experienced distress. Trenches were placed on both distressed and intact pavement. The base materials in all trenches were in good condition. The cause of distress was the debonding of AC layer. The materials from the first three trenches were similar. Trench 4 was from a different quarry.
		2	Good	4	14	
		3	Good	4	14	
		4	Good	4	14	
Fort Worth	FM 2415	1	Poor	2.5	7	Sites were selected because of problems with distress at the sites. Both distressed and fewer distressed areas were trenched. The bases were relatively thin and high in fine content.
		2	Poor	2.5	7	
	FM 2738	1	Poor	1.5	9	
	FM 51	1	Poor	2.0	9	
2		Poor	2.0	7.5		
Odessa	IH 20	1	Good	7	17	The site was heavily distressed. As per FWD, the base was weak, SPA and GPR did not confirm. During trenching, the base was found in good condition.
		2	Good	7	17	
Pharr	US 281	1	Poor	3	10	All base material in these projects were specified as Grade 1 base material, but exhibited some type of distress. Projects 1-4 used caliche bases which exhibited low strength and high moisture susceptibility. These bases had a high fine content (-#4 sieve) and behaved like a soil and not a base material. For example, Project 3 set up stiffness like a cohesive soil, but had low shear strength. None of these bases past Grade 1 requirement when retro tested. Projects 5-6 base material was a 50-50 blend of recycled concrete and caliche. These materials exhibited the same physical performance as the pure caliche (low strength, high moisture susceptibility). Projects 7-9 are crushed limestone base. Project 10 was a gravel base. These projects demonstrated high strength and fairly low to moderate moisture susceptibility. The distress in these sections was due to lack of compaction during construction. Meet Grade 1 physical requirements.
	FM 802	2	Poor	3	11	
	SH 48	3	Poor	3	12	
	FM 511	4	Poor	1.5	15	
	SH 100	5	Poor	7	10	
		6	Poor	7	10	
	FM 509	7	Good	7	8	
	BUS 83	8	Good	3	12	
	FM 3362	9	Good	3	12	
	US 83	10	Good	3	14	

are both affected by the layer thicknesses and moduli, as well as the manifestation of the distress. This is desirable in terms of locating weaker spots but is undesirable in terms of determining the moduli of the layers. In some of the sites, the trenching operation revealed that the distress was not due to weak base but due to problems with the AC or subgrade layer. As such, some of the well-performing base materials (e.g. in Odessa) were in distressed area; whereas some of the poor-performing bases were not distressed at all. In some instances, the material was of adequate quality but the cause of distress was inadequate thickness.

The index properties of the materials are shown in Table 6.10. In all cases, more than 40% of the materials pass through a No. 4 sieve. The largest aggregate is nominally less than 1 in. (25 mm). The liquid limit is typically above 20% with the plasticity index of as high as 15%. The plasticity tests were not carried out on the Pharr District materials. The optimum moisture content varies between 5% and 15%, while the maximum dry unit weight is as low as 104 pcf (16.5 kN/m^3) to as high as 145 pcf (23 kN/m^3). It is interesting to note that the index properties from trenches installed at the same project were quite similar, even though some of the trenches were in the distressed area and some in intact area. This indicates that there was not much difference in the index properties of the materials. As shown in Table 6.10, the in situ moisture content was for most sites quite different than the optimum moisture content. The difference is as high as 5% wet of optimum to about 3% dry of optimum. The preliminary results between the performance and the parameters measured are presented here.

The strength and stiffness parameters for each trench are shown in Table 6.11. The newly proposed triaxial tests and the tube suction tests were carried out on all but one material. On the other hand, the Texas Triaxial Tests were only carried out for the first three districts. The free-free resonant column tests were also carried out on all but one material. However, in two other occasions the soaked moduli were not determined. The DSPA tests were not carried out at two sites in Pharr because of conflict in scheduling. In the next section these parameters are related to the performance.

The first correlation was carried out between the angle of internal friction obtained from Tex-143-E and the performance as shown in Figure 6.12. It seems that at a minimum, an angle of internal friction of about 42 degrees is necessary to ensure that the base will not fail. We did not attempt to relate the angle of internal friction from Tex-117-E to performance because, in general the results from the new triaxial test procedure is more reliable and repeatable.

The second parameter explored was the modulus of the base after two days of dry back. The relationship between the performance and the seismic modulus is shown in Figure 6.13. As a preliminary number, it seems that a seismic modulus of about 100 ksi (700 MPa) is needed in order to ensure a well-performing base. It should be mentioned that there are several points under the poor performing materials that exhibit extremely high seismic moduli as well as angles of internal friction. These specimens, which belong to Fort Worth District, may need further investigation. The records indicate that they were inadvertently prepared dry of optimum.

In this particular study, as shown in Figure 6.14, no conclusive relation between the performance and the dielectric value can be drawn. Basically, the dielectric values for all materials are in the range considered as poor performing as per Saarenketo and Scullion (1997). One reason maybe

Table 6.10 – Index Properties of Sites Tested

District	Site	Trench	Compaction		Plasticity		Gradation					
			ω_{opt}	γ_{max}	LL	PI	1 1/4	7/8	5/8	3/8	#4	-#4
El Paso	Loop 375	1	5.8	143.1	26	13	2.8	12	20.7	34.0	52.0	48.0
		2	5.6	145.4	22	9	0.0	11.7	21.3	35.8	55.6	44.4
		3	5.7	145.1	24	13	3.5	13.9	23.8	38.7	59.0	41.0
		4	5.6	153.4	30	16	2.1	10.1	18.3	35.7	55.5	44.5
Fort Worth	FM 2415	1	7.4	131.3	33	18	3.0	8.8	17.5	35.0	54.3	45.7
		2	7.3	134.7	29	15	4.6	10.1	17.3	33.7	53.3	46.7
	FM 2738	1	7.4	135.5	18	5	2.6	10.3	18.4	31.9	47.9	52.1
	FM 51	1	6.3	135.4	15	2	0.6	2.1	5.6	14.9	30.8	69.2
		2	6.2	135.6	16	3	1.0	2.4	5.8	13.8	28.1	71.9
Odessa	IH 20	1	9.5	126.0	--	12	2.0	9.4	17.3	29.1	44.0	56.0
		2	9.5	126.0	--	13	2.0	9.4	17.3	29.1	44.0	56.0
Pharr	US 281	1	8.9	115.3	--	--	3.2	15.7	--	42.1	58.6	41.4
	FM 802	2	15.3	106.2	--	--	1.6	5.9	--	21.4	37.6	62.4
	SH 48	3	7.6	131.3	--	--	2.3	17.9	--	43.3	55.8	44.2
	FM 511	4	16.8	108.7	--	--	--	--	--	--	--	--
	SH 100	5	15.4	111.9	--	--	0.6	5.0	--	20.5	35.6	64.4
		6	15.3	111.3	--	--	0.0	8.5	--	27.6	43.6	56.4
	FM 509	7	8.4	118.5	--	--	1.8	21.6	--	50.9	64.8	35.2
	BUS 83	8	15.3	104.5	--	--	3.5	9.1	--	24.9	41.3	58.7
	FM 3362	9	13.8	104.4	--	--	2.9	9.5	--	26.5	43.5	56.5
	US 83	10	8.1	118.3	--	--	2.3	11.3	--	31.3	48.1	51.9

Table 6.11 – Strength and Stiffness Parameters of Sites Tested

District	Site	Trench	Base Performance	Triaxial Test (Tex-143-E)		Texas Triaxial Test (Tex-117-E)			Free-Free Resonant Column		Dielectric Constant	DSPA Modulus, ksi
				Angle of Internal Friction, degrees	Cohesion, psi	Class	Angle of Internal Friction, degrees	Cohesion, psi	Modulus, ksi	Modulus Ratio		
El Paso	Loop 375	1	good	43	18	2.7	57	5	168	0.61	16	140
		2	good	47	10	2.7	58	5	139	0.76	15	165
		3	good	55	12	2.7	56	5	224	0.74	16	112
		4	good	46	1	3.0	53	5	182	0.75	20	235
Fort Worth	FM 2415	1	poor	45	9	2.8	45	9	383	0.31	18	111
		2	poor	47	5	3.2	46	6	245	0.39	19	132
	FM 2738	1	poor	43	10	2.1	54	9	89	0.60	15	127
	FM 51	1	poor	31	14	2.8	45	9	632	0.13	17	120
		2	poor	48	8	2.7	45	10	598	0.23	17	141
Odessa	IH 20	1	good	47	9	2.7	49	8	109	0.39	17	127
		2	good	47	9	2.7	49	8	109	0.39	17	64
Pharr	US 281	1	poor	39	3	--	--	--	63	--	16	--
	FM 802	2	poor	14	2	--	--	--	16	--	24	--
	SH 48	3	poor	15	2	--	--	--	43	0.21	16	138
	FM 511	4	poor	--	--	--	--	--	--	--	--	118
	SH 100	5	poor	25	1	--	--	--	51	0.25	30	95
		6	poor	46	2	--	--	--	72	0.39	24	119
	FM 509	7	good	55	14	--	--	--	213	0.61	14	82
	BUS 83	8	good	53	5	--	--	--	182	0.59	15	103
	FM 3362	9	good	48	13	--	--	--	123	0.68	14	89
	US 83	10	good	51	11	--	--	--	103	0.53	17	115

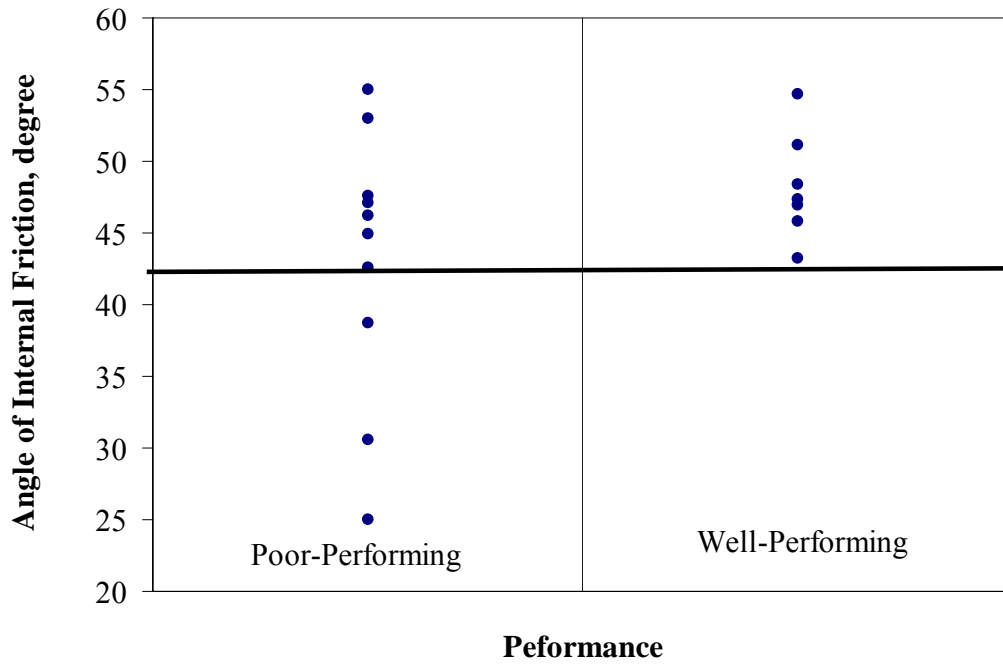


Figure 6.12 – Performance as Related to Angle of Internal Friction from New Triaxial Method (Tex-143-E)

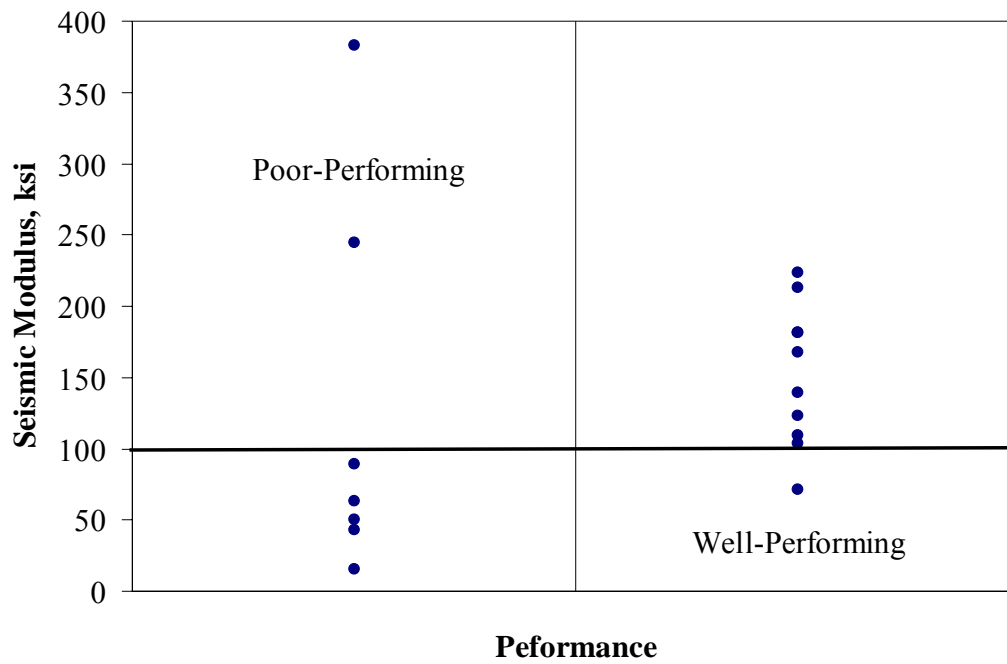


Figure 6.13 – Performance as Related to Seismic Modulus from Free-Free Resonant Column

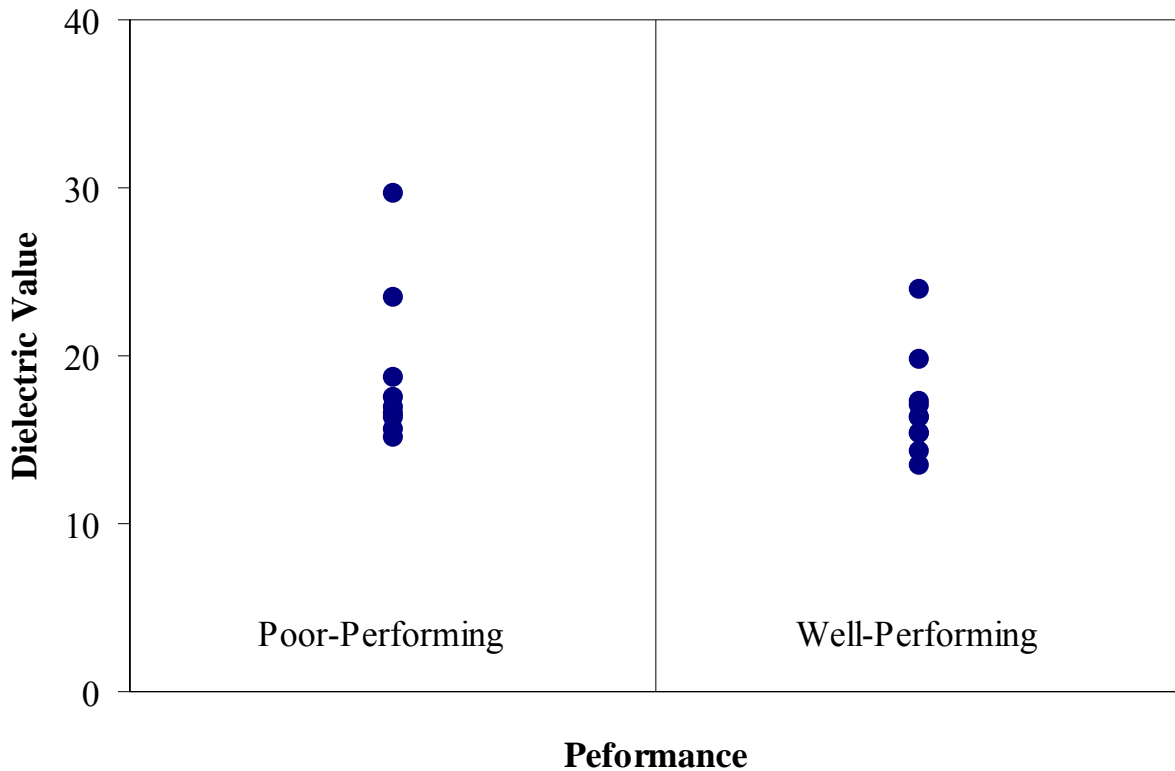


Figure 6.14 – Performance as Related to Dielectric Values from Tube Suction Tests

that the protocol followed here is somewhat different than that recommended by Saarenketo and Scullion.

The last parameter studied was the relationship between the modulus measured with the DSPA and the performance. As anticipated, the two parameters are not well-correlated (see Figure 6.15). This is anticipated because, despite the fact that in the laboratory tests a large number of parameters are controlled, a large number of parameters are varying in the field. Some important varying parameters are the environmental parameters (such as precipitation), length of time from completion, length of time since the distress appeared. A careful review of Tables 6.11 and 6.12 indicates that materials retrieved from the trenches at the same sites are more or less similar for almost all the tests carried out. Therefore, the reason for distress is either poor construction practice or transient changes in parameters such as moisture that may not be present at the time of trenching. For example, the Odessa site was tested shortly after a sizeable rain in the area. In this case, the base at the distressed area (Trench 2) was much wetter than the less-distressed area (Trench 1). In this case, the modulus from DSPA from Trench 2 is about half the modulus from Trench 1. During a forensic study in the same vicinity during an extended period of no participation, the base in the distressed area was significantly stiffer than the base in the intact area.

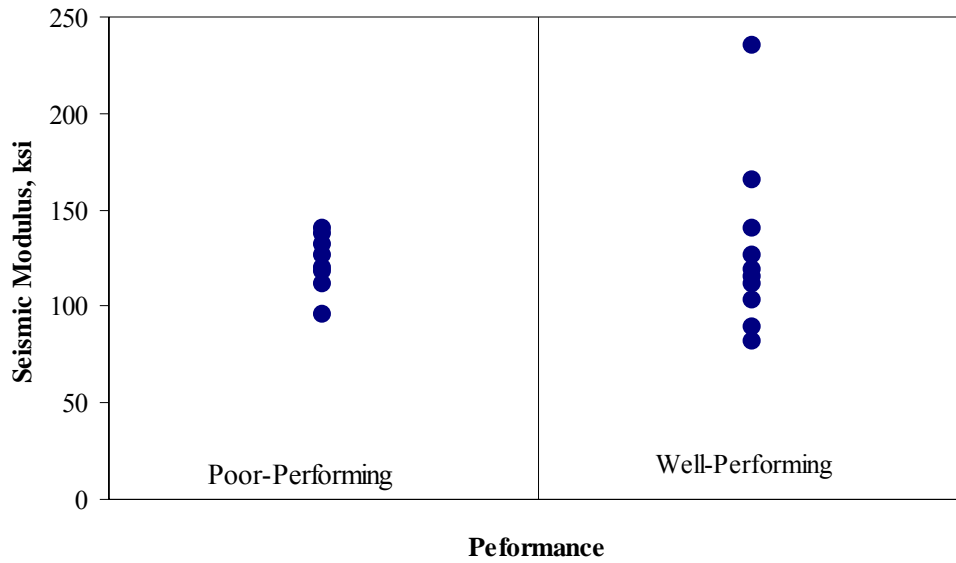


Figure 6.15 – Performance as Related to Seismic Modulus with DSPA

Generally, the DSPA would be a good tool for material characterization for old pavements at a given time, but without companion lab testing judging the relative quality of the material would be difficult. That is why, as proposed in Chapter 3, the quality management with the DSPA on the new project should be supplemented by field tests.

As indicated in Chapter 4, the third step of the proposed protocol consists of simulating seasonal variation in modulus. In that step, the variation in modulus and moisture with time is monitored first by drying back the specimen and then by allowing it to soak water. Typical results from a base material in El Paso are shown in Figure 6.16. Shortly after the specimen is prepared, the

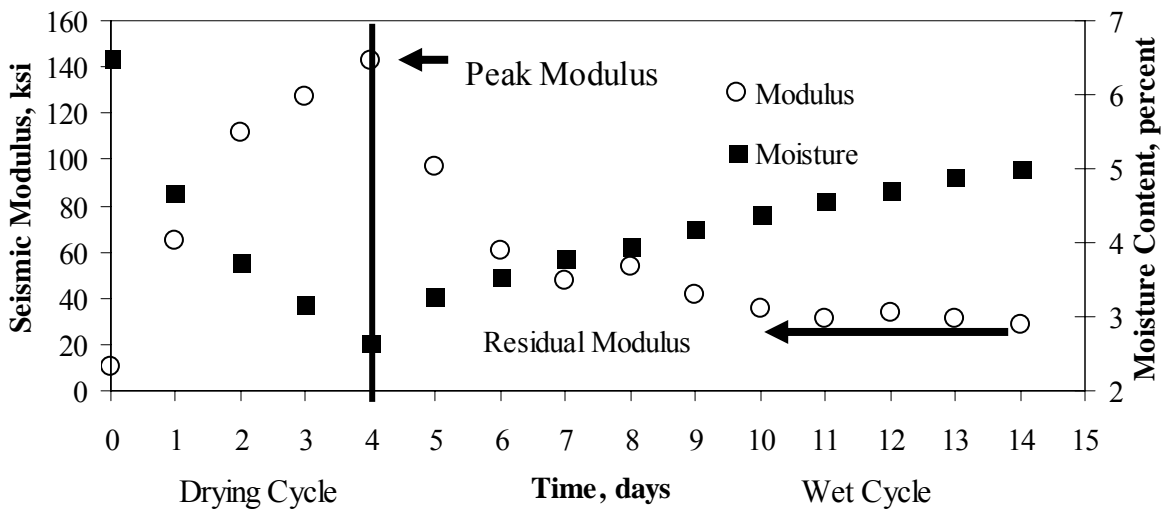


Figure 6.16 – Variation in Modulus and Moisture Content with Time for a Typical Base

modulus is about 10 ksi (70 MPa). However, after 24 hours the modulus is increased to about 60 ksi (420 MPa). In the first 24 hours, the moisture content is reduced from 6.5% (close to optimum moisture content) to about 5%. After 4 days of dry back, the modulus is about 140 ksi (960 MPa). However, after the specimen is exposed to water, the modulus drops drastically to about 30 ksi (210 MPa). The modulus at the completion of dry back period is called the peak modulus. Similarly, the modulus after the completion of soaking is called the residual modulus. Another performance indicator seems to be the ratio of the residual modulus to the peak modulus. In this case, the residual modulus is about 21% of the peak modulus.

We attempted to relate the performance to the ratio of the residual modulus and the peak modulus for all sites. This parameter is called the modulus ratio in Table 6.12. The variation between the performance and the modulus ratio is shown in Figure 6.17. It seems that for the existing database as long as the modulus ratio is greater than 0.4. The material is exhibiting a satisfactory performance.

In general, some promising trends between performance and the parameters measured from materials retrieved from the trenches have been observed. However, more data and experience are needed to establish definite values.

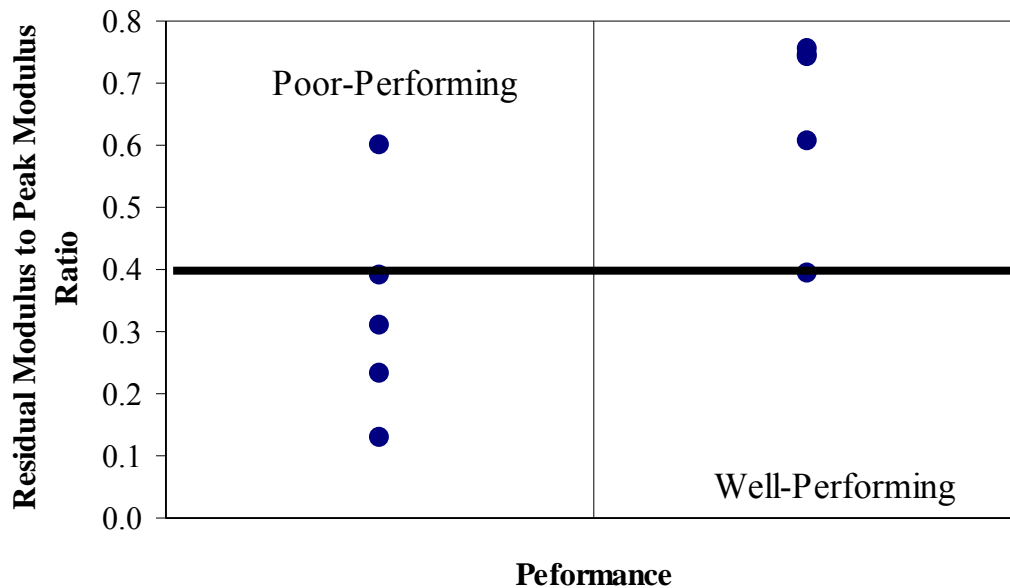


Figure 6.17 – Performance as Related to Seismic Modulus Ratio

Chapter 7

Closure

The focus of the study has been on measuring moduli with four inter-related seismic devices that measure moduli of materials nondestructively. Two of these are laboratory devices: the free-free resonant column device for testing base and subgrade and the ultrasonic device for testing AC cores and briquettes. The other two are field devices: the Portable Seismic Pavement Analyzer (PSPA) for testing AC layers and a version of it that works on the base and prepared subgrade layers (affectionately called DSPA for Dirt Seismic Pavement Analyzer).

Procedures have been developed to measure the moduli of each pavement layer shortly after placement and after the completion of the project. These procedures allow rapid data collection and interpretation. Thus, any problem during construction process can be identified and adjusted. The outcomes from this project exhibit that the proposed equipment and methodologies may strike a balance between the existing level of sophistication in the design methodology, laboratory testing and field testing. Performing the simplified laboratory and field tests along with more traditional tests may result in a database that can be used to smoothly unify the design procedures and construction quality control.

The major advantage of seismic methods is that similar results are anticipated from the field and laboratory tests as long as the material is tested under comparable conditions. This unique feature of seismic methods in material characterization is of particular significance, if one is interested in implementing performance-based specifications. The use of seismic moduli in pavement design, which is the other issue of significance, is currently being addressed under Project 0-1780 entitled Design Moduli from Seismic Measurements.

This report contains the results of an effort to address the issues related to the implementation of the methods and devices recommended in the day-to-day operation of TxDOT. The major issues addressed are the repeatability, reproducibility of the methods, means of relating the measured parameters to the design moduli, and relating the parameters to performance of the pavement.

For the AC layer, it was found the methodology proposed can be utilized to determine the quality of the completed layer. Through the complex modulus tests, the measured modulus can be readily related to the design modulus. The methods have also shown some potential in terms of estimating the degree of compaction for a given mixture. The primary construction parameter that impacts the seismic modulus seems to be the voids in total mix.

For the base layers, the method is well suited. The seismic modulus was related to the resilient modulus values for design purposes and to the angle of internal friction for material selection. The primary parameter that impacts the seismic modulus of base layer is the moisture content. Based on the results from eighteen sites within the state of Texas, the seismic moduli obtained from the free-free resonant column tests can be related to the performance.

An implementation project has already been approved for this project. The tasks to be undertaken as per the implementation plan are:

- Develop and deliver a comprehensive training course for engineers and technicians who conduct tests
- Assist TxDOT personnel to evaluate and modify procedures and test equipment to ensure their usefulness, user friendliness and versatility
- Recommend initial specifications for implementation of the methods by TxDOT personnel
- Compare existing QC/QA results with the outcome of these methods
- Recommend final specifications

References

- Abdallah, I., and Nazarian, S. (2003), "Program SMART: Determination of Nonlinear Parameters of Flexible Pavement Layers from Nondestructive Testing," Research Report 1780-4, Center for Highway Materials Research, the University of Texas at El Paso, TX
- Alexander, D. R. (1996), "In Situ Strength Measurements with Seismic Methods," Report from US Army Engineer Waterways Experiment Station, Vicksburg, Mississippi for the US Air Force Civil Engineering Support Agency, Tyndall AFB, Florida.
- Aouad, M. F., Stokoe, K. H., and Briggs, R. C. (1993), "Stiffness of Asphalt Concrete Surface Layer from Stress Wave Measurements," Transportation Research Board, No. 1384, Washington, DC, pp. 29-35.
- Barksdale, R. D., Alba, J., Khosla, P. N., Kim, R., Lambe, P. C., and Rahman, M. S. (1997), "Laboratory Determination of Resilient Modulus for Flexible Pavement Design," NCHRP Web Document 14, Federal Highway Administration, Washington, D.C., 486p.
- Ferry, J.D. (1970), "Viscoelastic Properties of Polymers," 2nd edition, John Willy, New York.
- Ke, L., Nazarian, S., Abdallah, I., and Yuan, D. (2001) "A Sensitivity Study of Parameters Involved in Design with Seismic Moduli," Research Report 1780-2, Center for Highway Materials Research, The University of Texas at El Paso, El Paso, TX.
- Kramer, S.L. (1996), Geotechnical Earthquake Engineering, Prentice Hall, Inc., Upper Saddle River, California.
- Naik, T. R., and Malhotra, V. M. (1991), Handbook on Nondestructive Testing of Concrete, CRC Press, Boca Raton, FL., pages 169-188.

- Nazarian, S., Baker, M., and Crain, K. (1997), "Assessing Quality of Concrete with Wave Propagation Techniques," *Materials Journal*, American Concrete Institute, Farmington Hills, MI, Vol. 94, No. 4, pp. 296-306.
- Nazarian, S., Yuan, D., and Tandon, V. (1999), "Structural Field Testing of Flexible Pavement Layers with Seismic Methods for Quality Control," *Transportation Research Record* 1654, Washington, DC, pp. 50-60.
- Richart, Jr., F.E., Woods, R. D., Hall Jr., J.R. (1970) *Vibrations of Soils and Foundations*, Prentice-Hall, Inc., Englewood Cliffs, NJ.
- Saarenketo, T and Scullion, T (1997) "Using Suction and Dielectric Measurements as Performance Indicators for Aggregate Base Materials," *Transportation Research Record* 1577, pp 37-44.
- Saeed, A., Hall, J. W Jr. (2001), "Determination of In Situ Material Properties of Asphalt Concrete Pavement Layers," Final Report for NCHRP, TRB and NRC, ERES Consultant Division of Applied Research Associates, Inc., 112 Monument Place, Vicksburg, Mississippi.
- Witzak, M.W., Bonaquist, R., Von Quintus, H., and Kaloush, K. (1999) "Specimen Geometry and Aggregate Size Effects in Uniaxial Compression and Constant Height Shear Tests," *Journal of Association of Asphalt Paving Technologist*, Volume 69, pp 733-793.

APPENDIX A
RESULT OF TTI

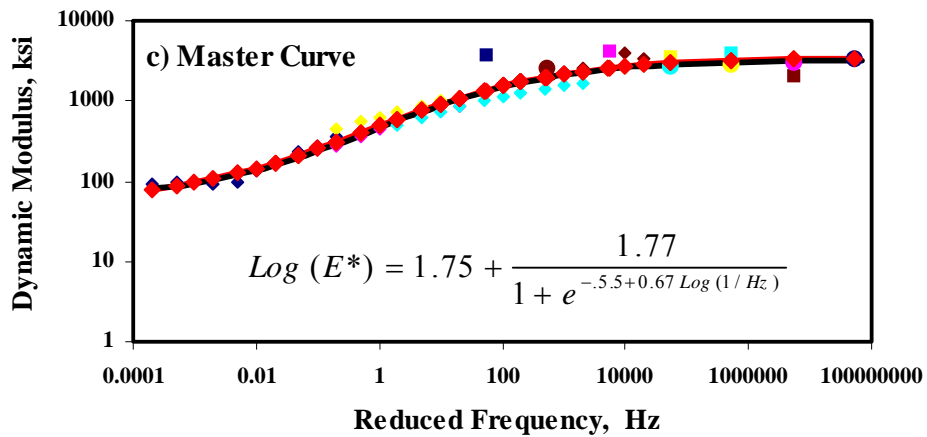
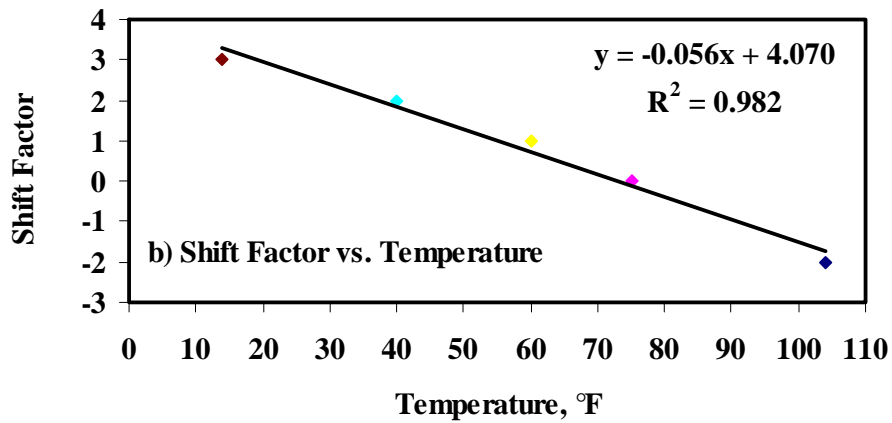
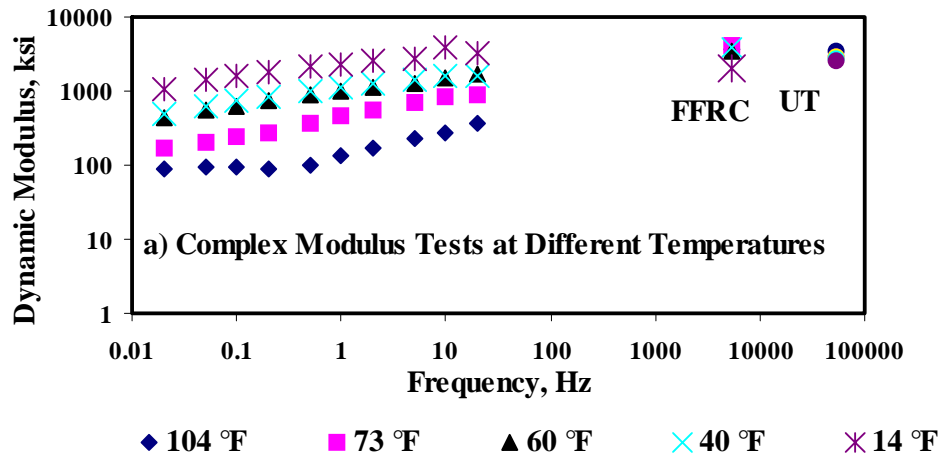


Figure A.1 - Data for Section 1-4

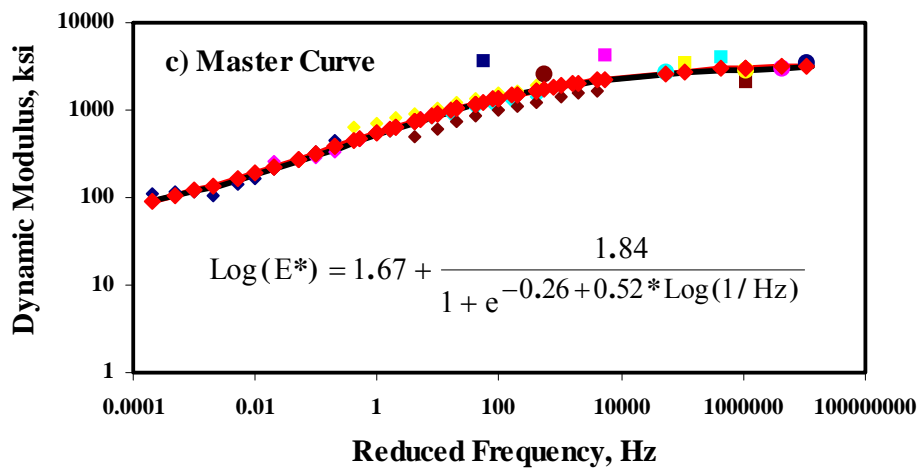
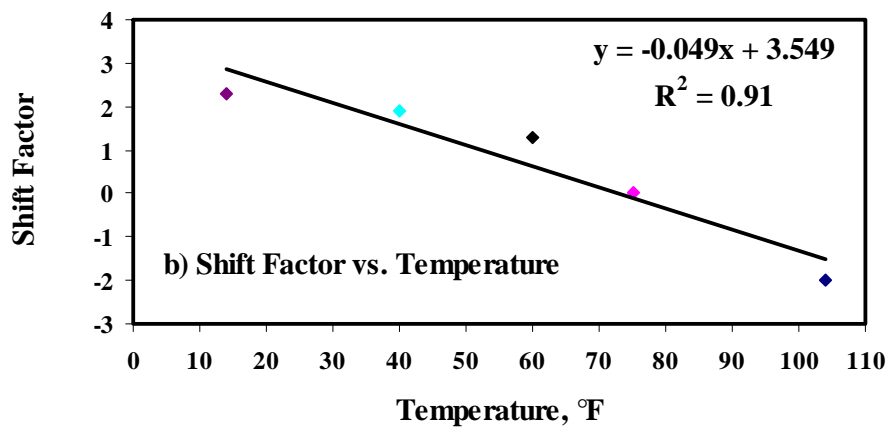
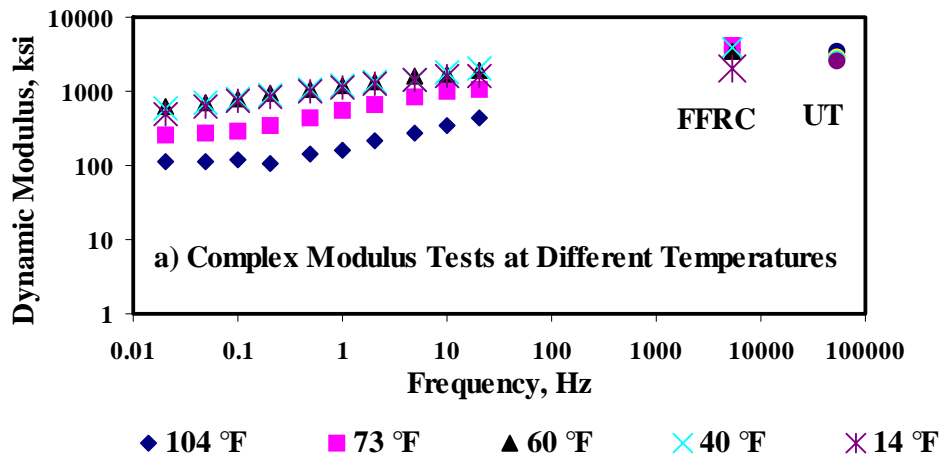


Figure A.2 - Data for Section 1-3

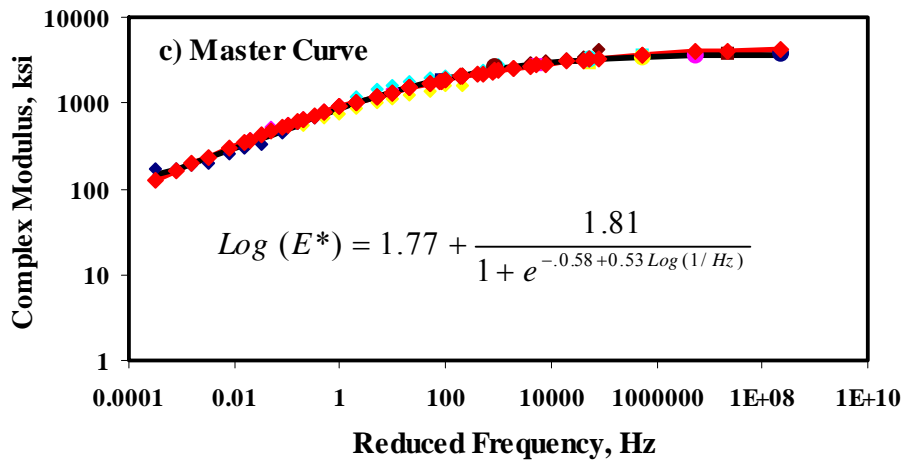
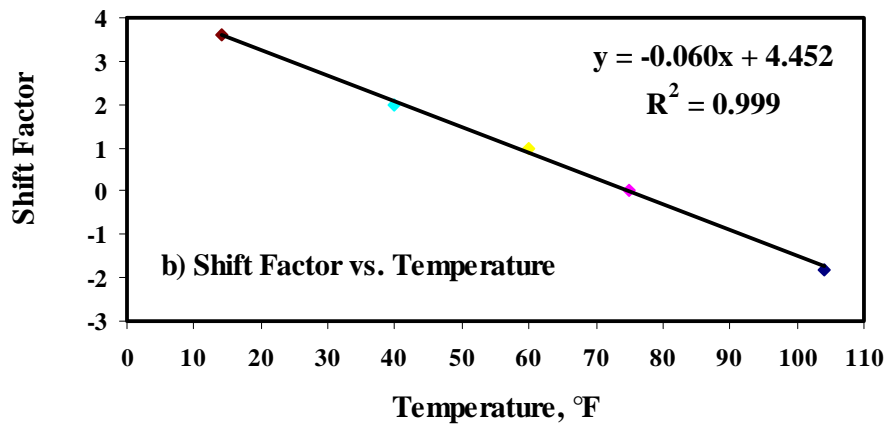
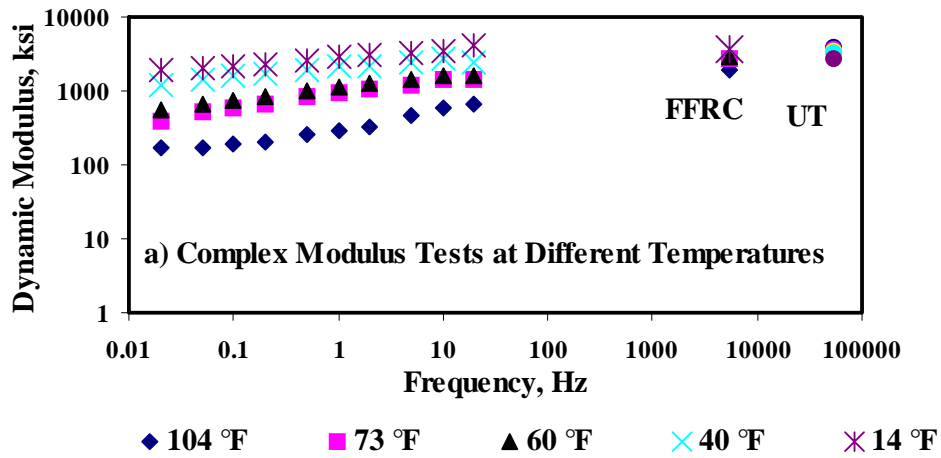


Figure A.3 - Data for Section 3-1

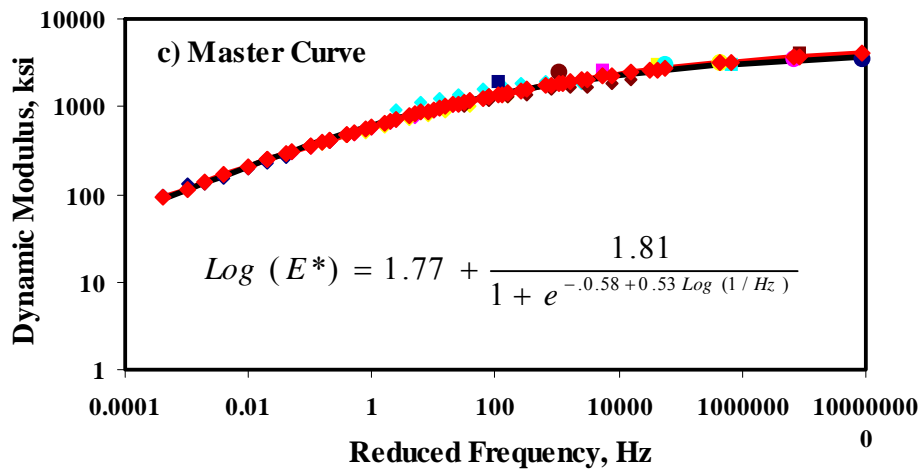
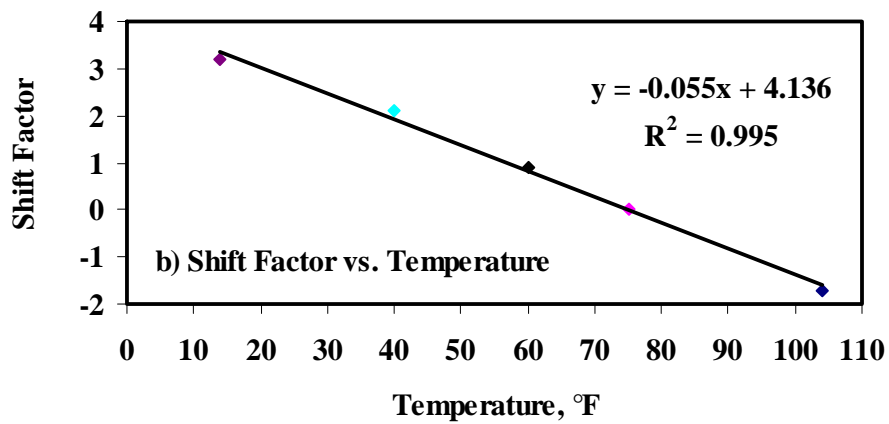
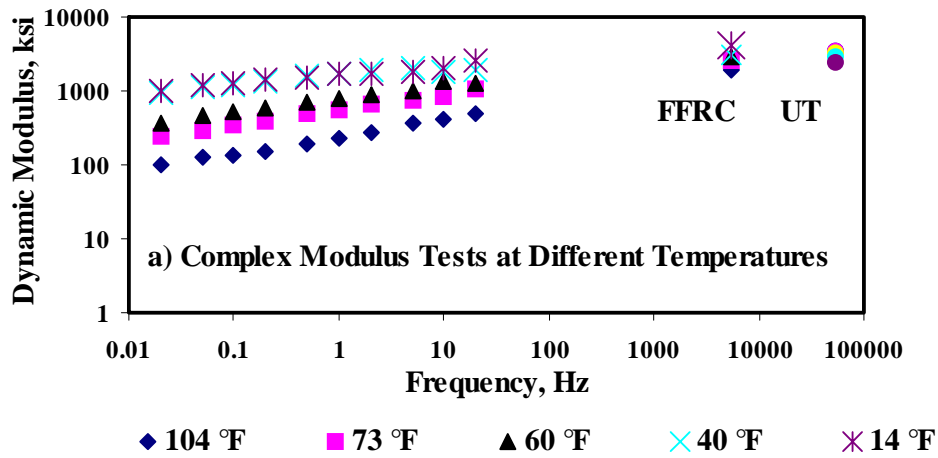


Figure A.4 - Data for Section 3-2

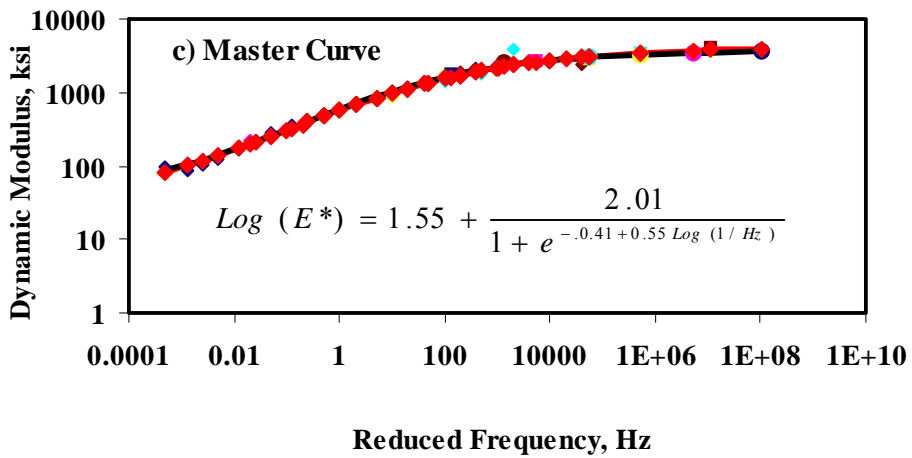
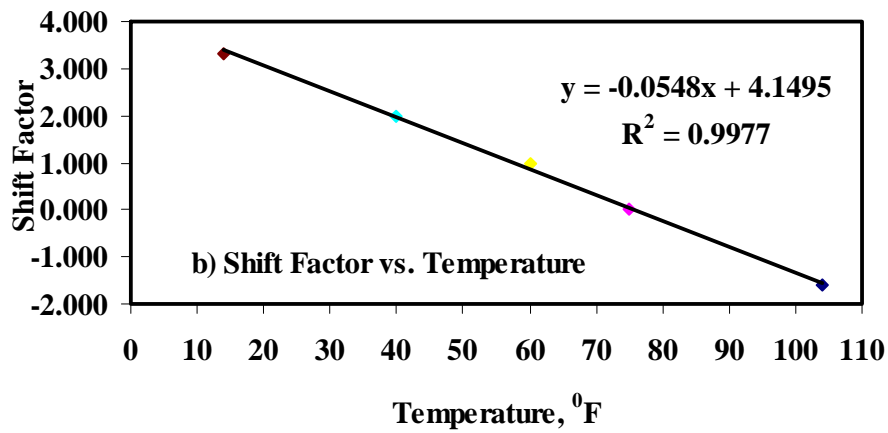
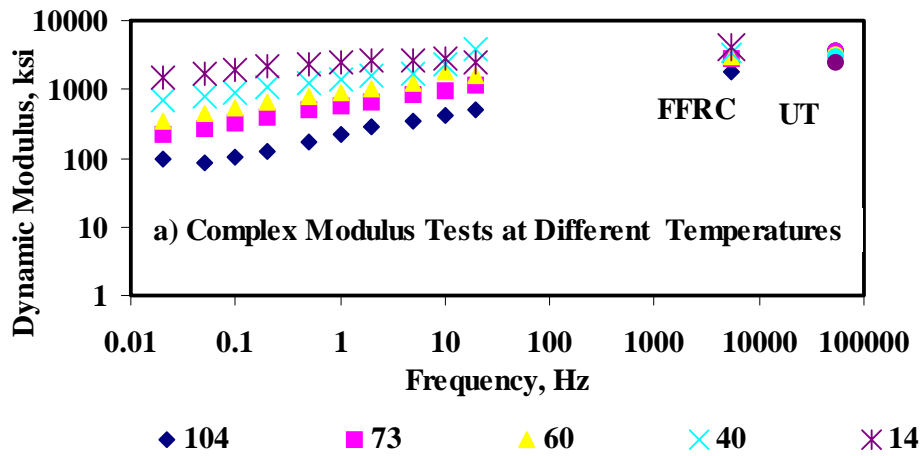


Figure A.5 - Data for Section 3-3

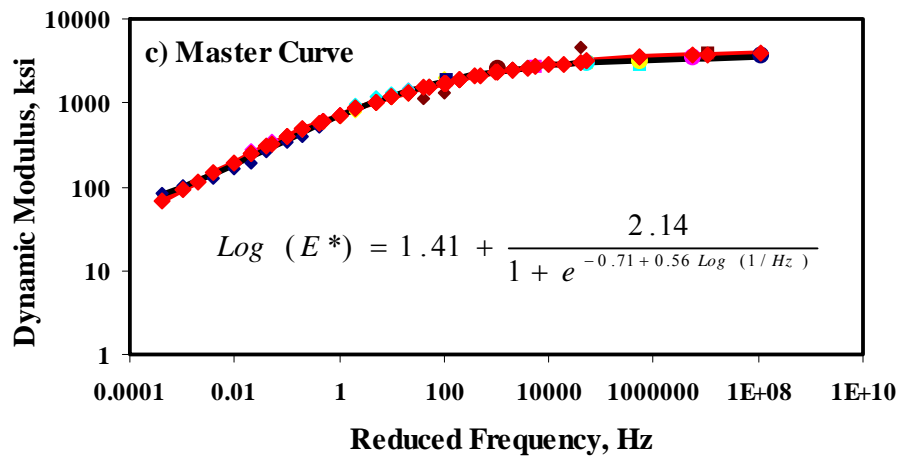
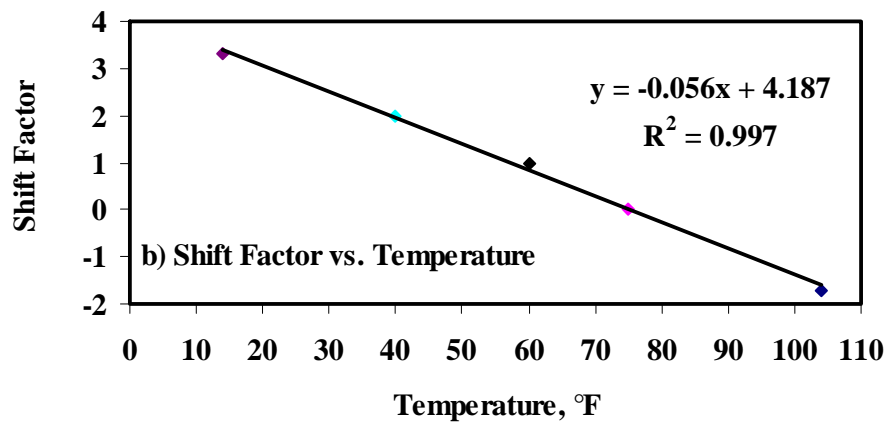
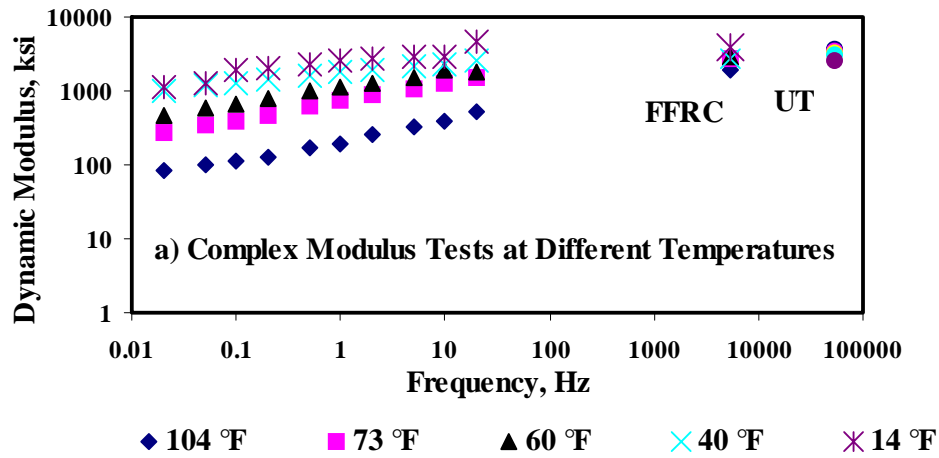


Figure A.6 - Data for Section 3-4

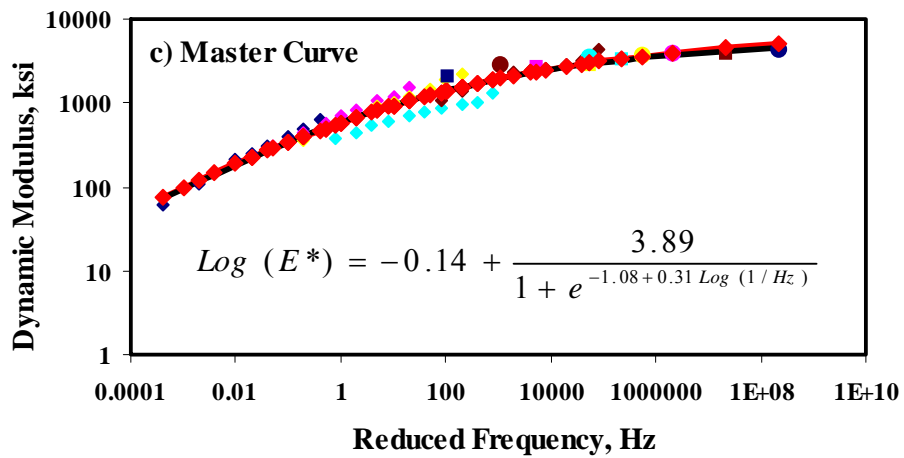
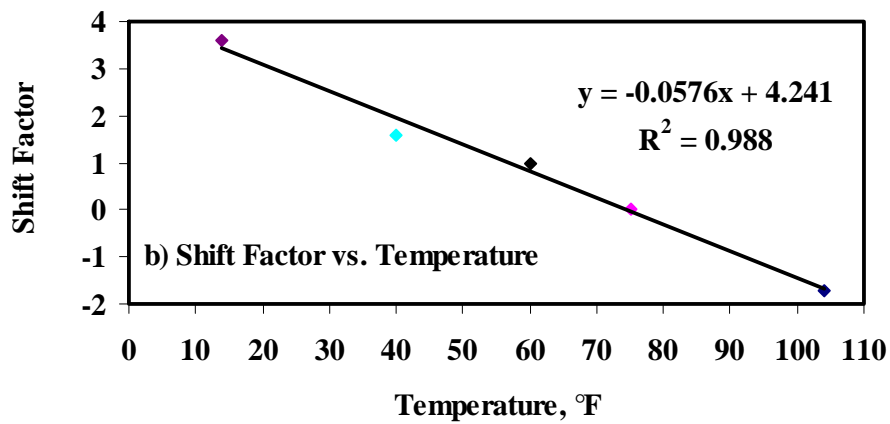
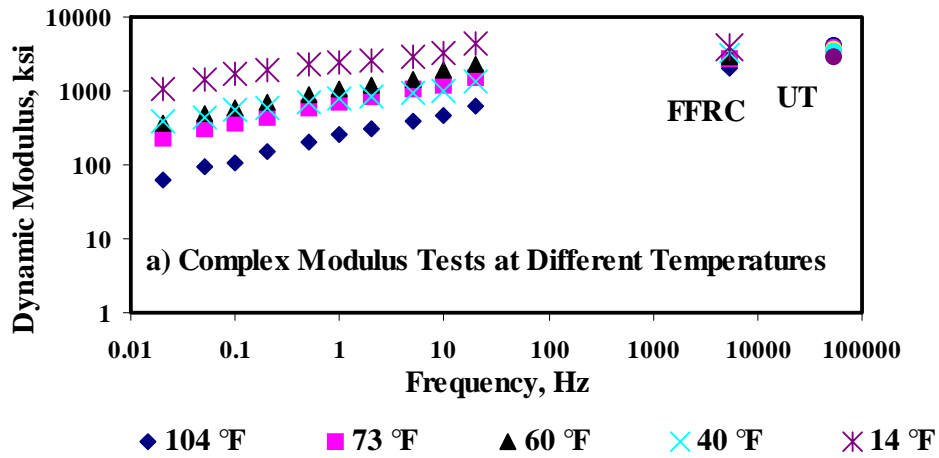


Figure A.7 - Data for Section 4-1

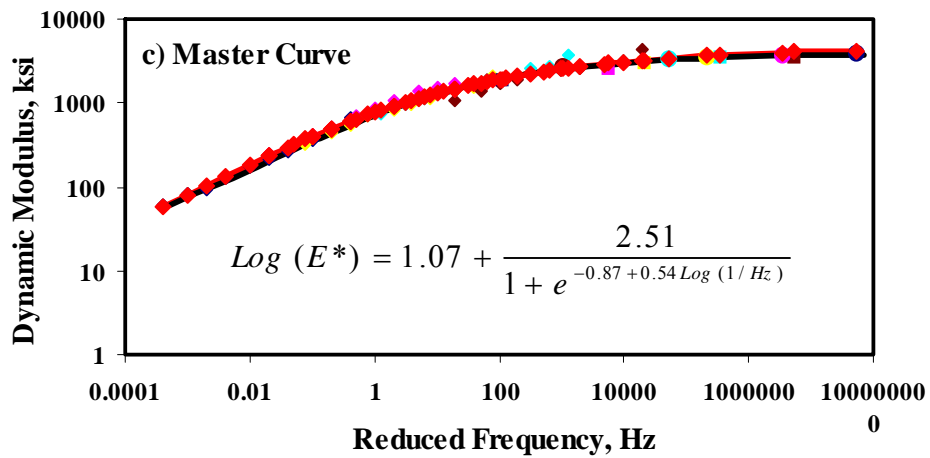
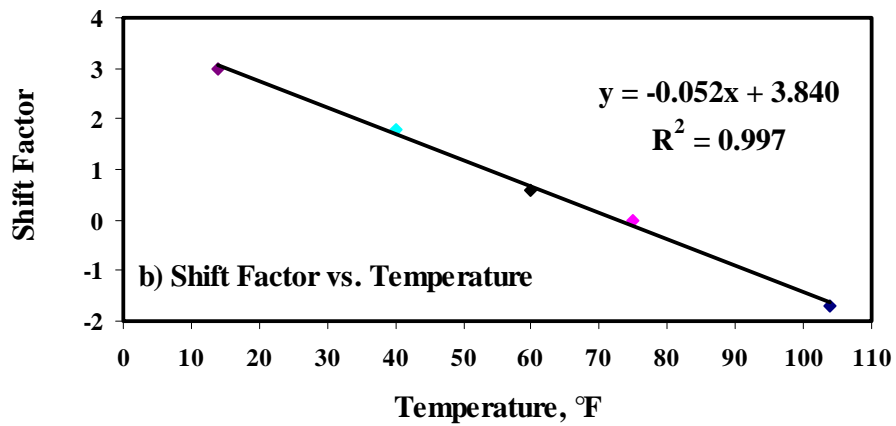
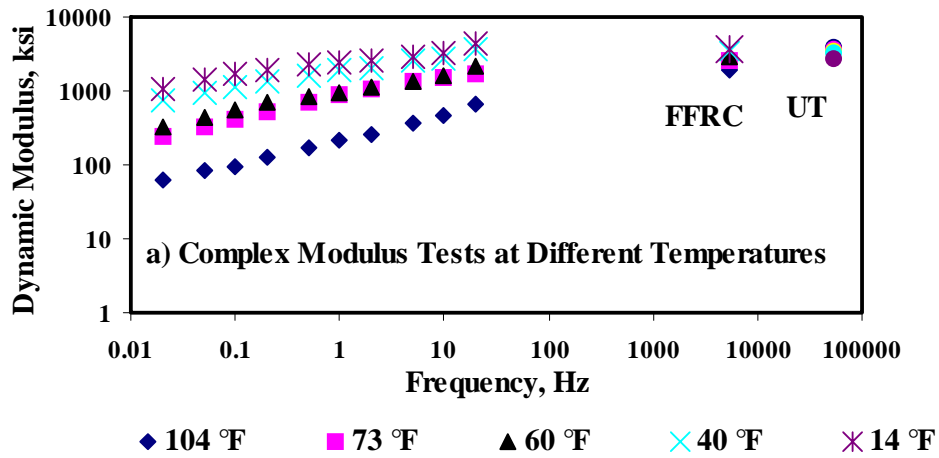


Figure A.8 - Data for Section 4-2

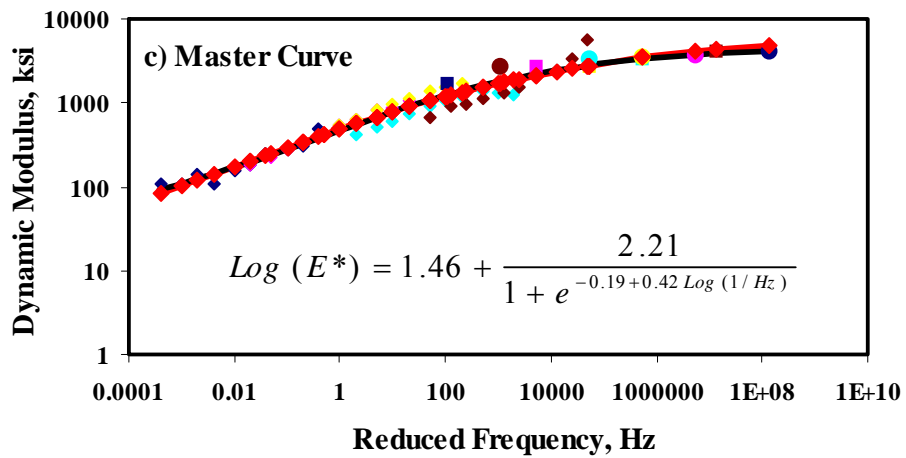
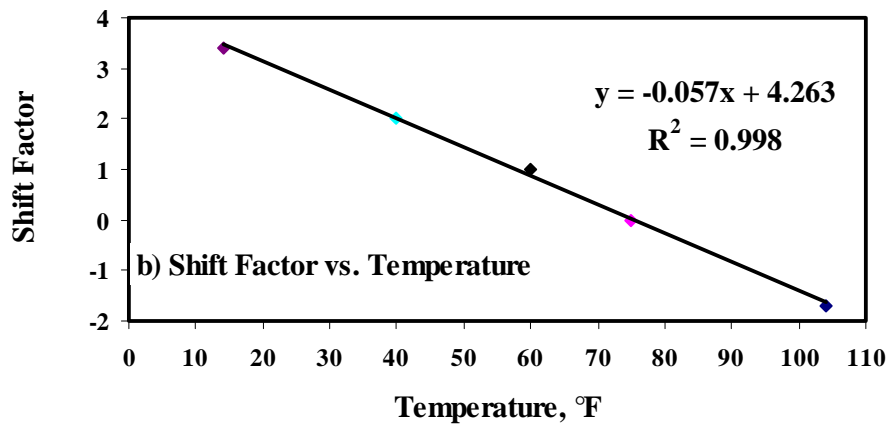
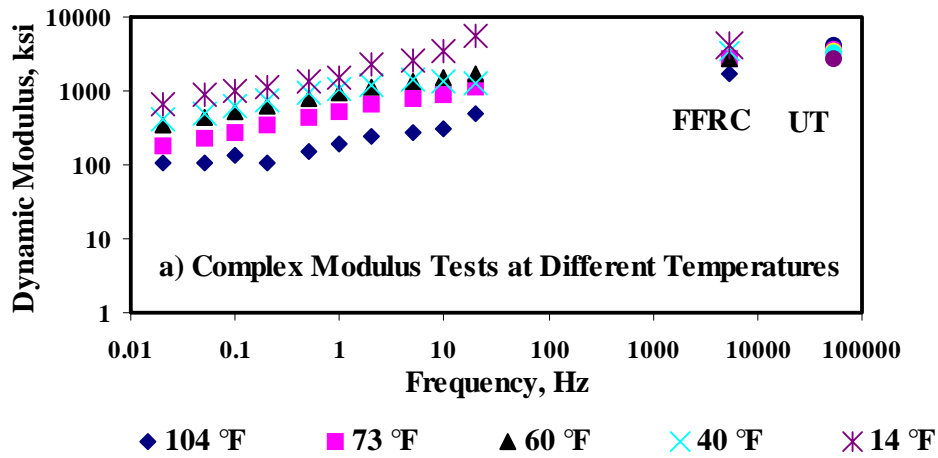


Figure A.9 - Data for Section 4-3

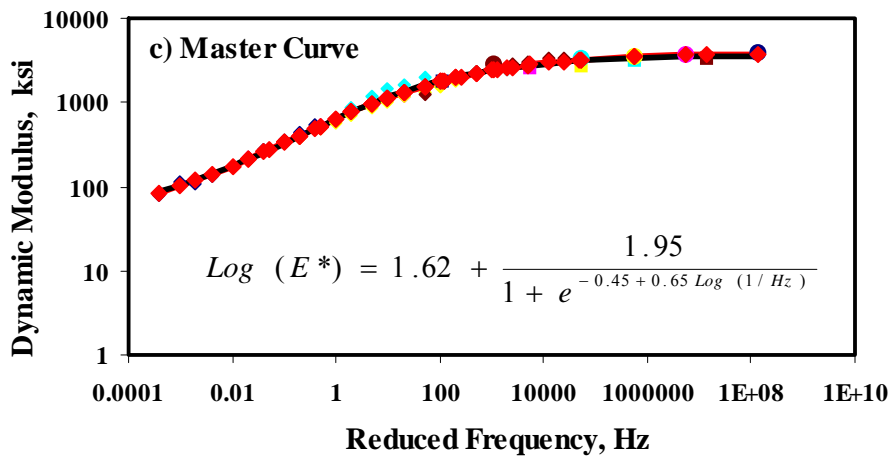
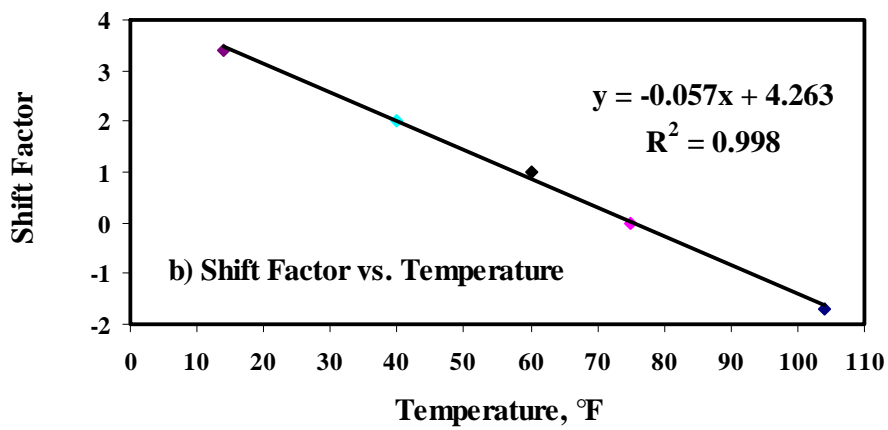
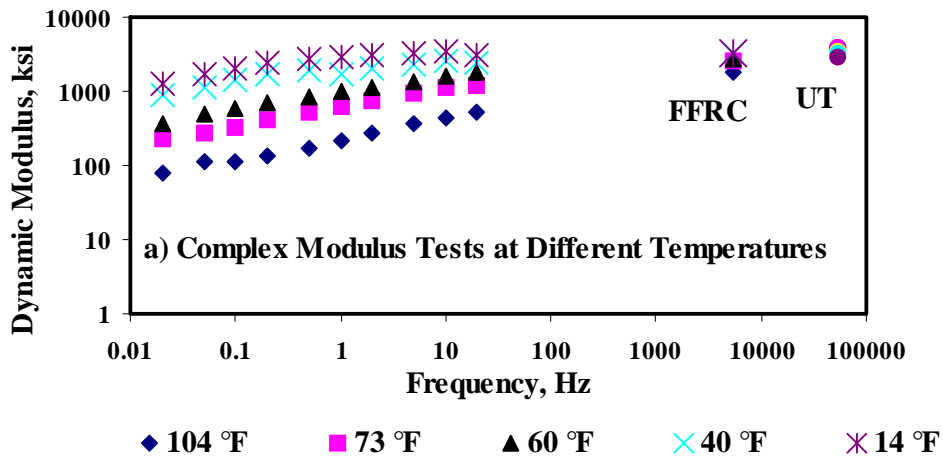


Figure A.10 - Data for Section 4-4

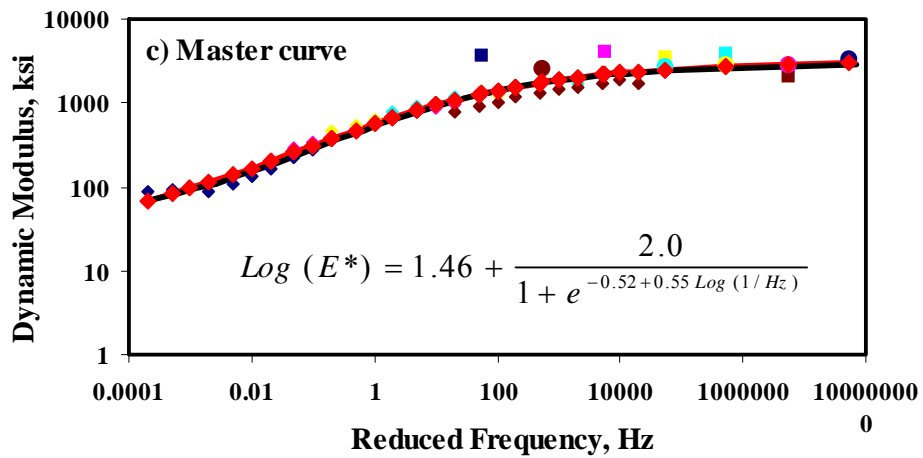
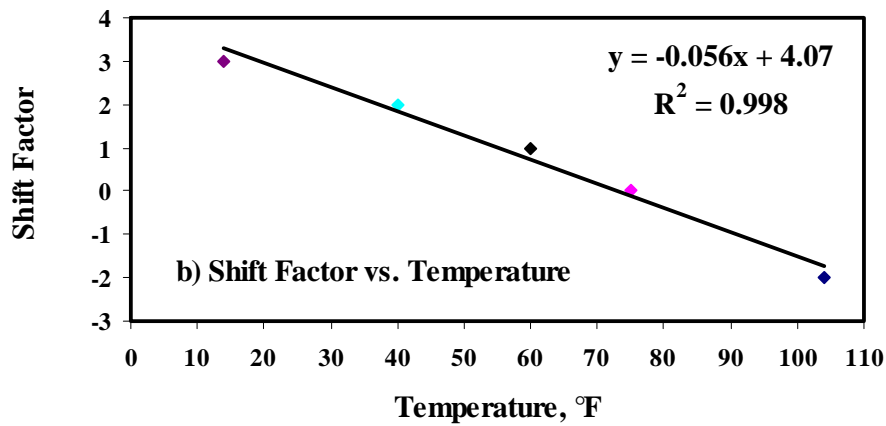
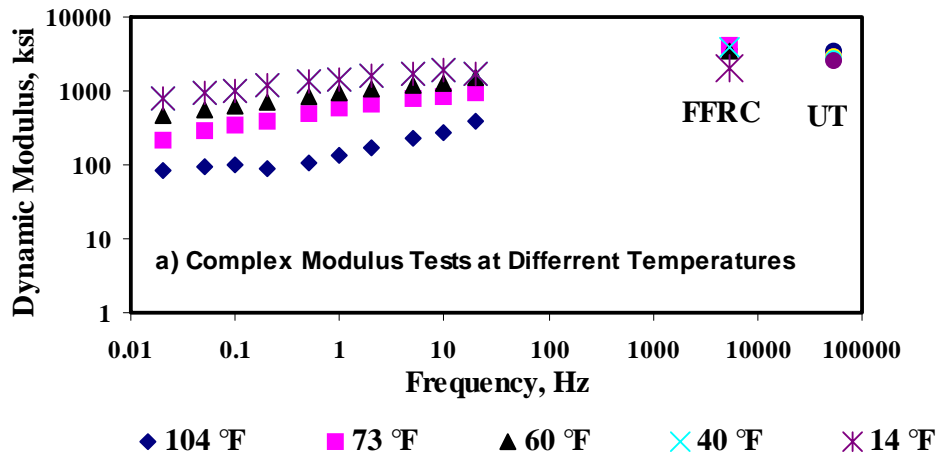


Figure A.11 - Data for Section 5-3

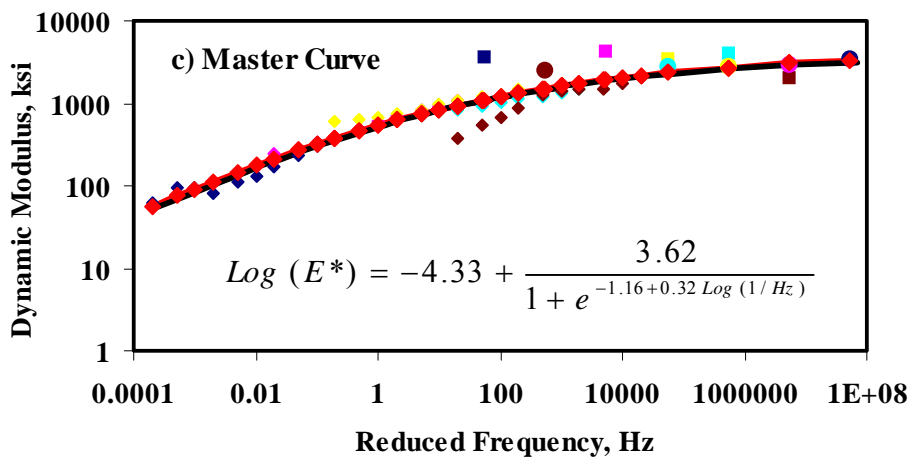
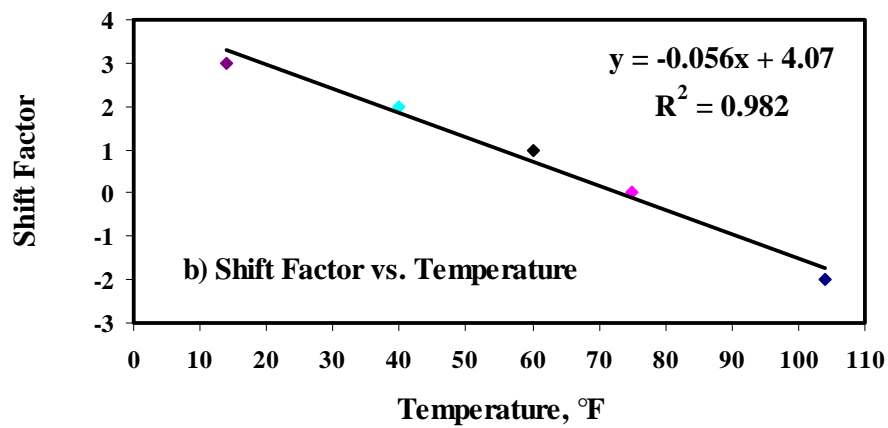
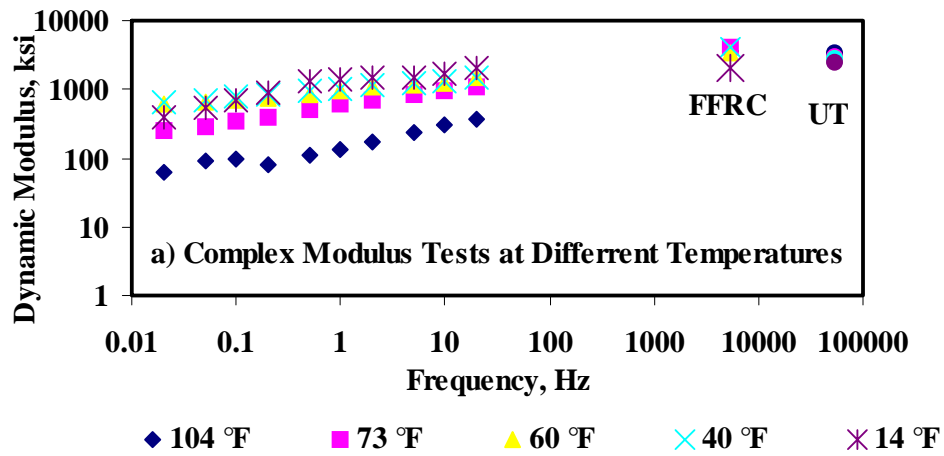


Figure A.12 - Data for Section 5-4

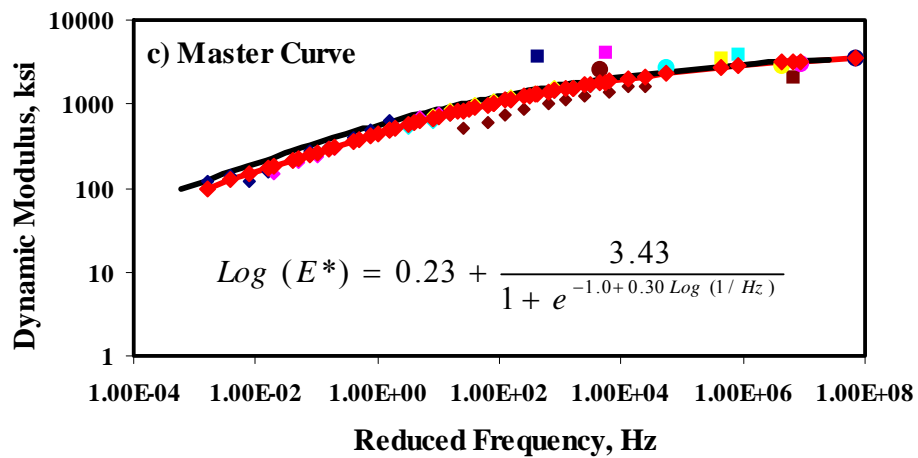
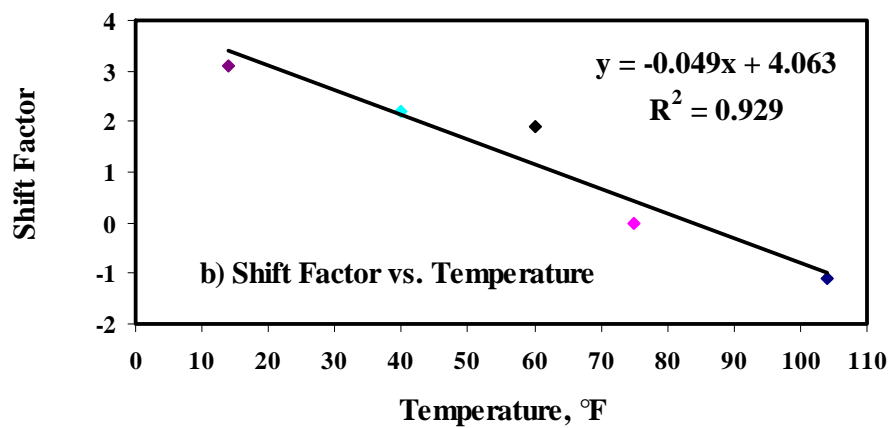
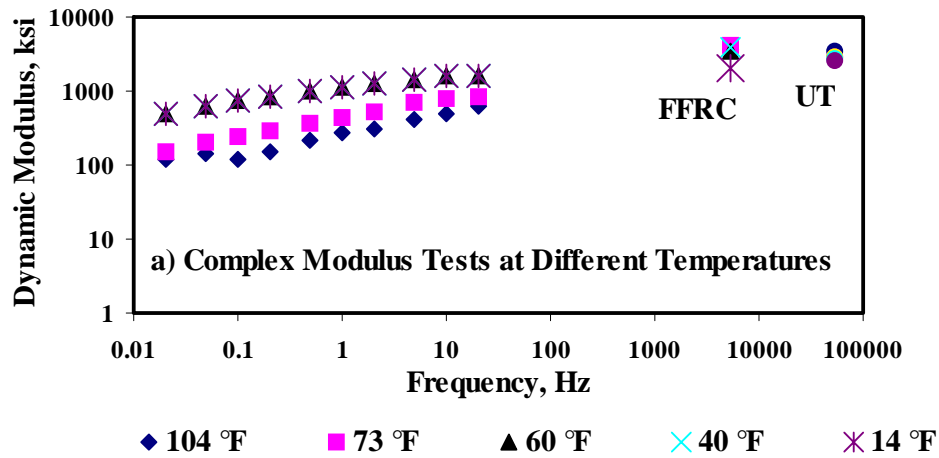


Figure A.13 - Data for Section 6-3

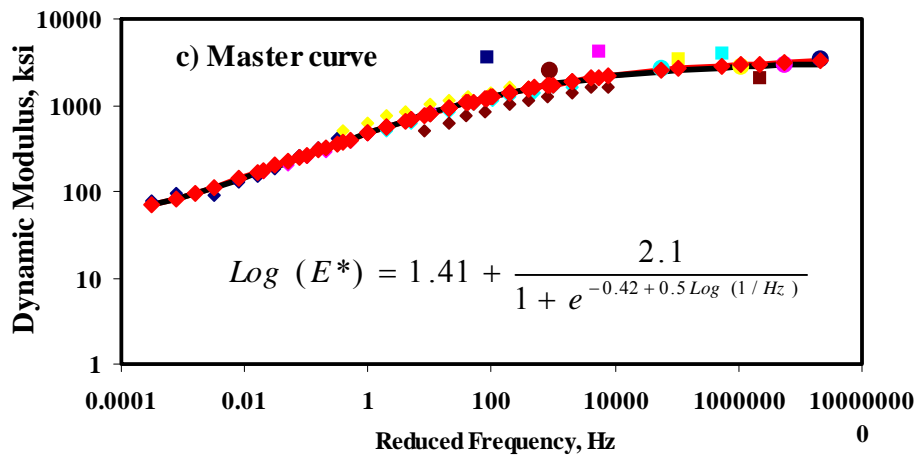
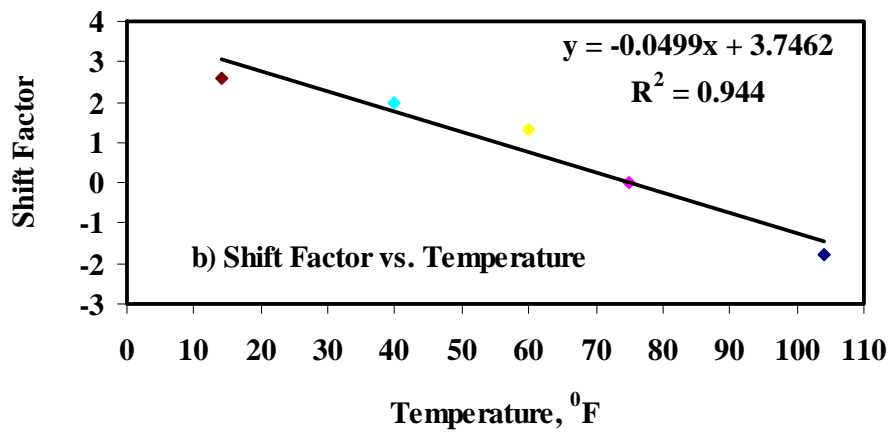
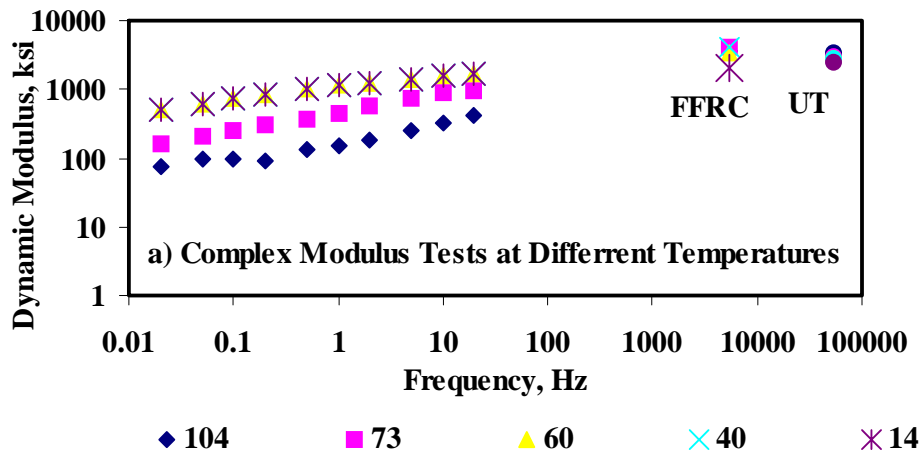


Figure A.14 - Data for Section 6-4

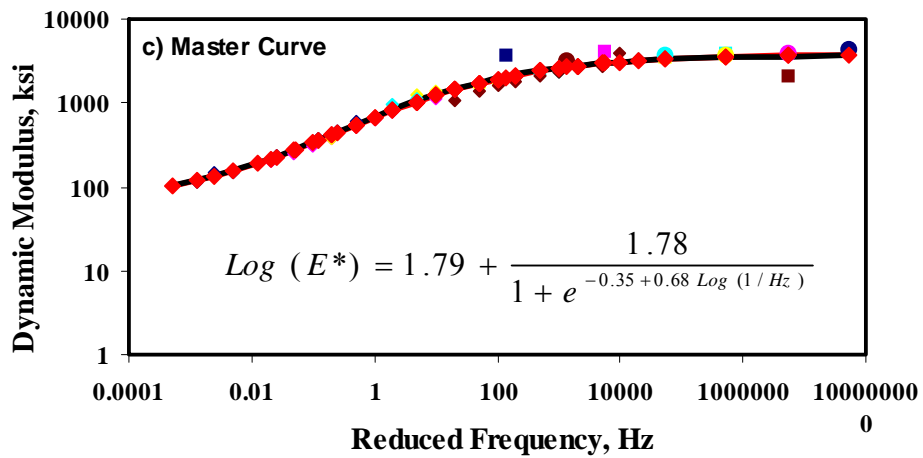
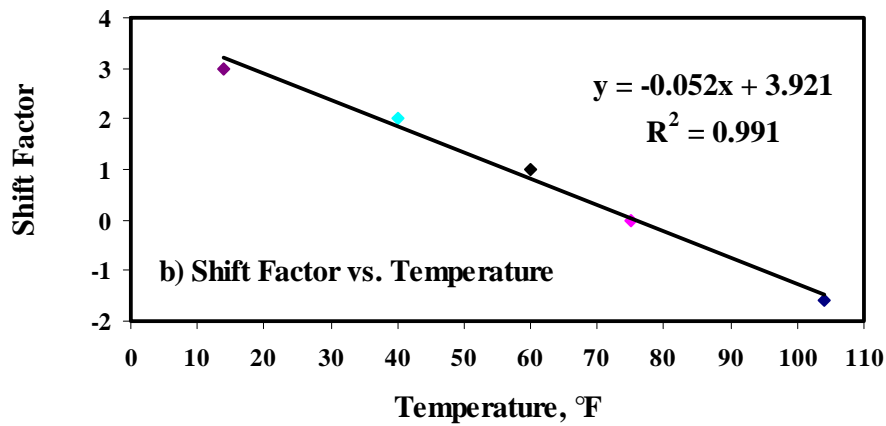
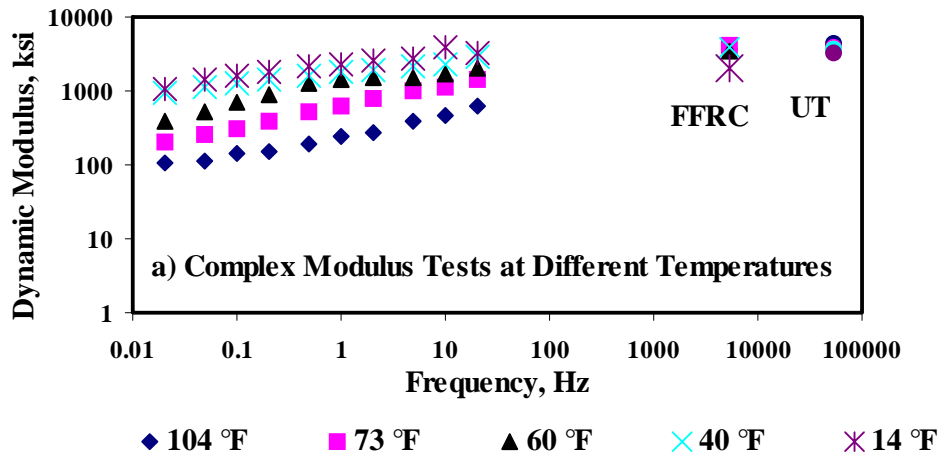


Figure A.15 - Data for Section 7-2

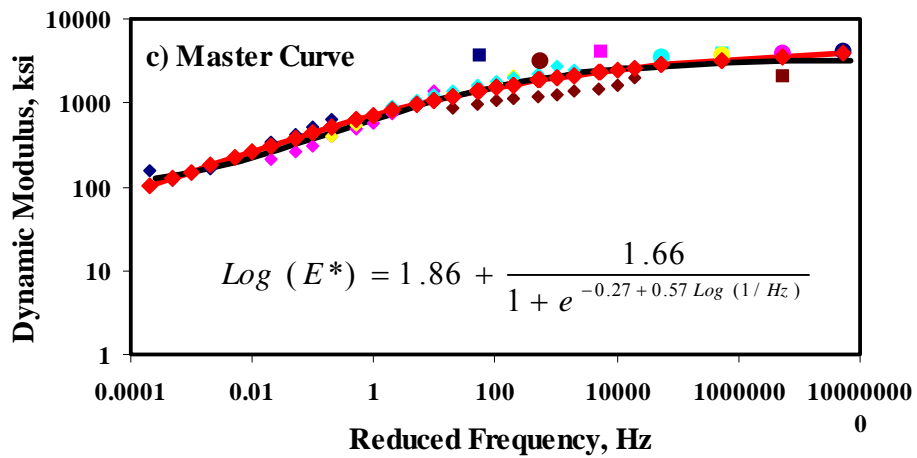
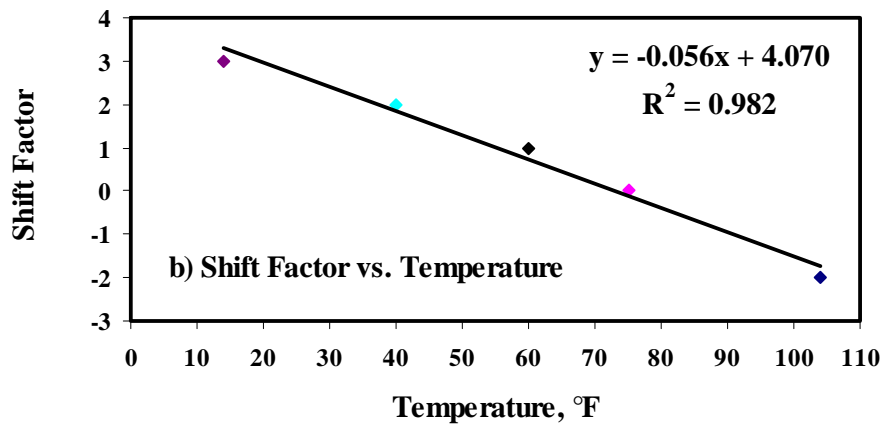
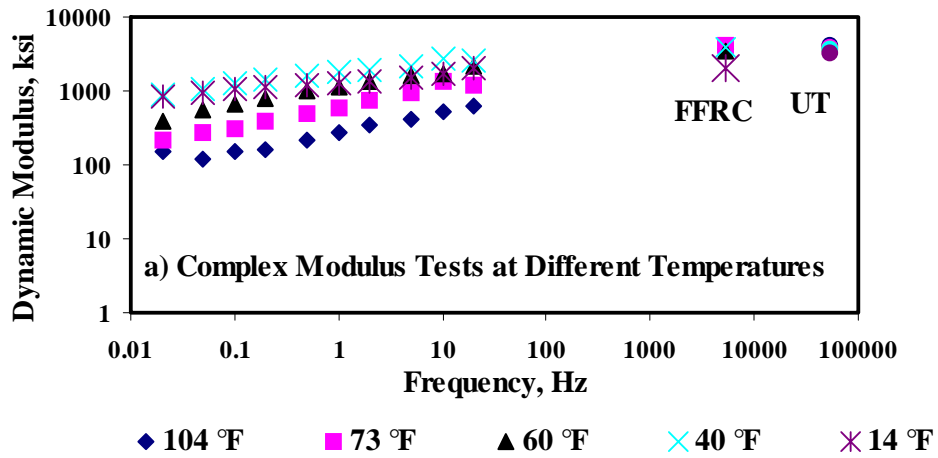


Figure A.16 - Data for Section 7-3

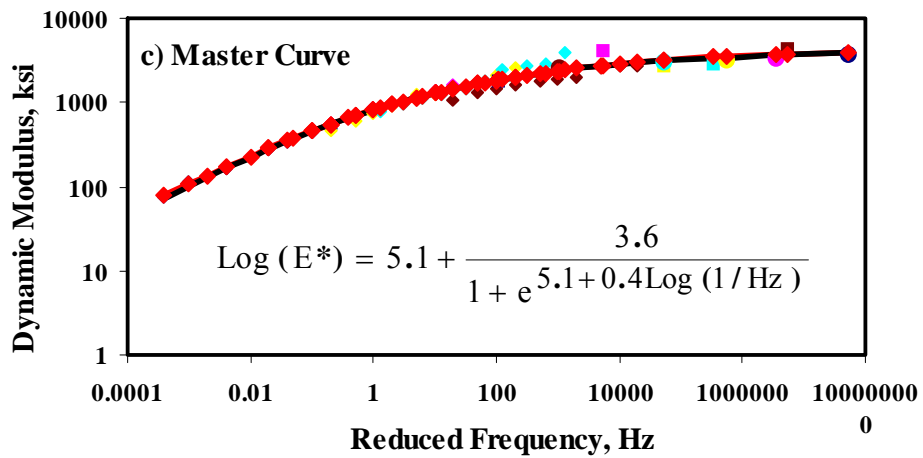
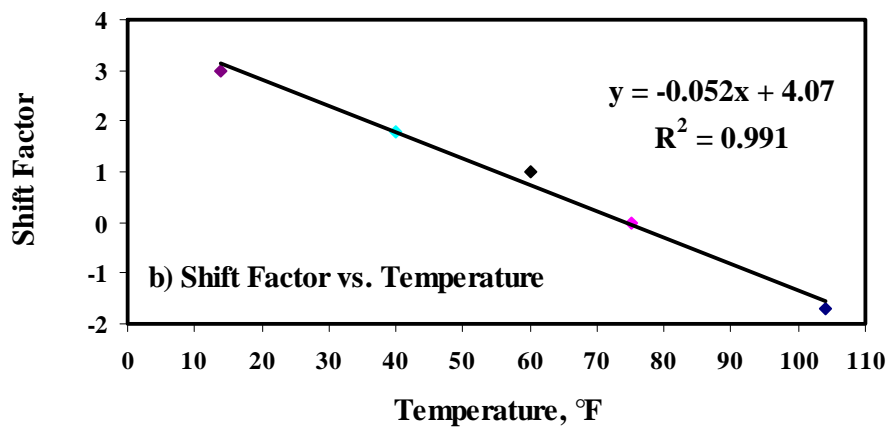
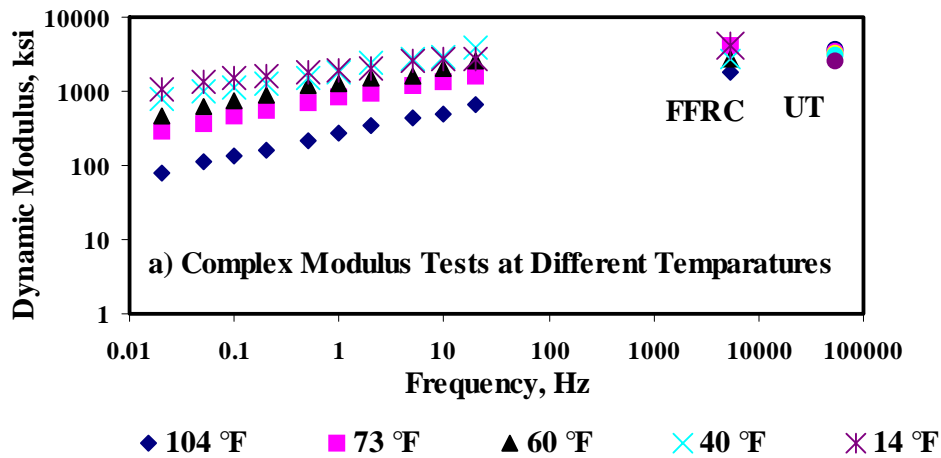


Figure A.17 - Data for Section 8-1

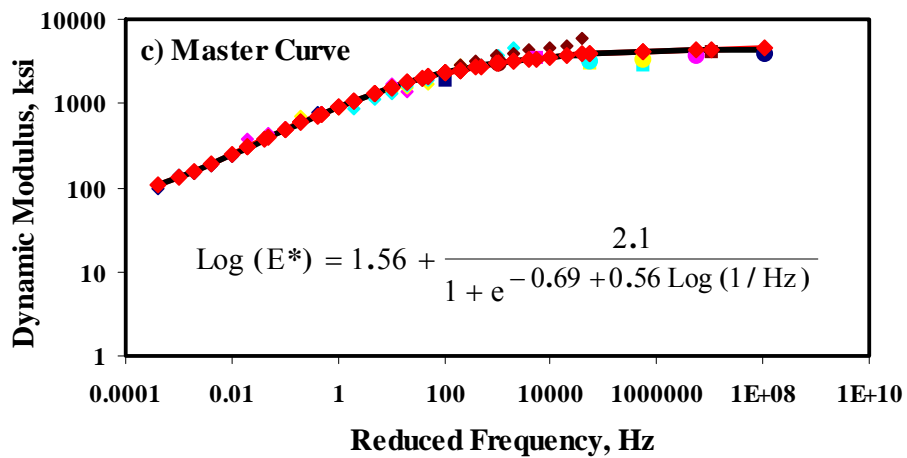
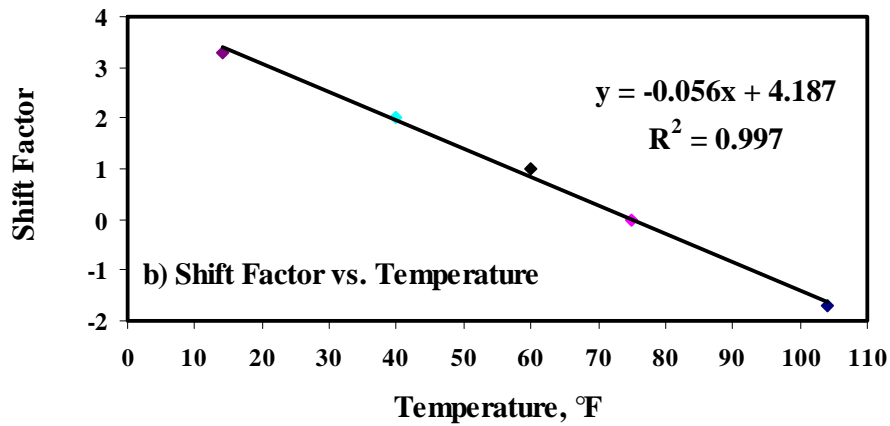
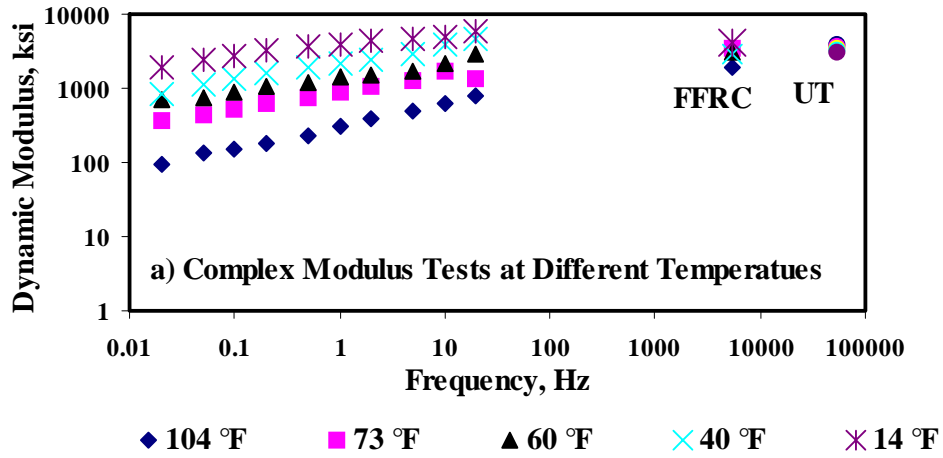


Figure A.18 - Data for Section 8-2

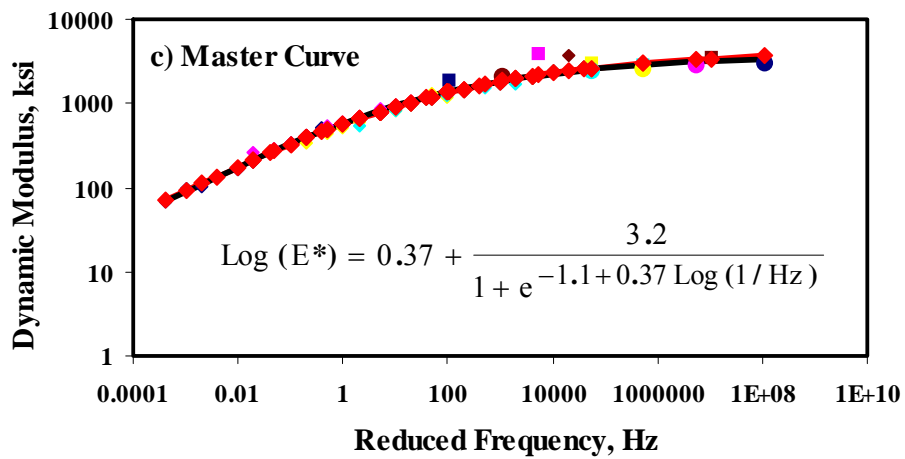
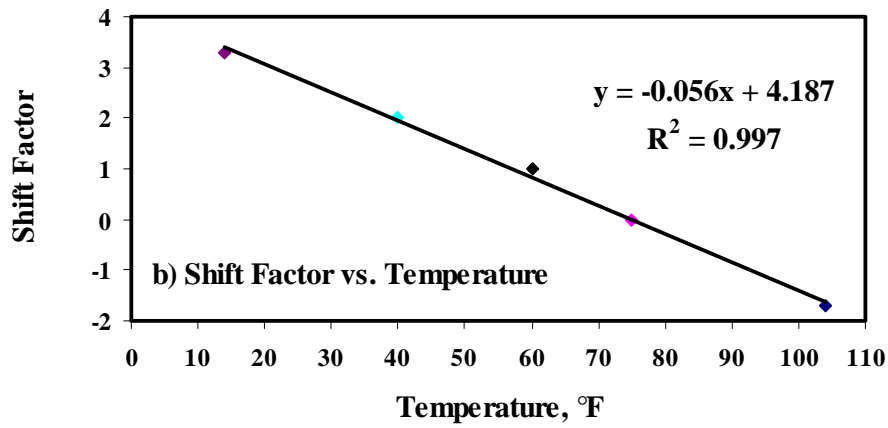
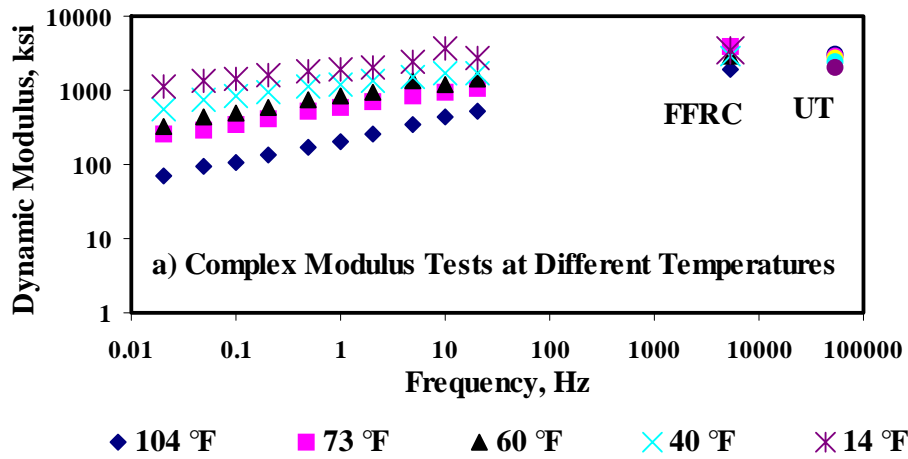


Figure A.19 - Data for Section 8-3

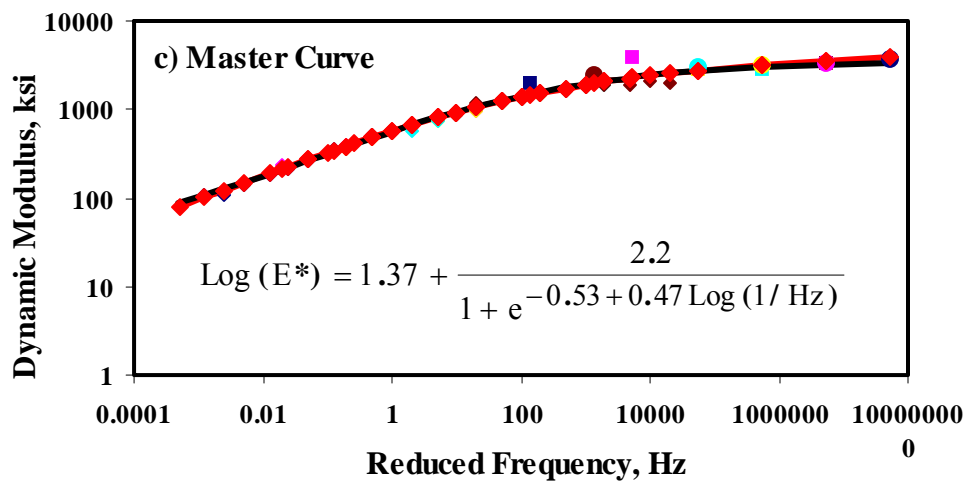
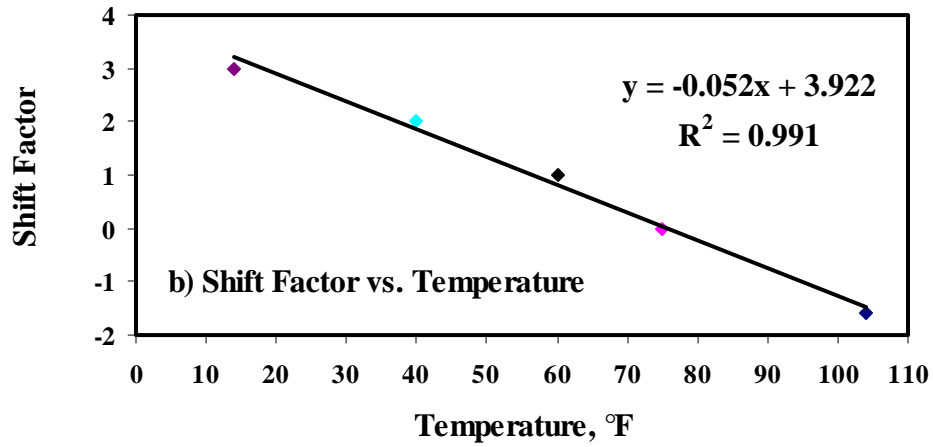
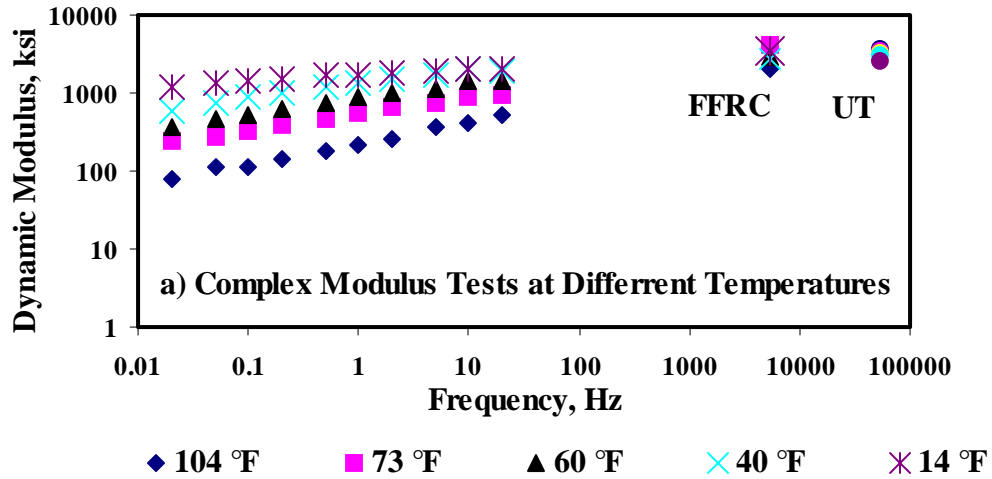


Figure A.20 - Data for Section 8-4

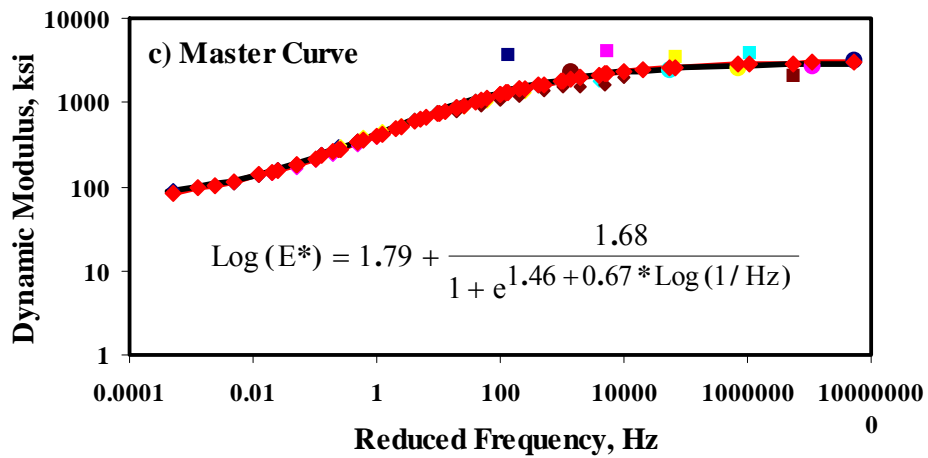
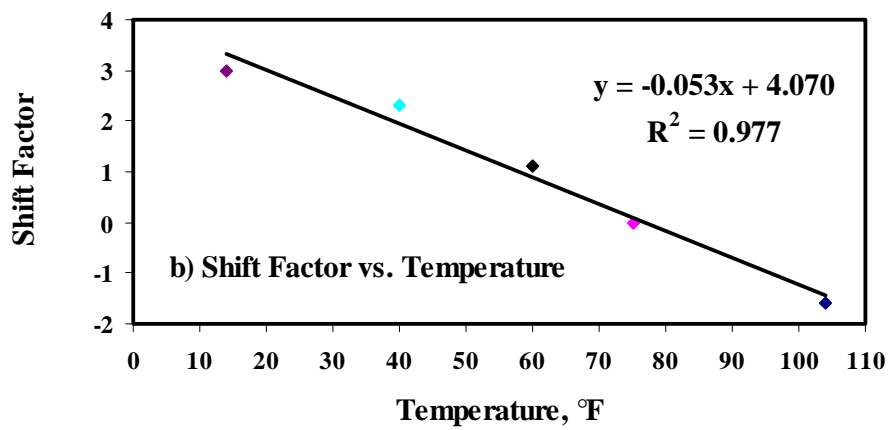
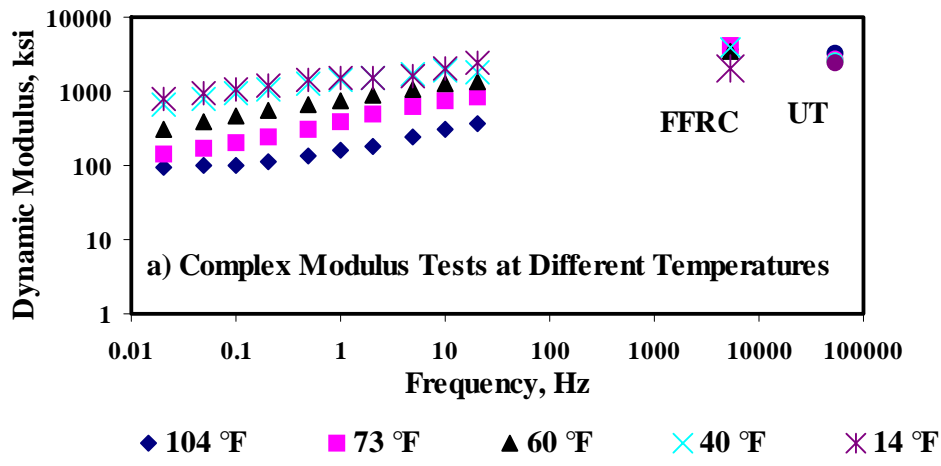


Figure A.21 - Data for Section 9-3

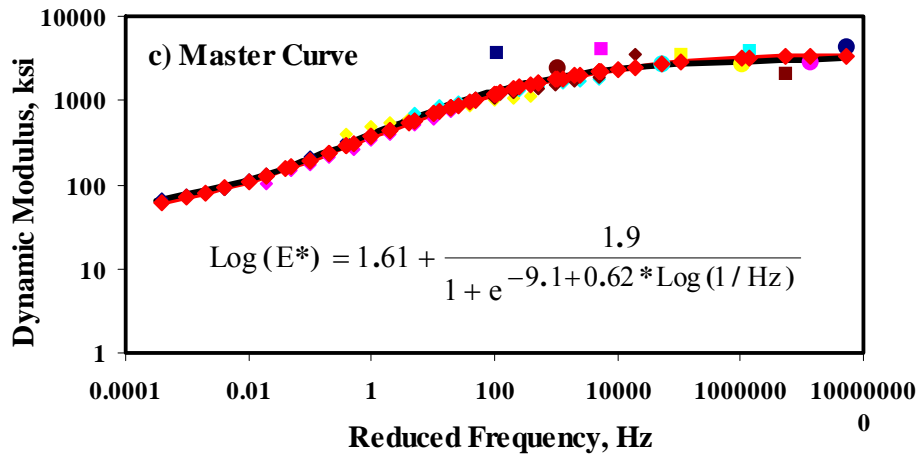
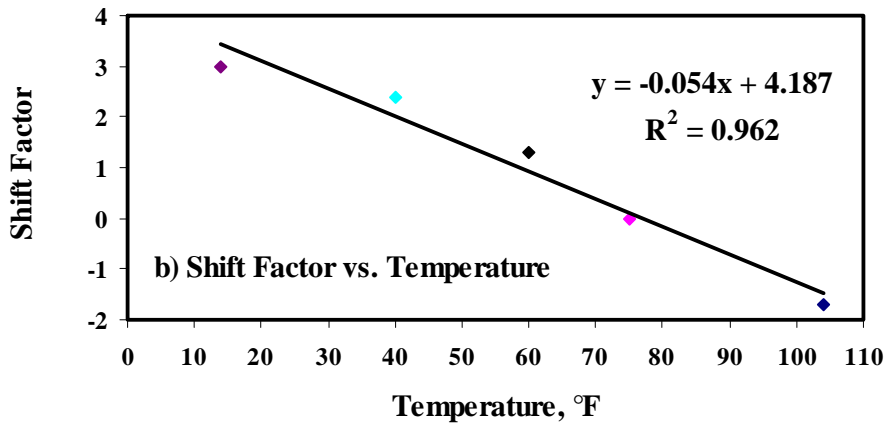
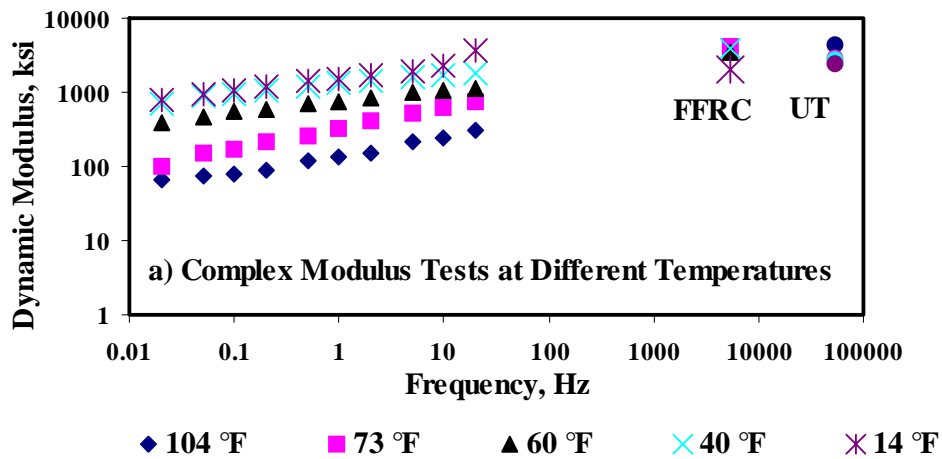


Figure A.22 - Data for Section 9-4

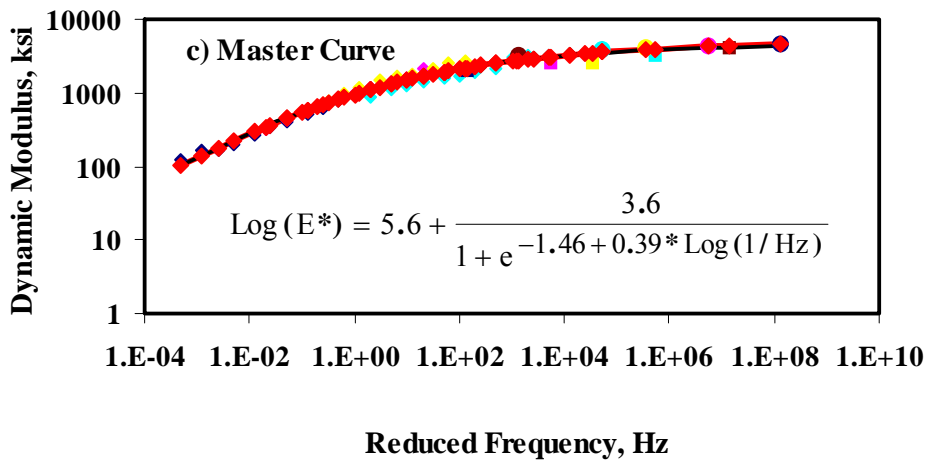
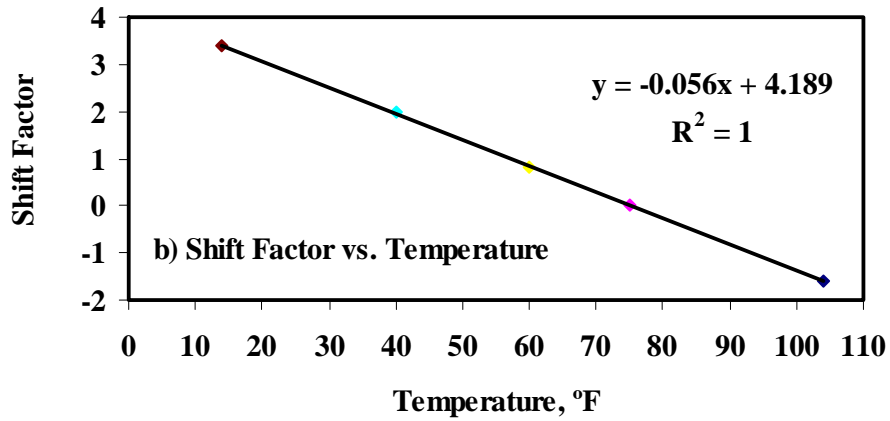
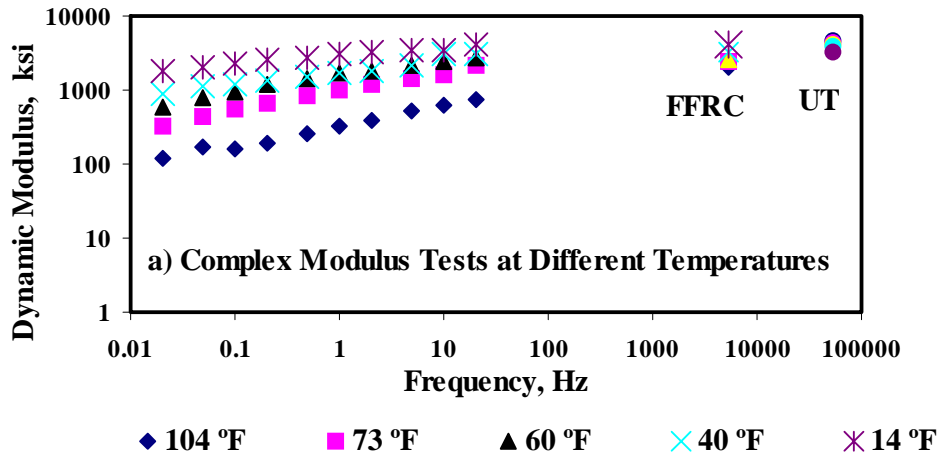


Figure A.23 - Data for Section 10-1

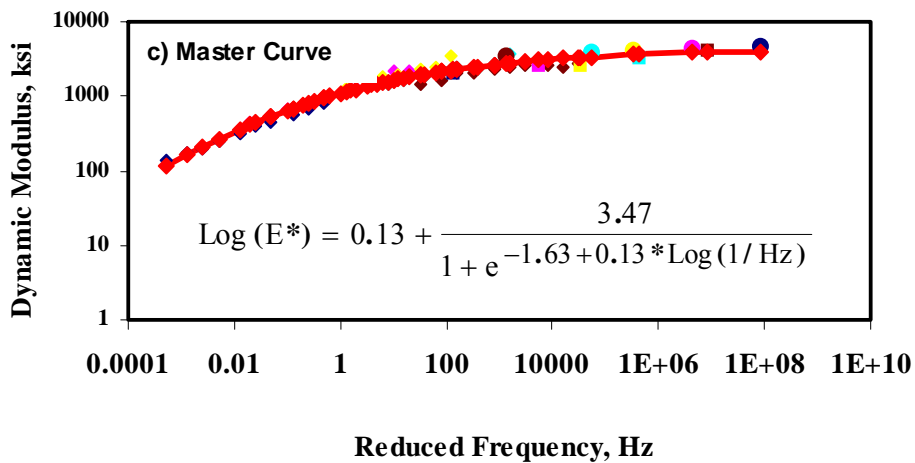
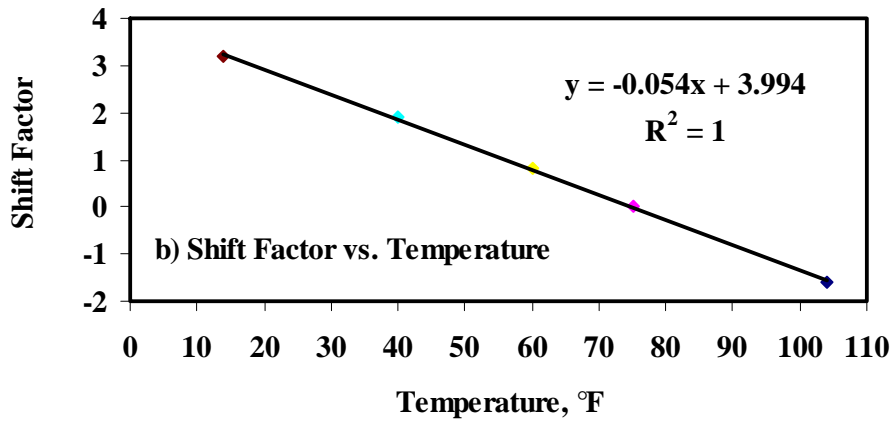
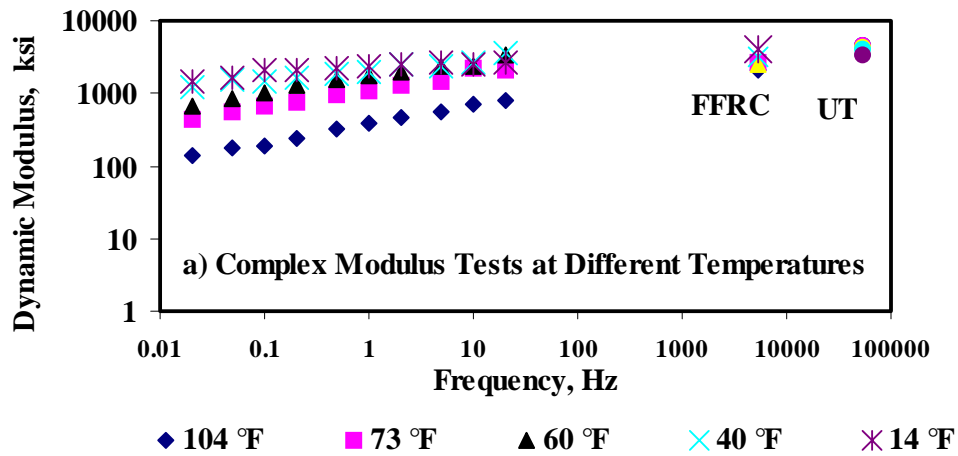


Figure A.24 - Data for Section 10-2

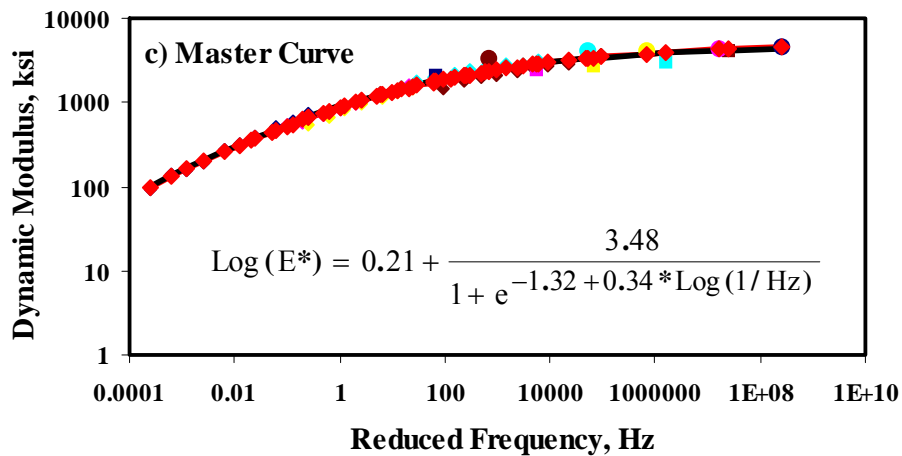
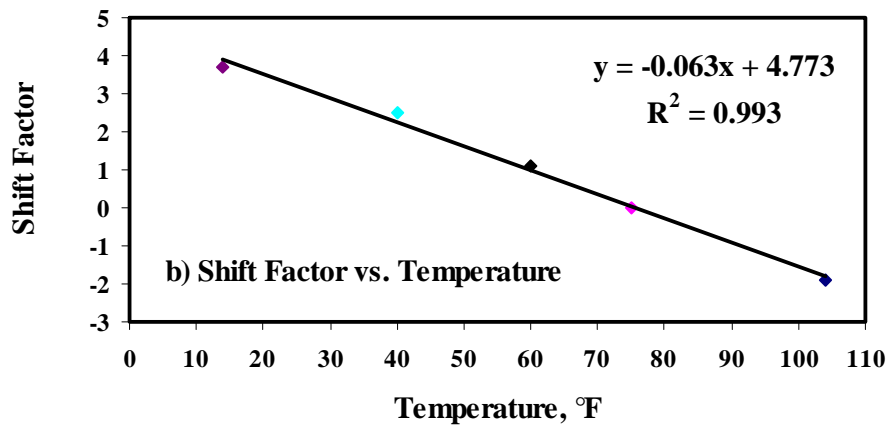
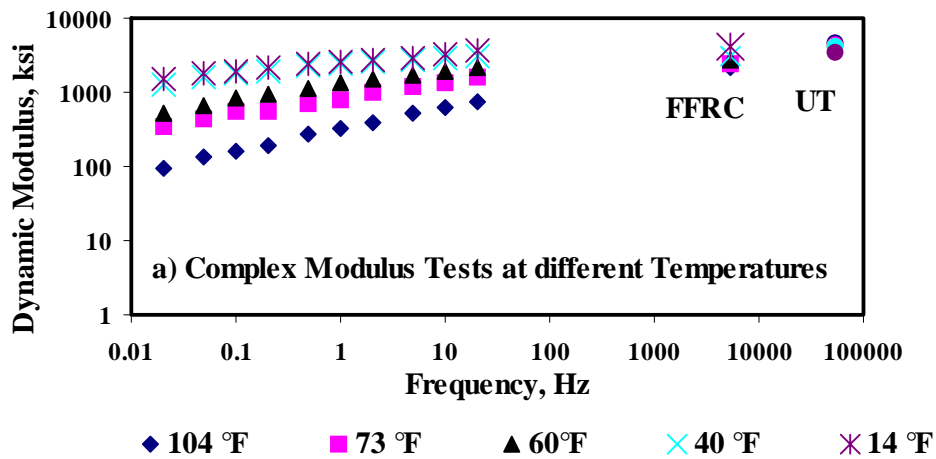


Figure A.25 - Data for Section 10-3

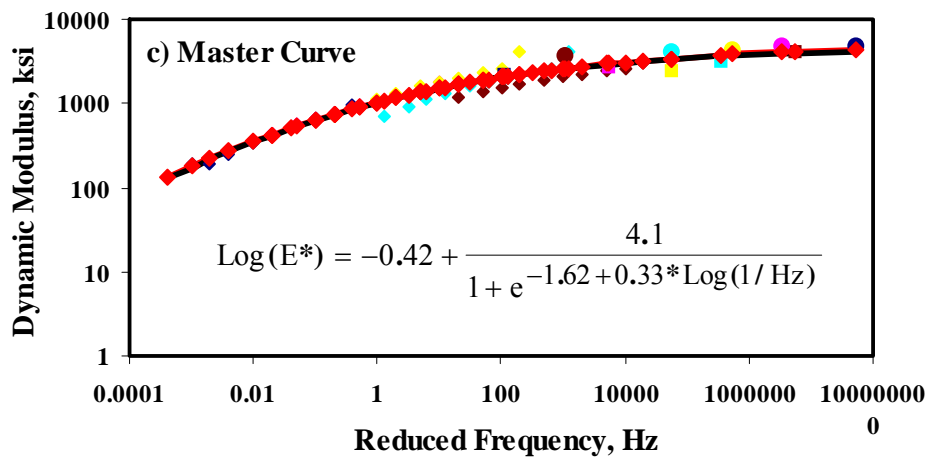
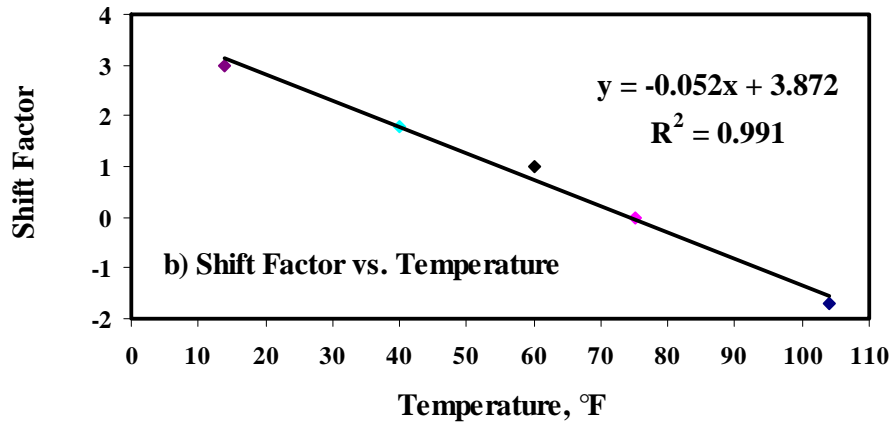
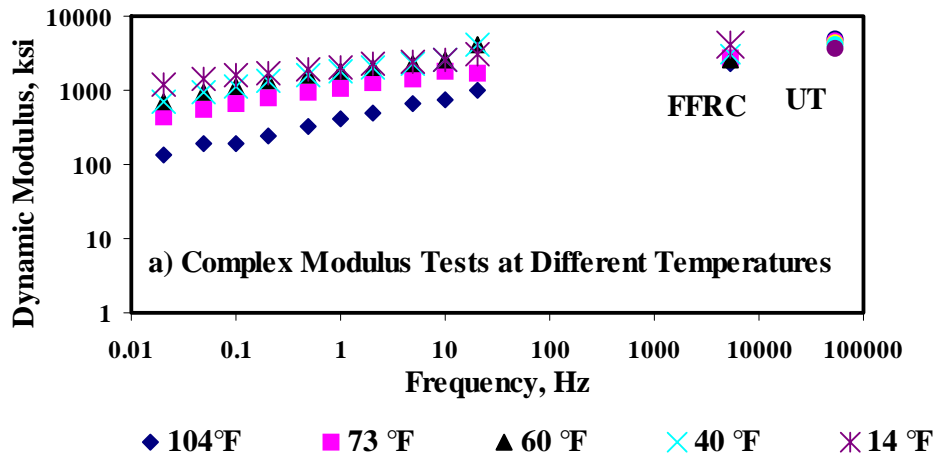


Figure A.26 - Data for Section 10-4

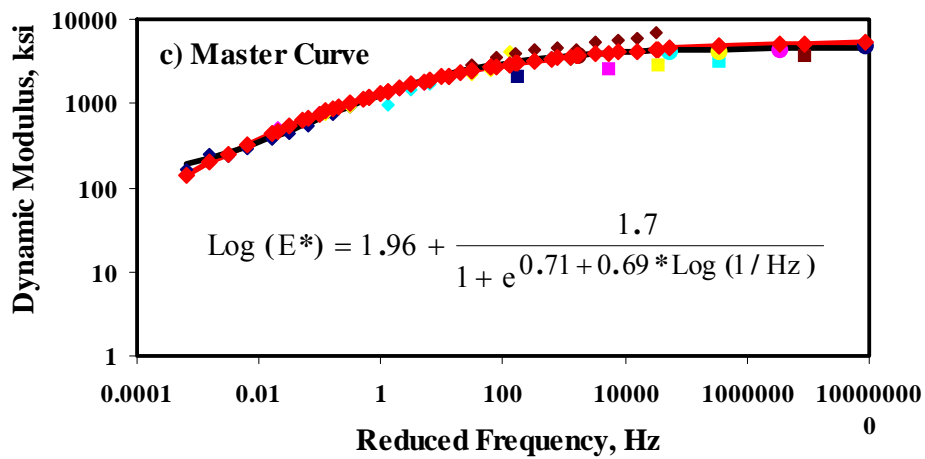
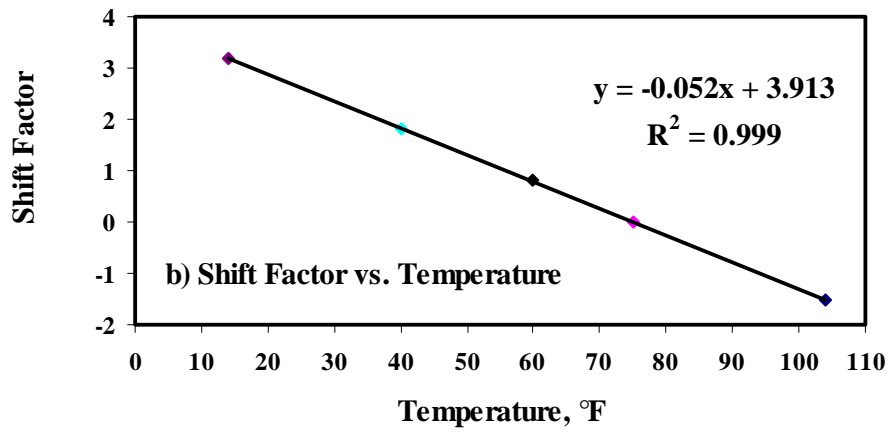
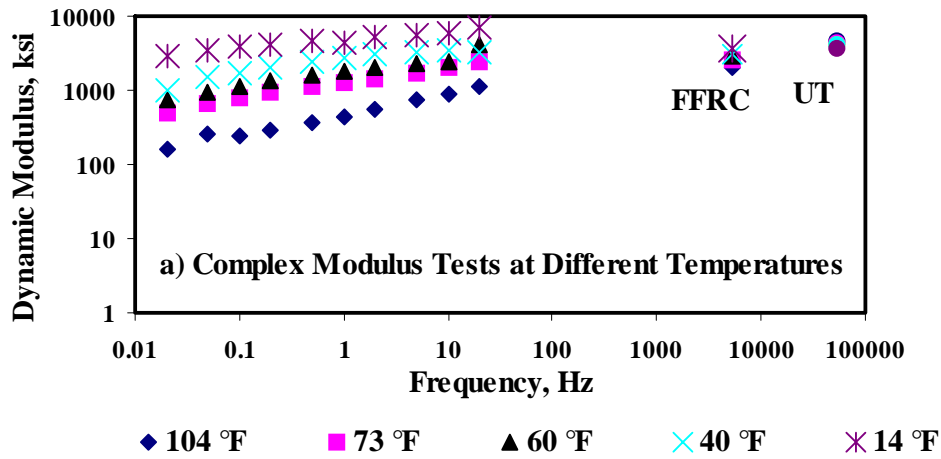


Figure A.27 - Data for Section 10-5

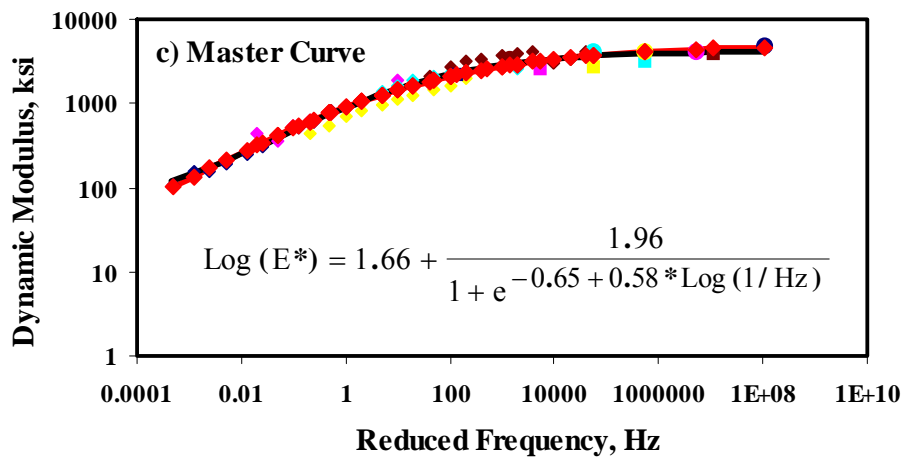
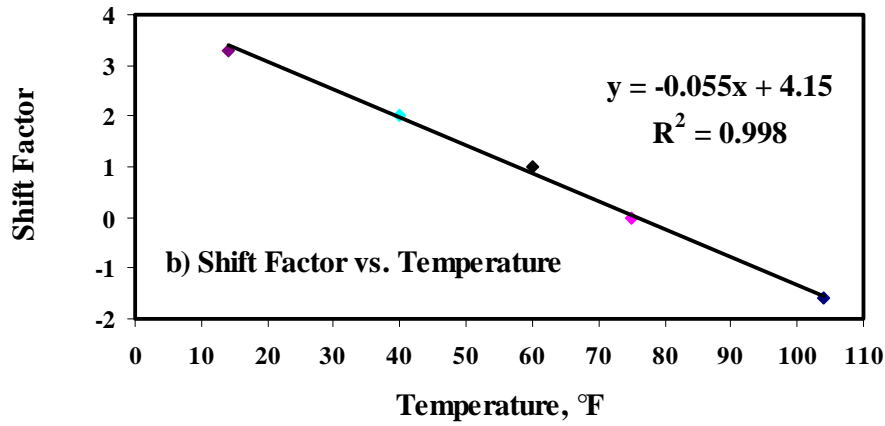
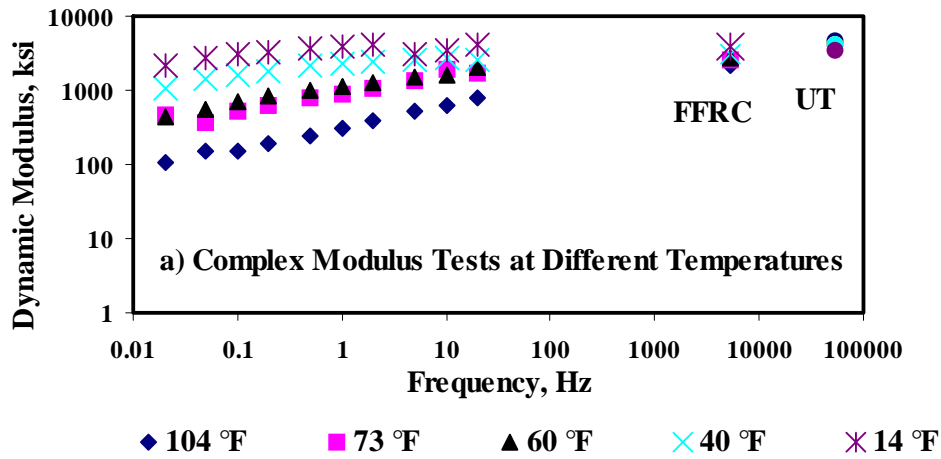


Figure A.28 - Data for Section 10-6